A thesis submitted for the degree of Doctor of Philosophy

MECHANICAL FACTORS AFFECTING THE ESTIMATION OF TIBIALIS ANTERIOR FORCE USING AN EMG-DRIVEN MODELLING APPROACH

by

Stuart C. Miller

Centre for Sports Medicine and Human Performance

School of Sport and Education

Dedicated to Mum, Dad, and my brother Iain who have supported me through everything.

Abstract

The tibialis anterior (TA) muscle plays a vital role in human movement such as walking and running. Overuse of TA during these movements leads to an increased susceptibility of injuries e.g. chronic exertional compartment syndrome. TA activation has been shown to be affected by increases in exercise, age, and the external environment (i.e. incline and footwear). Because activation parameters of TA change with condition, it leads to the interpretation that force changes occur too. However, activation is only an approximate indicator of force output of a muscle. Therefore, the overall aim of this thesis was to investigate the parameters affecting accurate measure of TA force, leading to development of a subject-specific EMG-driven model, which takes into consideration specific methodological issues.

The first study investigated the reasons why the tendon excursion and geometric method differ so vastly in terms of estimation of TA moment arm. Tendon length changes during the tendon excursion method, and location of the TA line of action and irregularities between talus and foot rotations during the geometric method, were found to affect the accuracy of TA moment arm measurement. A novel, more valid, method was proposed. The second study investigated the errors associated with methods used to account for plantar flexor antagonist co-contraction. A new approach was presented and shown to be, at worse, equivalent to current methods, but allows for accounting throughout the complete range of motion. The final study utilised the outputs from studies one and two to directly measure TA force *in vivo*. This was used to develop, and validate, an EMG-driven TA force model. Less error was found in the accuracy of estimating TA force when the contractile component length changes were modelled using the ankle, as opposed to the muscle.

Overall, these findings increase our understanding of not only the mechanics associated with TA and the ankle, but also improves our ability to accurately monitor these.

Acknowledgements

Contents

List of Abbreviations

θ	joint angle
$\%RMS_{diff}$	root mean square of the percentage difference
$\%RMSE$	relative root mean square error
COR	centre of rotation
CV	coefficient of variation
EMG	electromyography
EMG_{max}	maximal electromyogram signal recorded
ES	effect size
F	force
F_{iso}	isometric force
F_{mus}	muscle force
F_{TA}	Tibialis Anterior muscle force
GEO	geometric
GEO_{INS}	geometric-derived moment arms using line of action at tendon insertion and foot rotation for centre of rotation
$GEO_{INS,TAL}$	geometric-derived moment arm using line of action at tendon insertion and using talus rotation for centre of rotation
GEO_{RET}	geometric-derived moment arms using line of action at retinaculum and foot rotation for centre of rotation
$GEO_{RET,TAL}$	geometric-derived moment arms using talus rotation for centre of rotation calculation
GM	Gastrocnemius Medialis
GL	Gastrocnemius Lateralis
ICC	intraclass-correlation
LOA	line of action
M	moment
M_{DF}	dorsiflexor moment
M_J	joint moment
M_{PASS}	passive joint moment
M_{PF}	plantar flexor moment
MRI	magnetic resonance imaging
MTJ	muscle-tendon junction
MTU	muscle-tendon unit
MUAP	motor unit action potentials

MVC	maximal voluntary contraction
r	muscle moment arm
R^2	coefficient of determination
RMS	root mean square
RMSE	root mean square error
ROM	range of motion
SOL	Soleus
T_i	point (i=1-2) on talus used to track talus rotation in geometric method
TA	Tibialis Anterior
TE	tendon excursion
TE_{CORR}	tendon excursion-derived moment arms using change in muscle-tendon unit length
TE_{DF}	tendon excursion-derived moment arms using dorsiflexor rotations
TE_{PF}	tendon excursion-derived moment arms using plantar-flexor rotations
TS	Triceps Surae
v	velocity

Chapter One

General Introduction

The Role of Tibialis Anterior in Human Movement

Tibialis anterior (TA) is the largest muscle in the anterior compartment of the lower leg, accounting for over 60% of dorsiflexor volume (Fukunaga, Roy, Shellock, Hodgson, & Edgerton, 1996a, 1996b; Fukunaga et al., 1992). Its principal function is to dorsiflex the foot, but it also provides assistance during inversion due to its tendon inserting on the medial cuneiform and first metatarsal (Brenner, 2002). TA is important in locomotion where it controls foot-drop during heel-strike and foot-lift during the swing phase to prevent tripping (Byrne, O'Keeffe, Donnelly, & Lyons, 2007; Franz & Kram, 2013; Gazendam & Hof, 2007; Kyrolainen, Avela, & Komi, 2005; Scott, Murley, & Wickham, 2012). TA's activation magnitude and timing can be varied to adapt to varying gait conditions, including those relating to step rate and length (Chumanov, Wille, Michalski, & Heiderscheit, 2012), footwear (Cheung & Ng, 2010; Murley, Landorf, Menz, & Bird, 2009; Scott et al., 2012; Wright, Neptune, van Den Bogert, & Nigg, 1998) and inclination (incline and decline) (Franz & Kram, 2013; Lay, Hass, & Gregor, 2006; Lay, Hass, Richard Nichols, & Gregor, 2007) changes as well as treadmill use compared to overground gait (Lee & Hidler, 2008). Additionally, changes in the action (and role) of TA with age have also been documented during locomotion (Franz & Kram, 2013; Hortobágyi, Finch, Solnik, Rider, & DeVita, 2011; Hortobágyi et al., 2009). Because these conditions influence TA activation, they also influence the force it develops and its role during gait.

TA also appears to play an important role in determining the speed at which humans change from walking to running gaits in order to minimise the energy cost of locomotion, i.e. the walk-run transition (Segers, Lenoir, Aerts, & De Clercq, 2007). The activation of TA, and thus the dorsiflexor moment, has been shown to increase with increasing walking speeds but then decrease upon commencement of running (Bartlett & Kram, 2008; Hreljac, Imamura, Escamilla, Edwards, & MacLeod, 2008). In addition to, and maybe because of, TA's important role in gait, the muscle tends to be susceptible to overuse injuries such as chronic exertional compartment syndrome (Allen & Barnes, 1986; Edwards, Wright, & Hartman, 2005; Mouhsine, Garofalo, Moretti, Gremion, & Akiki, 2006; Touliopolous & Hershman, 1999). Chronic exertional compartment syndrome is associated with being an overuse injury related to an unaccustomed increase in activity (Allen & Barnes, 1986; Bong, Polatsch, Jazrawi, & Rokito, 2005; de Fijter, Scheltinga, & Luiting, 2006). It is most commonly found in athletes partaking in sports involving a "great deal of running" (Bong et al., 2005), such

as distance running, ball and puck sports (Edwards et al., 2005), or in those exposed to significant impact stress to the legs (Turnipseed, Hurschler, & Vanderby, 1995), such as military personnel (de Fijter et al., 2006).

TA Force Estimation

Recent increments in understanding of the importance of TA force output has also helped to improve our understanding of the neuromuscular factors influencing walking and running performance. For example, investigations into the (i) possible neural control strategies used by the central nervous system to perform walking (Neptune, Clark, & Kautz, 2009), (ii) regulation and control of impact forces during heel-toe running (Wright et al., 1998), (iii) production of propulsive forces during running (Hamner, Seth, & Delp, 2010) and (iv) effect of modifying the mechanical properties of structures within the lower limb (i.e. plantar flexor stiffness and length; Xiao & Higginson, 2010), have all required the estimation of TA forces in order to make calculations. Accurate quantification of TA force production is therefore an important goal to achieve in order to continue to further our understanding in many contexts.

In vivo muscle forces cannot be directly measured without the use of invasive methodologies such as the buckle transducer (Fukashiro, Komi, Järvinen, & Miyashita, 1995; Gregor, Komi, Browning, & Järvinen, 1991) or fibre-optic technologies (Arndt, Komi, Brüggemann, & Lukkariniemi, 1998; Finni, Komi, & Lepola, 2000). As such, non-invasive techniques, typically incorporating a modelling-based approach, are commonly used. Three different approaches to modelling muscle force have been predominant: inverse dynamics, forward dynamics, and EMG-driven modelling. An inverse dynamics approach uses Newton-Euler equations of motion (Zajac, Neptune, & Kautz, 2002) to calculate joint moments from external forces and kinematic data. This approach only calculates net joint moments; individual muscle forces cannot be accurately computed due to an indeterminate scenario. Nonetheless, muscle forces can be estimated using optimisation procedures that focus on the minimisation of the magnitudes of variables such as muscle fatigue, muscle stress or peak forces (Zajac et al., 2002). The second approach, forward dynamics, produces a set of muscle activation patterns that produce whole-body kinetics and/or kinematics that agree with measured values using a dynamical-model of the body (Delp et al., 1990). For example, an optimisation algorithm can be used to find the muscle activation patterns such that the simulation-generated trajectories of the kinematics and kinetics (and perhaps muscle

activation patterns) match the measurements as well as possible. The principal challenge within this approach is to determine how to specify the relative importance (i.e. the weighting) of each variable, because different weightings produce different muscle activation patterns, and thus tracking solutions (Zajac et al., 2002). It is not ideal to use electromyogram (EMG) signals as muscle activation inputs for the model because the quasi-random nature of the EMG signals increases model variability (Zajac et al., 2002). As such, the accuracy of this method is reliant on the optimisation approach used, and the target used to drive this optimisation. A third approach to estimating muscle forces, EMG-driven modelling, uses the EMG recorded during data collection to drive a set of muscle models. Commonly, the Hill-based model is used, incorporating force-length(Gordon, Huxley, & Julian, 1966b), force-velocity (Hill, 1938) and force-EMG (Lippold, 1952) sub-models (Buchanan, Lloyd, Manal, & Besier, 2004; Manal, Gravare-Silbernagel, & Buchanan, 2012; Olney & Winter, 1985; White & Winter, 1992; e.g. Zajac, 1989). When using an EMG-driven model, processing of the EMG signal (Potvin & Brown, 2004a; Sparto et al., 1998), the modality used to track the length and velocity of the contractile component (Fukunaga et al., 2001; Ito, Kawakami, Ichinose, Fukashiro, & Fukunaga, 1998; Lichtwark & Wilson, 2005), and the requirement to calibrate the model to the individual (which requires force being measured during a set of controlled contractions) provides challenges and requires methodological consideration.

When modelling approaches were first developed to estimate muscle forces the required model parameters, such as moment arm length, muscle length and tendon length, were obtained from cadaveric studies either directly or after scaling to the subject (e.g. Hoy, Zajac, & Gordon, 1990; White & Winter, 1992). However, scaled-generic models do not allow for accurate muscle force estimates due to anthropometric variability between individuals (Correa, Baker, Graham, & Pandy, 2011; Scheys, Spaepen, Suetens, & Jonkers, 2008; Scheys, Van Campenhout, Spaepen, Suetens, & Jonkers, 2008). A significant landmark in biomechanics research has thus been the development of medical imaging techniques, which have allowed detailed measurements to be made non-invasively *in vivo*. The advent of ultrasound and magnetic resonance imaging has facilitated ground-breaking discoveries, with a major discovery being that tendons and muscles do not work in phase during locomotion; e.g. a muscle may be shortening whilst the muscle-tendon unit is lengthening (e.g. Chleboun, Busic, Graham, & Stuckey, 2007b; Fukunaga et al., 2001; Ishikawa, Pakaslahti, & Komi, 2007; Lichtwark

& Wilson, 2005). Importantly, medical imagining techniques allow researchers to obtain the parameter values required to develop subject-specific models (Arnold, Salinas, Asakawa, & Delp, 2000; Zajac et al., 2002). The ability to directly measure variables such as muscle moment arms (Ito, Akima, & Fukunaga, 2000; Maganaris, 2000, 2004; Rugg, Gregor, Mandelbaum, & Chiu, 1990) as well as muscle (Fukunaga, Kawakami, Kuno, Funato, & Fukashiro, 1997; Maganaris, 2001) and tendon length and mechanical properties (Fukashiro, Itoh, Ichinose, Kawakami, & Fukunaga, 1995; Maganaris & Paul, 1999) is considered to have significantly improved the accuracy of musculoskeletal modelling (Correa et al., 2011; Scheys et al., 2008; Scheys et al., 2008).

TA force estimation has predominantly been achieved using either forward dynamics or EMG-driven modelling approaches. When TA force is a main output variable, an EMG-driven approach may be preferred. A forward dynamics approach requires the inclusion of multiple subject-specific parameters, in addition to those associated with the TA muscle-tendon unit (e.g.Xiao & Higginson, 2010). Although scale-based measurements could be incorporated, these may reduce the accuracy of the force estimates (Correa et al., 2011; Scheys et al., 2008; Scheys et al., 2008). Therefore, the use of an EMG-driven model may be preferred for TA investigations due to the focus being on a specific muscle.

EMG-driven musculoskeletal models require the inputs of force-length and force-velocity relationships with a scaling factor included for muscle activation intensity (i.e. amplitude). Importantly, the 'length' and 'velocity' must refer to that of the contractile unit itself (Ito et al., 1998) rather than the whole muscle-tendon unit, because changes in tendon length are rarely synchronous with changes in muscle length (Ichinose, Kawakami, Ito, Kanehisa & Fukunaga, 2000). Although variations in tendon length have been accounted for (i.e. removed) when measuring separate force-length (Maganaris, 2001) and force-velocity (Reeves & Narici, 2003) relationships in TA *in vivo*, this approach has not been applied to EMG-driven models used to estimate TA muscle force. Instead, muscle length has been assumed to vary with whole muscle-tendon unit length and thus modelled using ankle joint angle as the input variable (e.g.Olney & Winter, 1985; White & Winter, 1992); this method cannot therefore account for the discrepancy between these two variables due to tendon compliance (Ito et al., 1998).

A second issue associated with EMG-driven models is the requirement to quantify muscle force directly during a series of calibration contractions to allow for the model to be fitted to the individual. To estimate TA force magnitude, the ankle joint moment data are typically collected (e.g. using isokinetic dynamometry) during the calibration contractions. Muscle moment arm measurements (r), or cadaver- or model-based estimates (e.g. Buchanan, Lloyd, Manal, & Besier, 2005), then allows for the estimation of muscle force (F_{mus}) from joint moment (M) using the equation: $F_{mus} = M/r$. Although direct measurement of the muscle moment arm is somewhat complicated (Maganaris, 2004), it is necessary to incorporate this into the methodology to provide accurate muscular force estimates, as small variations in the moment arm value will strongly influence the model's output (Correa et al., 2011; Fath, 2012; Scheys et al., 2008; Scheys et al., 2008). Measurement of the TA moment arm is commonly performed using either the tendon excursion (Ito et al., 2000; Klein, Mattys, & Rooze, 1996; Maganaris, 2000; Spoor, van Leeuwen, Meskers, Titulaer, & Huson, 1990) or geometric (Maganaris, 2000; Maganaris, Baltzopoulos, & Sargeant, 1999; Rugg et al., 1990) methods. Importantly, these two approaches have been shown to produce different TA moment arm estimates (Maganaris, 2000), which is an issue also affecting other muscles (Fath, Blazevich, Waugh, Miller, & Korff, 2010; Maganaris, Baltzopoulos, & Sargeant, 2000; Wilson et al., 1999; Zhu, Duerk, Mansour, Crago, & Wilson, 1997), and thus may not be valid methods of deriving TA moment arm.

One final, yet important, consideration is the need to account for antagonist co-contraction of the plantar flexors prior to TA (i.e. dorsiflexor) force calculation. Although it is sometimes assumed that the antagonist co-contraction force is negligible (White & Winter, 1992), in fact the production of maximal dorsiflexor contractions without antagonist involvement is exceedingly difficult (Arampatzis et al., 2005; Billot, Simoneau, Van Hoecke, & Martin, 2010; Maganaris, Baltzopoulos, & Sargeant, 1998; Simoneau, Billot, Martin, & Van Hoecke, 2009). Importantly, accounting for plantar flexor co-contraction during a dorsiflexion contraction significantly alters the estimated moment (i.e. dorsiflexor moment was significantly different to joint moment; Billot et al., 2010). Therefore, it is necessary to account for plantar flexor co-contraction to allow calculation of the true dorsiflexor force from the resultant joint moment. A number of methods have been used to estimate plantar flexor moment during dorsiflexion, which focus on recording plantar flexor activation (i.e. EMG) and relating this to plantar flexor

moment. For example, the ratio between the maximal voluntary contraction (MVC) joint moment and the corresponding maximum EMG activity recorded (Aagaard et al., 2000; Reeves, Narici, & Maganaris, 2004a, 2004b), or the fitting of a simple model (commonly linear, curvilinear, or exponential; Billot et al., 2010; Kellis, Kouvelioti, & Ioakimidis, 2005; Mademli, Arampatzis, Morey-Klapsing, & Brüggemann, 2004, have both been used. However, differences in estimated plantar flexor moment between the different approaches are present, which suggests inaccuracies (Billot et al., 2010).

Improving TA Force Estimation Accuracy

The overall purpose of this thesis was to develop a subject-specific EMG-driven force model whilst accounting for methodological concerns outlined above, which would allow for the accurate estimation of TA muscle force during complex movement. To achieve this, three experiments were performed. The research presented in the first two experimental chapters (Chapters 3 and 4) aimed to develop appropriate methods for calculating TA force from joint moment data. Specifically, the purpose of the first study was to identify the most appropriate method of estimating TA muscle tendon moment arm, whilst the purpose of the second study was to determine the optimal method for accounting for plantar flexor antagonist co-contraction. Results from the first two studies were then used to provide an accurate method of TA force measurement, which could be used as the input for an EMG-driven force model that was developed and tested in the final study. The main purpose of this final study was to design an accurate, subject-specific, EMG-driven model that incorporated the change in muscle length and velocity, rather than the change in joint angle and angular velocity.

Chapter Two

Literature Review

Introduction

The overarching aim of this thesis is to investigate the methodological concerns related to measuring, and subsequently modelling, tibialis anterior force. As a bridge across the three studies (Chapters 3-5), this review will provide an overview of the processes involved in the development of force, and the action of this force at the joint. It will begin by introducing the three main acute factors (outside of fatigue) that affect force production of a muscle; length, velocity and activation. Following this, a description of the role the tendon and moment arm play in the transfer of muscle force to the joint will be provided. Although the order of muscle-to-joint has been employed within this chapter, common approaches to measuring muscle force work in the opposite direction (i.e. joint-to-muscle), such that the knowledge of the kinetics and kinematics of the joint are used to calculate force output of a muscle.

Effect of Length on Force

The force-length (also labelled 'length-tension', which will be used interchangeably) relationship was first properly described by a series of experiments (Gordon, Huxley, & Julian, 1966a, 1966b) set up to control for methodological concerns within earlier investigations (Ramsey & Street, 1940). Applying the then recently proposed sliding filament theory (Huxley & Niedergerke, 1954; Huxley & Hanson, 1954), the number of cross-bridges between actin and myosin was used to explain the variation in tension with changes to the length of the frog semitendinosus muscle. Peak tension was recorded at sarcomere lengths of 2.05-2.25 μm, with reductions in tension at lengths longer and shorter than this "optimal" region. Since these landmark studies, this relationship has been shown to hold true in skeletal muscles of varying species, including humans, although the exact lengths that the plateau region occurs on, and the rate of decline in force at lengths either side of this region, do vary across species (Gareis, Solomonow, Baratta, Best, & D'Ambrosia, 1992; Rassier, MacIntosh, & Herzog, 1999). This is largely thought to be because of different lengths of the thin actin filament across species, whereas the thick myosin filament is thought to be constant across species (approximately 1.6 μm, Burkholder & Lieber, 2001; Nigg & Herzog, 2006).

The force-length relationship of the muscle can be modelled using two components, an active and a passive component, with the summation of these two components making up the total force-length relationship of the muscle (Zajac, 1989). The active component

is that which is caused by the cross-bridge connection of actin and myosin, and the subsequent tension that is developed. However, recently a new addition to this theory has been proposed. Using a "multiple filament, spatially explicit model of the sarcomere that incorporates lattice spacing", Williams and colleagues demonstrated that the number of cross-bridge connections was not the only variable controlling the length-dependent development of active tension (Williams, Salcedo, Irving, Regnier, & Daniel, 2013). Approximately 20-50% of the tension is due to the spacing between the myosin and actin filaments; proposed to affect the direction and/or duration of the force that is produced during the power-stroke. Regardless of the mechanistic underpinnings causing the shape of the force-length relationship, the shape is consistent across sarcomeres, and summates up to a smooth quasi-inverted-U when measured at levels greater than that of the individual sarcomere (Hawkins & Bey, 1997; Leedham & Dowling, 1995; Maganaris, 2001; Marsh, Sale, McComas, & Quinlan, 1981).

Due to the constraints on joint range of motion (ROM) by anatomical features (i.e. bone and ligaments), the muscle does not transverse through its full length capabilities within the human body. The portion of the full force-length relationship that a muscle works upon *in vivo* appears to vary across muscle and species (Burkholder & Lieber, 2001; Lieber & Ward, 2011). Of those measured *in vivo*, the majority of human muscles appear to work predominantly along the ascending limb and plateau region of the sarcomere force-length relationship (Arnold & Delp, 2011; Burkholder & Lieber, 2001; Hawkins & Bey, 1997; Leedham & Dowling, 1995; Lieber & Ward, 2011; Maganaris, 2001), although some muscles work on the descending limb also (e.g. Lieber, Loren, & Fridén, 1994), whilst a wide range of operating positions have been found across species (Herzog, Guimaraes, Anton, & Carter-Erdman, 1991; Herzog, Read, & Ter Keurs, 1991; Lieber & Brown, 1992; Lieber et al., 1994; Lieber, Raab, Kashin, & Edgerton, 1992; Rack & Westbury, 1969).

The passive tension of a muscle becomes measureable when it is held at a length beyond its optimal length (defined as the point at which peak active tension is produced). At lengths beyond this position, an exponential increase in passive force is measured, with this continuing to increase until failure within the mechanical structure i.e. tearing of the muscle (Garrett, Safran, Seaber, Glisson, & Ribbeck, 1987). Although the tendon (see below) is the dominant factor in the passive tension of the muscle-tendon unit, the internal elastic resistance of the myofibril is the main component

affecting passive tension of the muscle itself (Magid & Law, 1985). Of the structures within the myofibril, it is hypothesised that the protein titin produces the greatest passive resistance to stretch, at least up to a sarcomere length of approximately 3.8 μm (Labeit & Kolmerer, 1995; Nishikawa et al., 2012; Prado et al., 2005). The shape of the passive length-tension relationship is commonly presented as an exponential model, spanning from the optimal length of the muscle (below which passive tension is not present) up to the point at which failure occurs (Garrett et al., 1987; Zajac, 1989).

The force-length relationship of the human TA *in vivo* has been investigated for both voluntary and stimulated contractions. Maximum TA force was found to be in the range of 157-644 N (ankle angles ˉ30° - 45°; dorsiflexion – plantar flexion) with a maximum force of 673 N at 30° plantar flexion (Maganaris, 2001). Marsh et al (1981) only reported ankle moments, but these were similar to those reported by Maganaris (2001) when electrical stimulation was used. When maximal voluntary contractions were performed, peak moments were double those measured with electrical stimulation (Marsh et al., 1981). In both studies, the TA was acting along the ascending and plateau region of the force-length relationship.

Effect of Velocity on Force

The effect of velocity on muscle force was first investigated during a series of pioneering studies (Fenn & Marsh, 1935; Hill, 1938, 1964). Since then, the "Hill-equation" has become routine in the biomechanical testing of muscle. There are two portions to the force-velocity relationship, with one having been investigated much more than the other (Nigg & Herzog, 2006).

As the muscle shortens under load, it is only able to produce force levels that are lower than that measured under isometric conditions. With increasing velocity of shortening, the force developed is reduced. Alternatively, the maximal shortening velocity of a muscle under load increases as the load decreases. The relationship between shortening velocity of muscle and force able to be produced follows a relationship first described by Hill (1938). This relationship for the concentric portion of the force-velocity relationship is a hyperbolic relationship. However, further studies have presented that this single-hyperbolic relationship may not be accurate at representing the true force-velocity relationship whilst the muscle is shortening. A "double-hyperbolic" relationship has been found to best model the concentric force-velocity data in rat

(Devrome & MacIntosh, 2007) and frog (Edman, 1988) muscle fibre. These findings suggest that the concentric portion of the force-velocity relationship has two distinct portions, both able to be modelled by a separate hyperbolic relationship, joining at approximately 78% of force produced under isometric loads (Edman, 1988). However, this model is unlikely to be required at the whole muscle and/or joint level as it appears that the summation of individual fibres "smooths" this potential double-hyperbolic relationship (Bobbert & Frank, 2012).

The relationship between load and velocity of shortening varies with the structure of the muscle being investigated. Specifically, longer muscles (i.e. a greater number of sarcomeres in series) can achieve a higher maximal shortening velocity, compared to muscles with a higher percentage of "slow-twitch" fibres (Baratta, Solomonow, Best, Zembo, & D'Ambrosia, 1995; Bottinelli, Canepari, Pellegrino, & Reggiani, 1996; Thorstensson, Grimby, & Karlsson, 1976). However, despite the differences between different muscles, the concentric force-velocity relationship of a given muscle has been shown to vary only along the force-axis, with length (Abbott & Wilkie, 1953; Scott, Brown, & Loeb, 1996; Matsumoto, 1967; Edman, 1979) and activation (Bigland & Lippold, 1954b; Podolsky & Teichholz, 1970) having no effect when the force-velocity relationship is normalised to the isometric force. As such, the effect of shortening velocity on muscle force appears to be well modelled by the Hill-equation (Hill, 1938).

Not as much is understood about the eccentric portion of the force-velocity relationship as is about the concentric portion (Nigg & Herzog, 2006). An important consequence of this is that a general model for the eccentric portion is not available. Various approaches have been used to model the eccentric portion of the force-velocity relationship such as a linear fit (Kues & Mayhew, 1996), an altered Hill-equation (Buchanan et al., 2004), or a linear extension of the concentric force-velocity relationship (Olney & Winter, 1985). Additionally, the rate of rise in force with increasing velocity is large over the slower velocities (especially compared to that seen in the concentric portion), leading to a plateau of the force measured during eccentric contractions at higher velocities (Lieber & Ward, 2011; Edman, 1988; Linnamo, Strojnik, & Komi, 2006; Zajac, 1989).

Effect of Activation on Force
Measurement of the electrical activity that occurs within the muscle as it is activated is enticing to measure. It is a step in the chain of events that produces muscle contraction,

and thus force, making it potentially a great variable to model force on. However, since the first investigation into the relationship between muscle activity and force (Lippold, 1952), the relationship between activation and force is still not fully understood (Staudenmann, Roeleveld, Stegeman, & van Dieën, 2010).

The discussion about the shape of the relationship is commonly made between whether it is linear or non-linear. The surface electromyogram (EMG) that is recorded is a result of not only the rate coding, but also the motor unit recruitment. Although the relationship between force output and rate coding or motor unit recruitment is like to be non-linear (Milner-Brown, Stein, & Yemm, 1973; Staudenmann et al., 2010), the combination of the two, as detected by surface EMG, appears to be linear. A linear relationship has been reported for many different muscles including calf and plantar flexors (Bigland & Lippold, 1954b; Hof & Berg, 1977a; Lippold, 1952), first dorsal interosseus muscle of the hand (Milner-Brown et al., 1973), biceps brachii (Moritani & deVries, 1978) and trunk musculature (Brown & McGill, 2008).

Although debate is present between whether the relationship between surface EMG and muscle force is linear or not, there have been suggestions that the non-linearity sometimes reported is due to methodological considerations. Specifically, muscle fatigue (Moritani & deVries, 1978), muscle length change (Hof & Berg, 1977b; Moritani & deVries, 1978), electrode configuration (Moritani & deVries, 1978), contraction intensity range (Kutch & Buchanan, 2001), antagonist co-contraction correction (Brown & McGill, 2008), inclusion of all muscles involved in the action (Hof & Berg, 1977b; Kutch & Buchanan, 2001) and the EMG filtering method (Potvin & Brown, 2004a; Staudenmann et al., 2010) have all been suggested to reduce linearity of the measured force-EMG relationship.

Transfer of Muscle Force to Joint Moment

Tendon

The force output of a muscle is not applied directly to the joint. Instead, it is applied to an elastic tendon, which then transfers force to the joint. The viscoelastic tendon is not a rigid structure as was originally believed. In fact, it is far from this, with changes in length occurring with only small amounts of force being applied to it. The consequences of this are huge for our understanding into areas such as motor control (Fukashiro et al., 1995; Muraoka, Muramatsu, Fukunaga, & Kanehisa, 2004), disabilities (Baddar et al.,

2002), the effects of fashion (Csapo, Maganaris, Seynnes, & Narici, 2010) as well as common movement patterns such as walking (Chleboun, Busic, Graham, & Stuckey, 2007a; Ishikawa et al., 2007; Lichtwark, Bougoulias, & Wilson, 2007), running (Ishikawa & Komi, 2008; Ishikawa et al., 2007; Lichtwark et al., 2007), hopping (Lichtwark & Wilson, 2005; Sano et al., 2012) and jumping (Fukashiro, Hay, & Nagano, 2006; Kurokawa, Fukunaga, & Fukashiro, 2001).

Mechanical properties of tendon are due to its viscoelastic properties. Specifically, the presence of prior stretch (i.e. hysteresis Maganaris & Paul, 2000a), rate of stretch (Theis, Mohagheghi, & Korff, 2012), duration held at end range of motion (Ryan et al., 2010) and number of stretches (Maganaris, 2002; Maganaris, Baltzopoulos, & Sargeant, 2002) all acutely affect the behaviour of the tendon. These are in addition to the more permanent properties of tendon such as thickness and length (Arampatzis, Peper, Bierbaum, & Albracht, 2010; Kubo, Kanehisa, & Fukunaga, 2002; Reeves, Narici, & Maganaris, 2003). These mechanical properties of tendon, and the variability between people (Arampatzis, Karamanidis, Morey-Klapsing, De Monte, & Stafilidis, 2007), affect the interaction between muscle and joint.

Moment Arm

When tension is developed within the tendon, it is applied as force to not only the muscle, but also the bone-segment it is attached to. This results in a rotation of the segment around the joint that it is constrained by. The magnitude and strength of this rotation is a product of the force applied by the tendon and the distance that this force is from the centre of rotation i.e. the moment arm. The moment arm is often overlooked when discussing strength and/or velocity at the joint, most likely due to the inability for changing the moment arm without surgical intervention (Koh & Herzog, 1998). However, knowledge of the moment arm is paramount when studying either the muscle or tendon, as it is the only non-invasive direct way of calculating muscle force.

Before the advent of medical imaging availability, moment arm measurements were undertaken using cadavers, with these being used to estimate moment arms *in vivo* (Boyd & Ronsky, 1998; Hughes, Niebur, Liu, & An, 1998; Spoor & van Leeuwen, 1992). However, imaging techniques such as ultrasound and magnetic resonance have allowed for *in vivo* moment arms to be directly measured (Fath et al., 2010; Hashizume et al., 2011; Ito et al., 2000; Maganaris, 2004; Sheehan, 2007, 2012; Tsaopoulos,

Baltzopoulos, & Maganaris, 2006; Tsaopoulos, Baltzopoulos, Richards, & Maganaris, 2007). Two techniques are commonly used to measure the muscle-tendon unit's (MTU) moment arm *in vivo*. The tendon excursion (Fath et al., 2010; Ito et al., 2000; Maganaris & Paul, 2000b; Tsaopoulos et al., 2006) method uses the ratio of MTU length change to joint angle rotation as the calculation for moment arm. This method is based on the principle of virtual work (Antman & Osborn, 1979), and requires that the work performed by the MTU (*force × Δlength*) is equal to the work performed by the joint (*moment × Δangle*). This assumption applied to the tendon excursion method allows the moment arm (traditionally presented as *moment / force*) to be calculated as *Δlength / Δangle*. The geometric method is commonly performed using magnetic resonance imaging (Sheehan, 2007, 2012; Wilson & Sheehan, 2009) or X-ray (Tsaopoulos et al., 2007) and measures the moment arm as the distance between the centre of rotation and the MTU line of action. This method requires the centre of rotation (commonly using the "Reuleaux method"; Reuleaux & Kennedy, 1876) to be calculated and the MTU line of action to be located.

Although both approaches to measuring the moment arm are theoretically sound, differences between the two approaches are commonly reported. Interestingly, the magnitude of these differences is not consistent across studies. For example, studies utilising both methods have shown variations (Boyd & Ronsky, 1998; Maganaris, 2000; Maganaris et al., 2000), no difference (Spoor & van Leeuwen, 1992), smaller (Fath et al., 2010) and larger (Hughes et al., 1998; Wilson et al., 1999; Zhu et al., 1997) TE-derived moment arms when compared to GEO-derived moment arms. Common presentation is that the tendon excursion method is invalid, as it does not take into account the length changes of the tendon. However, if this were the only reason, moment arm values would always be smaller when derived using the tendon excursion method (i.e. a reduced Δlength for a given Δangle), which they are not. As such, other mechanisms must be the cause for this discrepancy, although no in-depth investigation has been performed (Manal, Cowder, & Buchanan, 2013).

Summary

The measurement of muscle force *in vivo* is dependent on accounting for many variables. Specific to the purpose of this thesis are muscle activation, length and velocity, tendon length changes, and the MTU moment arm. Each of these affect the relationship between muscle force and joint moment. When quantification of muscle

force is required *in vivo*, unless invasive methodologies are to be used, knowledge of the moment arm and the interaction between tendon and muscle are essential. However, when modelling approaches are employed, the relationship between muscle force, activation, length and velocity are required to develop a subject-specific model.

Chapter Three

Tendon Excursion and Centre of Rotation Methodologies for Tibialis Anterior Moment Arm Determination: Accounting for Sources of Error and Violations of Assumptions

ABSTRACT

Accurate estimates of tibialis anterior muscle force is important in many contexts linked to human movement and injury. Two approaches commonly used to estimate moment arm are the tendon excursion (TE; using ultrasonography) and geometric (GEO; using magnetic resonance imaging) methods. Previously, poor agreement between TE- and GEO-derived moment arm estimates has been reported. The purposes of this study were to (1) assess the impact of different variations to the two methods of moment arm estimation and (2) determine how these different variations affect the agreement between the methods. For TE, differences between moment arm estimates calculated from plantar- and dorsiflexion rotations were found at ⁻15° ankle angle (0° = neutral; effect size [ES] = 0.84; p = 0.045). Large errors in moment arm estimates across the range of motion (p = 0.001) were found when inevitable tendon length changes (11 ± 4 mm for 60° rotation; p = 0.001) were not corrected for. For GEO, the estimated moment arm was reduced at ⁻15° when discrepancies between talus and foot joint rotations were accounted for or an alternative tendon line of action was used (located as the tendon inserts onto the foot), either separately (ES = 0.46 and 0.58 respectively; p > 0.05) or together (ES = 0.89; p > 0.05). TE-derived moment arms were smaller than GEO-derived moment arms (ES = 0.68 to 4.86, varying by angle) before accounting for sources of error, however moment arm values were similar after error correction (p > 0.05). Nonetheless, the shape of the moment arm-joint angle relationship was curvilinear for TE but linear for GEO. The results indicate that the TE method should be used for tibialis anterior moment arm estimation after accounting for tendon length changes during joint rotation.

INTRODUCTION

The muscle-tendon unit (MTU) moment arm is an important factor influencing the external transfer of internal force, and thus influences movement performance. Knowledge of its magnitude is a pre-requisite for the estimation of muscle forces from joint moment measurements (Biewener, Farley, Roberts, & Temaner, 2004; Hansen, Aagaard, Kjaer, Larsson, & Magnusson, 2003), which is commonly required in musculoskeletal models (Buchanan et al., 2004) or for the quantification of MTU characteristics (Maganaris, 2001; Maganaris & Paul, 2002; Rosager et al., 2002). Precise measurement of moment arms is essential because small variations introduced by measurement error (Ackland, Lin, & Pandy, 2012) or by the scaling of generic models based on anthropometry (Correa et al., 2011; Scheys et al., 2008) can significantly impact muscle force estimates.

The tibialis anterior (TA) muscle plays an important role in human movement (Cappellini, Ivanenko, Poppele, & Lacquaniti, 2006) and is a main site of musculoskeletal injuries such as chronic anterior compartment syndrome (Blackman, 2000). Thus, accurate estimates of TA forces are important in many contexts (Koh & Herzog, 1998), which in turn requires accurate knowledge of the TA moment arm. Two techniques commonly used to obtain the TA moment arm are the tendon excursion (TE; Maganaris, 2004; Spoor et al., 1990) and the geometric methods (GEO; Maganaris, 2000). The TE method is based on the principle of virtual work, where moment arm is estimated as the derivative of MTU length with respect to joint angle during passive joint rotation. It has been used in cadaveric studies (Klein et al., 1996; Spoor et al., 1990) and, more recently, in conjunction with ultrasound imaging techniques *in vivo* (Ito et al., 2000; Maganaris, 2004). In contrast, the GEO method estimates the moment arm as the perpendicular distance between the MTU line of action and the corresponding joint centre of rotation (COR), with the COR determined using the Reuleaux graphical method (Reuleaux & Kennedy, 1876). The GEO method is commonly used with magnetic resonance (MRI) or x-ray imaging techniques, which allow the clear visualisation of the relevant tendon and bony joint structures (Maganaris, 2000).

Both methods are subject to important assumptions however, which may introduce error into the moment arm estimates. For the TE method, the work performed by the MTU (force × Δlength) is assumed to be equal to the work performed by the joint (moment ×

28

Δangle). The moment arm, which is traditionally presented as the ratio between joint moment and MTU force, can then be calculated as the ratio of MTU length change to joint angle change (i.e. moment arm = moment / force = Δlength / Δangle). When the TE method has been used in cadaver-based studies, weights were suspended from the "free" end of the MTU to allow for a constant force to be applied to the MTU. This constant force prevented any changes in length of the muscle and tendon as the ankle joint was rotated, allowing for the movement (i.e. Δlength) of the MTU to be tracked and used to estimate moment arm. When applying the TE method in vivo, previous studies have tracked the muscle-tendon junction (MTJ) or the aponeurosis-muscle fascicle intersection using ultrasound imaging during joint rotation (Ito et al., 2000; Maganaris, 2000). In doing so, only the change in length of the MTU proximal to the point being tracked is included in the calculation of MTU moment arm. However the change in length of the TA tendon (distal to the MTJ) can contribute up to 45% to MTU length change during passive joint rotation (Herbert, Moseley, Butler, & Gandevia, 2002). Consequently, the moment arm estimated using MTJ displacement could be nearly half that when estimated using MTU length change. In addition to the method used to account for MTU length change, the movement direction (i.e. plantar- vs. dorsiflexion) could also affect moment arm estimates. The reason for this is that force levels within the muscle and tendon can vary differently between MTU shortening and lengthening due to their different hysteresis (Morse, Degens, Seynnes, Maganaris, & Jones, 2008; Tilp, Steib, & Herzog, 2011). Therefore, a difference between muscle lengthening and shortening would be recorded for a given joint angle change when tracking the MTJ. This variation would result in different moment arm estimates. Thus, both the choice of the method of tracking MTU length changes (i.e. muscle or muscle and tendon) and the choice of joint rotation direction are likely to influence TA moment arm estimates.

For the GEO method, the COR is located using the Reuleaux method (Reuleaux & Kennedy, 1876), in which the movement of a segment (typically, the talus for the ankle joint COR) is tracked between two angular positions equidistant either side of the angle of interest. In practice, these two joint positions are typically defined by the angle enclosed by the sole of the foot and the lower leg (subsequently referred to as "foot angle"; Maganaris, 2000; Rugg et al., 1990). Thus, the assumption is made that foot angle change is reflective of talus angle change. However, this has been shown not to be the case, because talus rotation is non-linearly related to foot rotation (Chen, Siegler, &

Schneck, 1988; Lundberg, Goldie, Kalin, & Selvik, 1989; Siegler, Chen, & Schneck, 1988). This could lead to errors in µ COR estimation, and therefore the TA moment arm. A second methodological issue within the GEO method relates to the location of the line of action of the TA. In previous studies, the line of action was assumed to be a line connecting the most proximal and distal points of the extensor retinaculum (Maganaris, 2000; Rugg et al., 1990). However, because the TA tendon inserts onto the foot and thus exerts its force anteriorly to the retinaculum, the line of action would be more accurately obtained at the tendon's insertion onto the foot (i.e. a line bisecting the tendon at the insertion into the first metatarsal). These two lines of action (retinaculum and insertion) are not likely to be similar because the path of the tendon passes anteriorly to the ankle's joint centre and curves over the foot, thus changing its path (i.e. line of action) prior to insertion on the medial cuneiform and first metatarsal bones (Brenner, 2002).

The individual, and combined, effects of these potential sources of error (i.e. rotation direction and tendon length change for the TE method, and talus rotation and line of action location for the GEO method) on both the estimated moment arm and the agreement between the two methods (i.e. TE and GEO methods) have not been investigated. Given this, the first aim of the present study was to examine the potential impact of different methodological approaches to both TE- and GEO-based moment arm estimates. Regarding the TE methods, we assessed how the direction of passive ankle rotation (plantar- vs. dorsiflexion) would affect TA moment arm estimates, and whether these estimates would be dependent upon how MTU shortening is modelled (i.e. muscle alone vs whole MTU length change). Regarding the GEO method, we determined whether foot angle change was indicative of talus angle change, and whether the method of modelling the tendon line of action (retinaculum vs. tendon insertion) would affect TA moment arm estimates. The second aim of this study was to examine the impact of the different methodological approaches on agreement between moment arms obtained from TE and GEO methods.

METHODS

Subjects

Eight adults (7 men and 1 woman) who were free from musculoskeletal injury gave their informed consent and volunteered for the study (age = 28 ± 4 yr, height = 1.81 ± 0.06 m, mass = 77.1 ± 9.3 kg; µ ± SD). Ethics approval was granted by the Brunel

University Ethics Committee, and all procedures were conducted in accordance with the Declaration of Helsinki.

Testing Overview

The subjects reported to the lab on two separate days (TE and GEO testing were performed separately) at least one week apart and at the same time of day. All subjects abstained from exercise for 48 hours before testing. Prior to the testing days, each subject went through a familiarisation session in which the methods involved in both the TE and GEO testing protocols were extensively practiced.

On both testing days, each subject performed three sub-maximal isometric contractions (at 50, 75 and 90% of perceived maximum voluntary effort) and five maximal contractions of both the plantar- and dorsiflexors (foot in the neutral position and the knee straight, 0°). This was done to pre-condition the respective tendons (Maganaris, 2003; Magnusson, Narici, Maganaris, & Kjaer, 2008) in order to minimise changes in tendon stiffness and muscle thixotropy (Axelson, 2005) during the testing. Prior to TE measurements, subjects were also re-familiarised with the passive ankle rotation manoeuvre (see below) by slowly rotating the ankle through its full ROM.

Tendon Excursion Method

The subjects were positioned in an isokinetic dynamometer (Biodex System 3, Biodex Medical Systems, Inc., NY) so that the lateral malleolus was aligned with the COR of the dynamometer and the relative knee and hip angles in the sagittal plane were at 0° and 85°, respectively (0° being full extension). Hook-and-loop straps were securely fastened over the metatarsals to prevent movement of the foot relative to the footplate, and straps were placed tightly across the thigh, torso and waist to limit movement of the upper body, leg and ankle joint. A foot angle of 0° was taken as neutral (taken when the sole of the foot was perpendicular to the tibia), with plantarflexion being a positive angle and dorsiflexion being negative. Each subject's full ROM was determined and used as the ROM during testing. The ankle was then rotated passively at $20°·s^{-1}$ through its ROM for three consecutive rotations (start and finish in dorsiflexion); the three consecutive rotations accounted for one test. A 10-MHz, 50-mm linear-array, B-mode ultrasound probe (Esaote Megas GPX, Genova, Italy) was housed in a custom-made

foam case and strapped to the anterior lower leg in line with the TA tendon-aponeurosis complex in order to track the muscle-tendon junction (MTJ) during the passive ankle rotations (Fig. 3.1). An electroconductive gel was placed on the surface of the probe prior to fixation to aid acoustic contact, with a thin echo-absorbent strip being placed on the skin under the probe to allow probe movement to be accounted for. The ultrasound images were continuously recorded to VHS tape at 25 Hz and synchronised with the dynamometer-derived joint angle data using a 5-V electrical trigger (model DS7A stimulator, Digitimer, Hertfordshire, UK). The joint angle data underwent analogue-digital conversion at 1000 Hz and were captured using Spike 2 software (version 5, CED, Cambridge, UK).
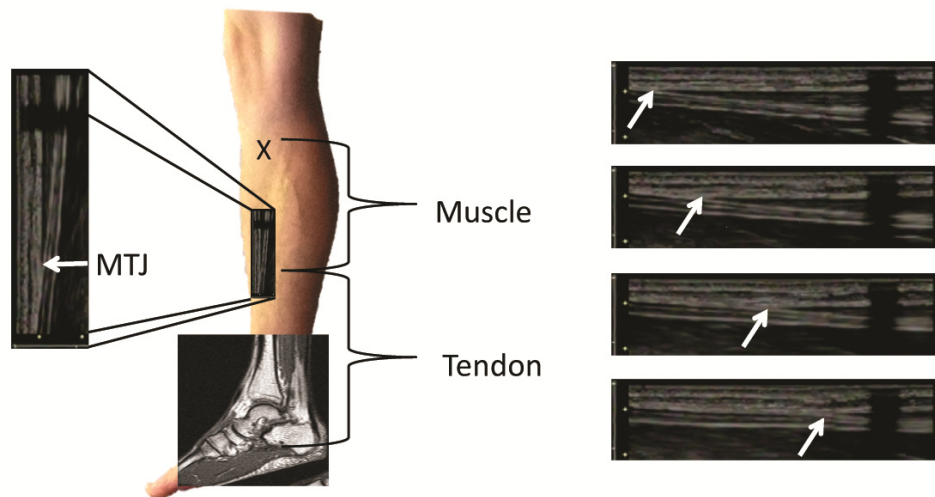
Figure 3.1: The muscle-tendon junction (MTJ; *left* and indicated by arrow at *right*) position change due to foot rotation was used to calculate the change in muscle length. The proximal head of the muscle (X) attaches directly to the tibia and thus was assumed to not move with foot rotation. Change in tendon length was calculated using magnetic resonance images of the ankle in different positions (see Fig. 3.2)

Processing Methods (TE)

Displacement of the MTJ (ΔMTJ) was manually digitised across all frames (50 Hz; Peak Motus, Peak Performance Technologies Inc., Colorado) and the data low-pass filtered with a sixth-order, zero-lag, Butterworth filter with a 1-Hz cut-off frequency. This filter was chosen based on the knowledge of the movement frequency being approximately 0.17 Hz, with analysis of the power density spectrum supporting this. Joint angle data were filtered using a 14-Hz low pass, fourth-order, zero-lag Butterworth filter (Winter, 2009). For each test, ΔMTJ was differentiated with respect to joint angle (θ) through the ROM over which constant angular velocity was achieved.

The moment arm was calculated using plantar- and dorsiflexion rotations separately, with differentiation being performed over a 2° angle range. Both ankle rotation directions were analysed in order to examine the potentially different effects of muscle and tendon stretch and hysteresis (Spoor et al., 1990). The moment arm values from all three rotations of the same direction (i.e. plantar- or dorsiflexion) were combined and a second-order polynomial was fitted to the moment arm-joint angle data to allow calculation of the moment arm at each angle. Moment arms derived using the TE method were named using the direction of rotation, i.e. TE_{PF} or TE_{DF}, for moment arms derived using plantar- or dorsiflexion rotations, respectively. Intra-experimenter reliability (digitisation of ultrasound video and subsequent processing of same data three times) of the digitising procedure was high (coefficient of variation = 7.4, 1.0, 2.1 and 2.0% for 30, 15, 0 and ⁻15°, respectively).

Previously, Fath and colleagues (2010) fitted both second- and third-order polynomials to the ΔMTJ–θ data and then differentiated these to estimate the Achilles tendon moment arm. During preliminary analysis, this method was found to not be suitable for the full ROM. The direction of the third-order polynomial, and thus the resultant second-order polynomial, was highly dependent upon the data at the end ROM; Fath et al. (2010) focussed their analysis of the moment arm on the neutral (0°) joint position. The second-order polynomial was not fitted to the ΔMTJ–θ data as differentiating this would result in a linear moment arm-angle relationship; previous research has shown the moment arm-angle relationship to be non-linear for the TA (Ito et al., 2000; Maganaris, 2000; Spoor et al., 1990). Furthermore, differentiation ranges up to 30° have been used for estimation of the moment arm using the TE method (Ito et al., 2000; Maganaris, 2000). During preliminary analysis, although differences in estimated moment arms were less than 3 mm (maximum difference between differentiation ranges for n=8) when differentiation ranges of 2, 4, 10, 20 and 30° were used, the intra- (three tests where subjects remained seated in the dynamometer and the ultrasound probe remained in place) and inter-test (three tests where the subject was removed from the dynamometer and the ultrasound probe removed before each repeat test) reliabilities were improved when the smaller ranges were used. Thus a 2° differentiation range was used for the TE method for the main analysis.

Tendon Elongation

In previous studies in which the TE method was employed *in vivo*, the change in position of the TA MTJ was differentiated with respect to foot angle (Ito et al., 2000; Maganaris, 2000), allowing the authors to only account for length change proximal to this point. Therefore, if a change in length of the tendon occurred during the passive rotation, an error in the estimated moment arm would occur. The change in tendon length was therefore calculated in the present study by subtracting the change in muscle length (measured from the ultrasound images; Fig. 3.1) from the change in MTU length (measured from MRI scans, described below and shown in Fig. 3.2). As the proximal insertion point of the MTU did not move during testing, any change in MTU length would be caused by rotation of the ankle. Using the MRI scans and a DICOM viewer (OsiriX; version 3.7.1; US) the tendon was tracked through 3-D space from the most distal insertion point on the medial cuneiform to 5 cm proximal to the distal head of the tibia (located in the MRI slice in which the TA tendon passed anterior to the tibia head; see Fig. 3.2) at each joint position. The change in length of the tendon across successive joint rotations was accepted as the change in MTU length due to ankle rotation. Muscle length change can be considered equal to the change in MTJ position recorded from the ultrasound because the distal end of the muscle moves during ankle rotation whilst the proximal head is directly fixed to the stationary tibia. The change in tendon length was calculated by subtracting the change in muscle length from the change in MTU length for each 15° rotation (Fig. 3.1). The moment arm was then estimated using the TE method using the change in MTU length instead of the change in MTJ position to correct for potential changes in tendon length (TE corrected; TE_{CORR}).
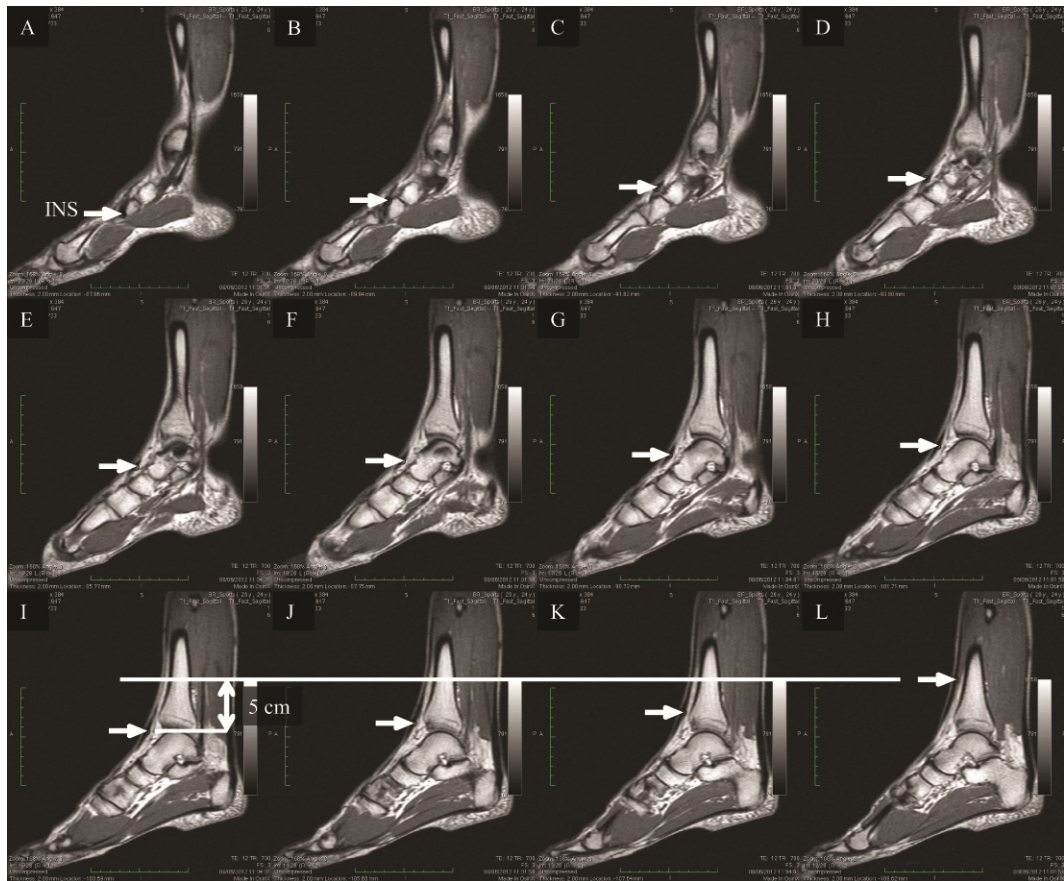
Figure 3.2: The tibialis anterior tendon was tracked (centroid of each tendon slice indicated by white arrow) from the most distal insertion point (INS: image A) on the medial cuneiform to 5 cm proximal (image L) to the distal head of the tibia. The point on the tibia head was located in the MRI slice (image I) in which the TA tendon passed anterior to the tibia head. The change in length of the tendon across successive foot rotations (45, 30, 15, 0 and ⁻15° plantar flexion) was used as the change in MTU lenth due to foot rotation. The change in MTJ position (see Fig. 3.1) was subtracted from the change in MTU length due to foot rotation to calculate tendon length change.

Geometric Method

For the GEO method, magnetic resonance imaging (MRI) scans were taken of the ankle joint as described by Fath et al. (2010). The subject rested supine within the MRI scanner (Siemens Magnetom Trio syngo MR 2004A, Erlangen, Germany). Localising scans were performed to determine the orientation of the lower leg before sagittal plane images (TR = 600 ms, TE = 12 ms, 3 excitations, 300 mm field of view, 2 mm slice thickness, 25 slices) were taken of the foot, ankle and lower leg. The foot was securely strapped to specifically shaped wooden blocks that ensured the ankle joint was held at the required foot angle, with scans being taken at 15° increments from 45° (plantarflexion) to ⁻30° (dorsiflexion) to allow for the moment arm to be calculated at

30, 15, 0 and ⁻15°. All procedures and analyses for the geometric method were located in 2-D in the sagittal plane.

Processing Methods (GEO)

Moment arm calculation involved two stages: (1) determining the location of the COR using the geometric method presented by Reuleaux (Reuleaux & Kennedy, 1876), and (2) measuring the perpendicular distance between the COR and the line of action of the tendon (Fath et al., 2010; Maganaris, 2004). All processing was performed using a DICOM viewer (OsiriX; version 3.7.1; US) and a custom MATLAB program (v. R2011b, Mathworks, USA).

Changes in position of the talus from 45-15°, 30-0°, 15-⁻15° and 0-⁻30° were used to calculate the COR for 30, 15, 0 and ⁻15° joint angles, respectively. The tibia was assumed to be the stationary segment with the rotation of the talus representing the rotation of the foot. One point was placed anteriorly (T_1) and one point posteriorly (T_2) to the talus in the neutral image. The talus outline and points were then traced and superimposed onto all subsequent images. The coordinates (assigned by the Osirix software) of these points (T_1 and T_2 for all angles) were then exported into MATLAB where the COR was calculated. The perpendicular bisector of the two T_1 points from the foot position 15° either side of the ankle angle of interest was calculated geometrically. This was repeated for the two T_2 points, with the point at which these two perpendicular bisectors met being taken as the COR. Here we used the foot angle to create the angular distances, and subsequently to model the talus rotation, in line with previous studies (Maganaris, 2000; Rugg et al., 1990). Because foot rotation and talus rotation may not be synonymous (Chen et al., 1988; Lundberg et al., 1989; Siegler et al., 1988), a second approach was also used (see below).

The TA tendon travels along a curved path anterior to the ankle. As such, the true line of action of the TA tendon force can be difficult to determine. To maintain consistency with previous studies (Maganaris et al., 1999; Rugg et al., 1990), the action line of the TA was modelled as a straight line connecting the proximal and distal points on the tendon slice at the retinaculum. The perpendicular distance (calculated geometrically using the coordinates of the COR and the two points locating the tendon line of action) from the TA action line that passed through the centre of rotation was recorded as the

moment arm. Processing of data at each angle was performed three times with the mean being taken as the moment arm (GEO retinaculum; GEO_{RET}). The mean ± SD coefficients of variation (CV) across subjects for each angle were 6.2 ± 3.2, 3.6 ± 1.6, 4.9 ± 4.1 and 3.3 ± 2.1% for 30, 15, 0 and ⁻15°, respectively.

Talus vs. Foot Rotation

An important assumption underlying the use of the GEO method is that the magnitude of foot rotation is synonymous with talus rotation, which may not be accurate (Chen et al., 1988; Lundberg et al., 1989; Siegler et al., 1988). The rotation of the talus was therefore examined in relation to the change in foot angle by measuring the angle between the line connecting T_1 and T_2 (Fig. 3.3) for successive 15° foot rotations relative to the tibia. This was repeated three times for each rotation with the mean being used for analysis (mean ± SD CV across subjects for each rotation was 8.2 ± 5.0, 6.5 ± 3.7, 5.2 ± 2.1, 6.4 ± 2.5 and 8.8 ± 4.8% for the 45-30°, 30-15°, 15-0°, 0-⁻15° and ⁻15-⁻30° rotations, respectively). To assess the effect that a discrepancy between the talus rotation and foot rotation has on the estimated moment arm, the GEO_{RET} method calculations were repeated using the change in talus angle instead of change in foot angle (retinaculum line of action with talus correction; $GEO_{RET,TAL}$) to determine COR. Because MRI scans were only taken at 15° foot angle increments, a 2nd order polynomial was fitted to the coordinates of T_1 and T_2 against talus angle (R^2 [mean ± SD] = 0.99 ± 0.02 and 0.98 ± 0.04 for T_1 and T_2, respectively). These curves were then used to determine the location of the talus markers at any talus angle. The centre of rotation at 30, 15, 0 and ⁻15° ankle angles were then calculated (Reuleaux method; see above) using the rotation of T_1 and T_2 from the talus position 15° either side of the talus angle at the ankle angle of interest. Using this new COR, the moment arm was then calculated, as above, using the straight line connecting the proximal and distal points on the tendon slice at the retinaculum. This was performed three times for each moment arm estimation, with mean ± SD CVs across subjects for each angle of 3.7 ± 2.2, 2.5 ± 1.2, 2.4 ± 1.4 and 2.0 ± 1.3% for 30, 15, 0 and ⁻15°, respectively.
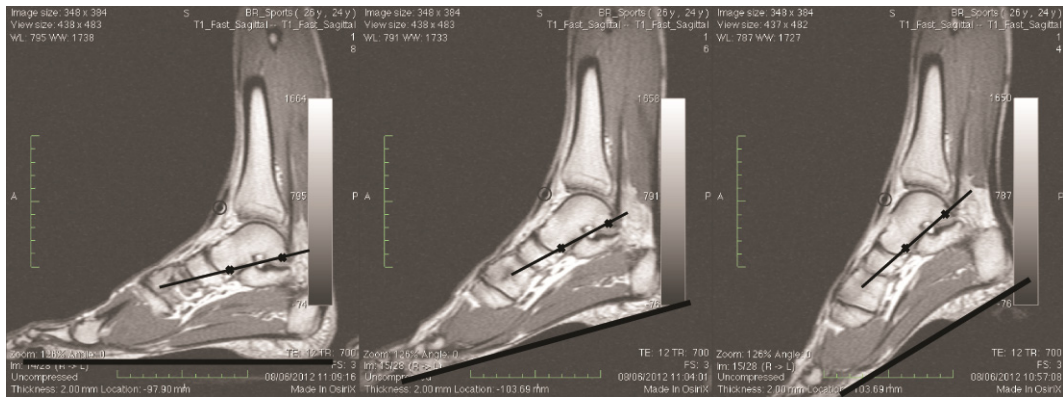
Figure 3.3: The rotation of the talus was examined in relation to the rotation of the foot across all ankle angles (only three shown). The rotation of the talus was modelled using a line connecting two points; one point placed anteriorly and one point placed posteriorly to the talus in the neutral image (*left*). The foot rotation was modelled using a line placed over the sole of the foot.

Tendon Line of Action

As presented above, the line of action of the TA tendon force was estimated from the point of which it passes the extensor retinaculum. In fact, the TA tendon curves anteriorly past the ankle and, therefore, this location may not be valid. We therefore investigated the effect on the estimated moment arm of using a line of action taken near the insertion of the tendon on the foot. For this purpose, the centroid of the tendon slice was manually located within the three MRI slices proximal to the slice in which the insertion first became observed (see Fig. 3.4). This resulted in the mean ± SD tendon segment lengths (distances between the centroid of the tendon within the first and third MRI slice used) being 18.4 ± 5.9, 17.0 ± 5.6, 17.7 ± 4.7 and 16.8 ±3.9 mm for the 30, 15, 0 and ⁻15° foot angles, respectively. A linear fit was applied to the 2D coordinates (sagittal plane) of the centroids from the three MRI slices, which acted as the new line of action. The moment arm was geometrically calculated as the perpendicular distance between the new line of action and the COR, using either the COR estimated using the original method (GEO insertion; GEO_{INS}) or the talus correction method (TAL insertion; $GEO_{INS,TAL}$). This was performed three times for each moment arm estimation, with mean ± SD CVs across subjects for each angle of 7.1 ± 2.8, 5.0 ± 2.5, 6.0 ± 4.1 and 3.0 ± 1.8% for GEO_{INS} and 4.9 ±3.3, 3.0 ± 1.8, 3.8 ± 2.4 and 2.7 ±1.8% for $GEO_{INS,TAL}$ for 30, 15, 0 and ⁻15°, respectively.
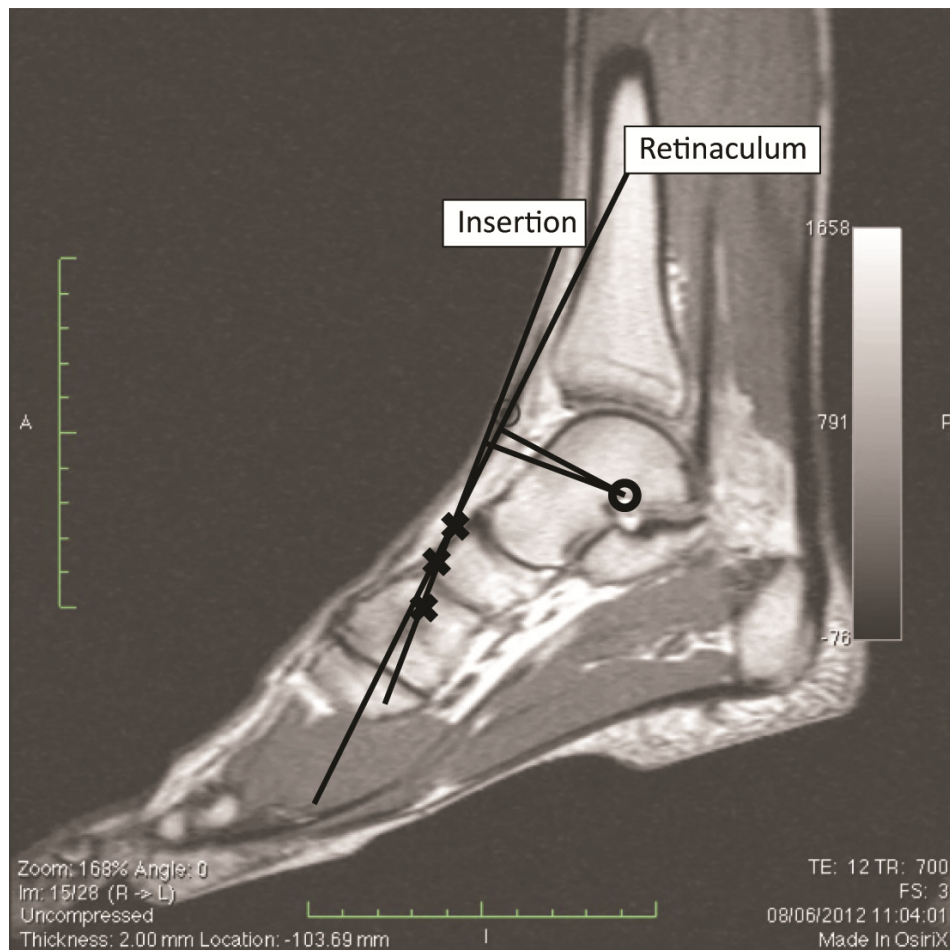
Figure 3.4: Two approaches to modelling the line of action of the tibialis anterior tendon were used. The first used a straight line connecting the proximal and distal points on the tendon slice at the retinaculum (labelled *Retinaculum*). The second (labelled *Insertion*) modelled the line of action as a linear fit being fitted to the 2D (sagittal plane) coordinates of the centroid of the tendon slice within the three MRI slices proximal to the slice in which the insertion first became observed.

Statistical Analysis

The effect of rotation direction on moment arm estimate using the TE method (i.e. TE_{PF} vs. TE_{DF}) was analysed using a two-way ANOVA with repeated measures (2 × 4; direction × angle). Least significant difference post-hoc pairwise comparisons were used at each angle following a significant interaction.

The difference in change in length of the muscle and tendon was assessed using a 2 × 5 (tissue × angle) repeated measures ANOVA. Planned repeated comparisons were performed following a significant interaction effect to locate the angle ranges in which length change differed between the muscle and tendon. To determine the joint range over which the muscle and tendon were lengthening, a one-way repeated measures

ANOVA was performed for each tissue, with repeated planned comparisons being used to establish over which range the length change was occurring.

Differences between foot rotation (set to 15° using wooden blocks) and talus rotation were assessed using a one-sample t-test for each rotation. Consistency of talus rotation across the range of motion, which is required for the Reuleaux method, was assessed using a one-way repeated measures ANOVA. Planned repeated comparisons were performed comparing talus rotations over consecutive 15° ankle rotations.

To assess the effect of different methodological approaches to the tendon excursion (TE) method on moment arm estimations, a two-way ANOVA (3 × 4; method × angle) was used. The uncorrected moment arms were derived from the dorsiflexion and the plantar flexion directions separately, which were compared with the corrected TE method. For the geometric (GEO) method, the effect of different methodological approaches was assessed using a two-way ANOVA (4 × 4; method × angle). The individual and combined effects of accounting for talus rotation and the alternative location of the line of action were assessed for the GEO method. Significant interactions within the two-way ANOVAs were followed up with Bonferroni corrected one-way ANOVAs at each of the four angles. Significant main effects of method within either the two-way (if interaction was not significant) or one-way ANOVA were followed up with simple planned comparisons between moment arm estimates before and after accounting for the individual assumptions, i.e. TE_{PF} v TE_{CORR} and TE_{DF} v TE_{CORR} for the tendon excursion approach, and GEO_{RET} v $GEO_{RET,TAL}$, GEO_{RET} v GEO_{INS} and GEO_{RET} v $GEO_{INS,TAL}$ for the geometric approach.

A two-way ANOVA with repeated measures (5 × 4; method × angle) was used to investigate the effect of the assumptions on the agreement between TE and GEO moment arm estimates. Follow-up analyses were similar to above, with Bonferroni corrected one-way ANOVA at each angle. Simple planned comparisons (TE_{PF} v GEO_{RET}, TE_{DF} v GEO_{RET}, TE_{CORR} v $GEO_{INS,TAL}$) were performed following a significant main effect of method within either the two-way (if interaction was not significant) or one-way ANOVA. The consistency between the TE and GEO methods before and after accounting for the individual assumptions was assessed using a two-way random intraclass correlation with absolute agreement (de Vet, Terwee, Knol, & Bouter, 2006).

Effect sizes (ES) were calculated using Cohen's *d*. The pooled SD was used as the standardizer, being calculated as the square root of the mean variances (Cohen, 1988; Fritz, Morris, & Richler, 2012). The Greenhouse-Geisser correction was used in some instances where the assumption of sphericity was violated within the ANOVA (assessed using Mauchly's test of sphericity). Statistical significance was accepted at $p < 0.05$. Data are presented as mean ± SD.

RESULTS

Tendon Excursion Method

Effect of Direction of Ankle Rotation

A significant interaction of rotation direction (TE_{PF} vs. TE_{DF}) and angle was evident (interaction effect: $p = 0.047$), with moment arm estimates being similar at 30° ($p = 0.27$), 15° ($p=0.49$) and 0° ($p = 0.41$) between TE_{PF} and TE_{DF}, but moment arms obtained using TE_{PF} were larger than those obtained using TE_{DF} at ⁻15° (ES = 0.84, $p = 0.045$). Both TE_{PF} and TE_{DF} were used for subsequent comparison with TE_{CORR} and $GEO_{INS,TAL}$ because of this difference in estimated moment arms.

Tendon Length Change

The TA muscle and tendon both lengthened as the ankle was plantarflexed. However, most of this length change occurred in the muscle (Fig. 3.5). Specifically, muscle length increases were greater than the tendon for the ⁻15-0 (ES = 4.6, $p < 0.001$), 0-15 (ES = 4.7, $p < 0.001$) and 15-30° (ES = 1.3, $p = 0.1$) rotations. Towards the end of the rotation (30-45°), more of the increase in MTU length was taken up by the tendon (ES = 1.2, $p = 0.09$). As such, measurement of MTJ displacement was considered not to be a valid representation of the displacement of the tendon insertion.
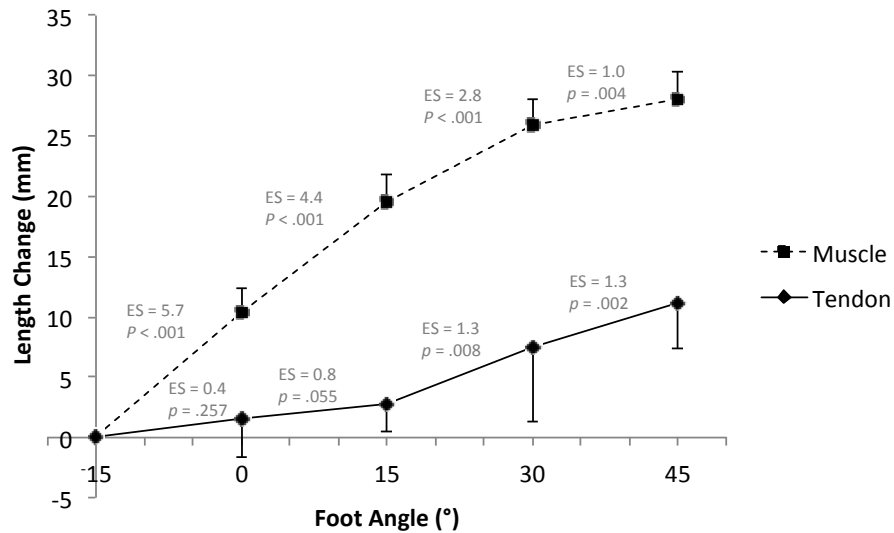
Figure 3.5: Tibialis anterior muscle and tendon length change during passive foot rotation (¯15° dorsiflexion to 45° plantarflexion at 20°·s⁻¹). The length change is reported relative to the length at 15° dorsiflexion. Effect sizes (ES) show the change in length for each tissue across 15° rotations. The change in muscle length was greater than the change in tendon length for ¯15-0 ($p < 0.001$), 0-15 ($p < 0.001$), and 15-30° ($p = 0.1$) rotations, but tendon lengthening was greater for the 30-45° rotation ($p = 0.094$).

Tendon length change (relative to -15°) $= 0.00304 \times \theta^2 + 0.09443 \times \theta + 0.79592$; ($R^2 = 0.999$), where $\theta =$ foot angle; accuracy to five decimal places is required for accurate estimation.

Geometric Method

Talus Rotation

Talus rotation was not consistent across the 15° ankle rotation increments ($p = 0.042$), and was always less than 15° ($p < 0.05$). Although differences between successive rotations were not significantly different (planned repeated comparisons), moderate to large effect sizes were calculated between the ¯30-¯15 and ¯15-0° (ES = 0.65, $p = 0.28$), 0-15 and 15-30° (ES = 0.83, $p = 0.16$), and the 15-30 and 30-45° (ES = 0.99, $p = 0.096$) rotations (Fig. 3.6). Therefore, the change in angle between the sole of the foot and the tibia shaft (i.e. foot angle) cannot be used to represent the change in the talucrural joint angle (i.e. talus rotation).
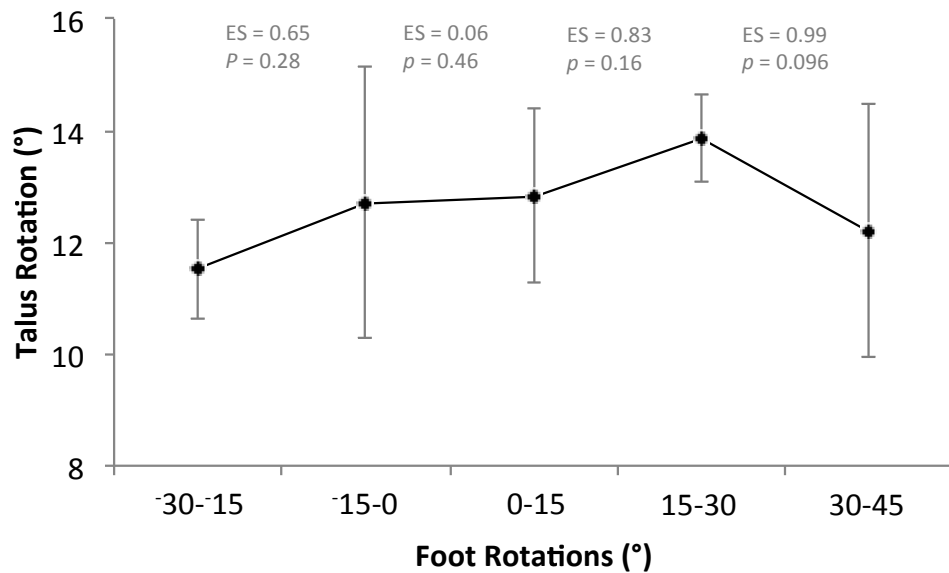
Figure 3.6: Talus rotation resulting from each 15° foot rotation across the ROM. Effect sizes (ES) indicate differences in rotation of the talus for successive 15° foot rotations.

Agreement between TE and GEO Methods and the Effect of Different Methodological Approaches

Accounting for each of the three methodological variations (tendon length change, TE_{CORR}; talus rotation, $GEO_{RET,TAL}$; location of the line of action, GEO_{INS}) had different effects on the estimated moment arm (Fig. 3.7). For the TE method, estimates of moment arm after accounting for tendon length changes (TE_{CORR}) were larger than moment arm estimates using either TE_{PF} or TE_{DF} ($p = 0.001$ for both). The effect of accounting for tendon lengthening was similar for TE_{PF} and TE_{DF} at 30, 15, and 0°, but not at ⁻15° where there was a larger effect for TE_{DF} compared to TE_{PF} (ES = 1.02 and 0.20, respectively; Fig. 3.7), although this interaction effect did not reach significance ($p = 0.051$).

Accounting for either talus rotation ($GEO_{RET,TAL}$), an alternative line of action (GEO_{INS}), or both ($GEO_{INS,TAL}$) within the GEO approach did not significantly alter the moment arm estimates (main effect $p = 0.48$; interaction effect $p = 0.15$). However, estimates made at ⁻15° did produce moderate to large effect sizes when sources of error were accounted for. Specifically, moment arm estimates were smaller after accounting for talus rotation, an alternative line of action, or both at ⁻15° (ES = 0.46, 0.58, and 0.89, respectively; Fig. 3.7).

43

Agreement between TE and GEO was assessed before (i.e. TE_{PF} v GEO_{RET} and TE_{DF} v GEO_{RET}) and after (i.e. TE_{CORR} v $GEO_{INS,TAL}$) accounting for assumptions. Before accounting for assumptions, agreement was poor at 30, 15, and ⁻15° when either TE_{PF} or TE_{DF} was compared with GEO_{RET} (Fig. 3.8). At 0°, although differences between the uncorrected TE and GEO methods were non-significant, moderate to large effect sizes were calculated (0.68, $p = 0.20$; and 0.92, $p = 0.11$; for TE_{PF} v GEO_{RET} and TE_{DF} v GEO_{RET}, respectively). Following correction for the three assumptions, agreement was good between TE_{CORR} and $GEO_{INS,TAL}$ for ⁻15° ($p = 0.80$), 0° ($p = 0.46$) and 15° ($p = 0.61$), although a large effect was seen at 30° (ES = 1.20, $p = 0.052$). There was an improvement in agreement between TE and GEO-derived moment arms at all angles after all assumptions had been accounted for (Fig. 8). However, despite the reduction in the magnitude of difference between the TE and GEO methods after assumption correction, the consistency (two-way random ICC with absolute agreement) between the TE and GEO methodologies was still poor for each angle (Table 3.1).

Although no significant differences were seen between TE_{CORR} and $GEO_{INS,TAL}$, visual inspection of the two curves (Fig. 3.8) shows differences in the relationship between moment arm and ankle angle. To assess the nature of this, each subject's individual moment arm–joint angle dataset was fitted with both a linear and second-order polynomial. The root mean square of the percentage difference (%RMS$_{diff}$) between the linear and second-order polynomials was then calculated for TE_{CORR} and $GEO_{INS,TAL}$, with a paired t-test being used to compare between the two methods. The use of a second-order polynomial improved the curve fit more for TE_{CORR} than $GEO_{INS,TAL}$ (ES = 1.00, $p = 0.094$). This indicates that the relationship between moment arm and ankle angle is more curvilinear when the moment arm is estimated using TE_{CORR} compared with $GEO_{INS,TAL}$.
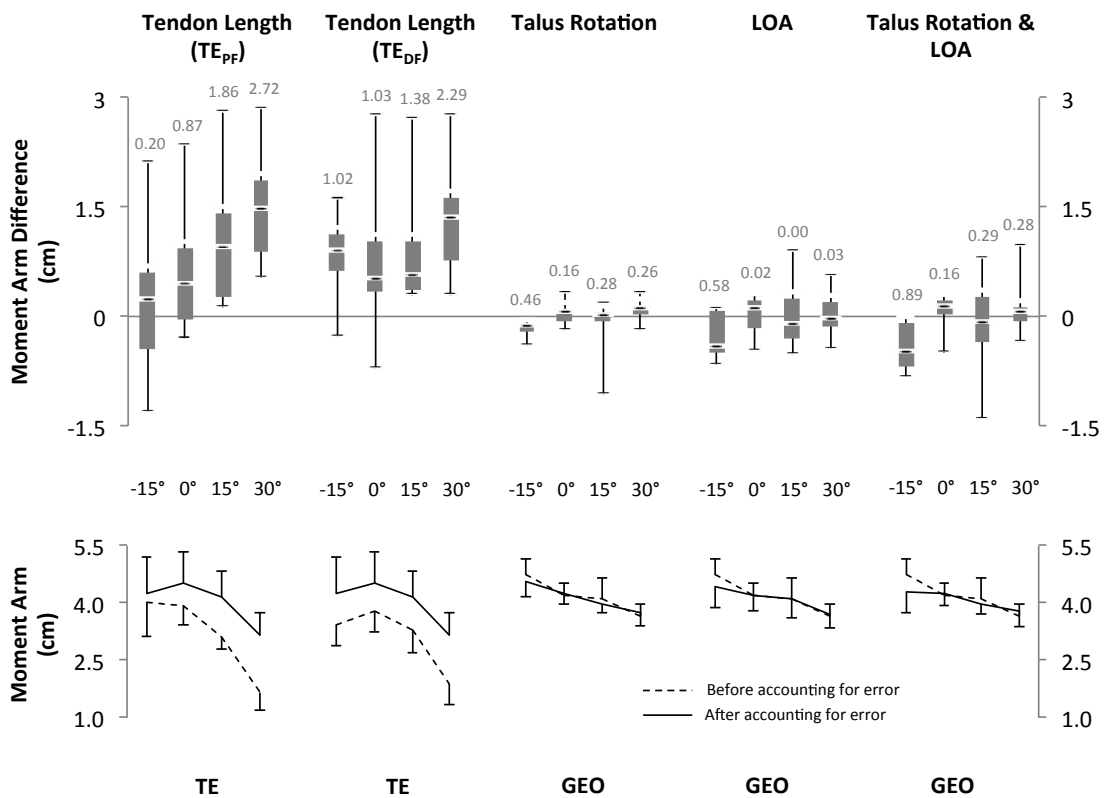
Figure 3.7: The effect of assumptions on TA moment arm estimates for TE and GEO methods. Overall, tendon length change affected moment arm values across all angles (TE; $p = 0.001$, main effect of method when change in MTJ was tracked during either plantar- [TE_{PF}] or dorsiflexion [TE_{DF}]) whilst talus rotation inconsistencies and changes in the location of the tendon line of action changed the moment arm estimate at ⁻15° (GEO). Effect sizes (shown above the box plot) show the standardised effect of accounting for the source of error at each angle. Box plots (top) show median (centre marker), $25^{th} - 75^{th}$ percentile range (box) and minimum and maximum (end of bars). Line graphs (bottom) show the mean and SD. When using the TE method, it may be more practical to track the MTJ during ankle rotation. If this method is employed, a moment arm correction to account for tendon length change is presented below. These provide the magnitude of difference between the mean moment arms estimated before and after tendon length change has been accounted for. Therefore, the output should be added to the estimated moment arm when the MTJ is tracked. For plantarflexion rotation = $0.00008 \times \theta^2 + 0.02770 \times \theta + 0.58850$ ($R^2 = 1.00$), and for dorsiflexion rotations = $0.0054 \times \theta^2 + 0.00243 \times \theta + 0.72550$ ($R^2 = 1.00$), where $\theta =$ foot angle (°; fitted using data between -15° - 30°, therefore caution must be employed when attempting to extrapolate).
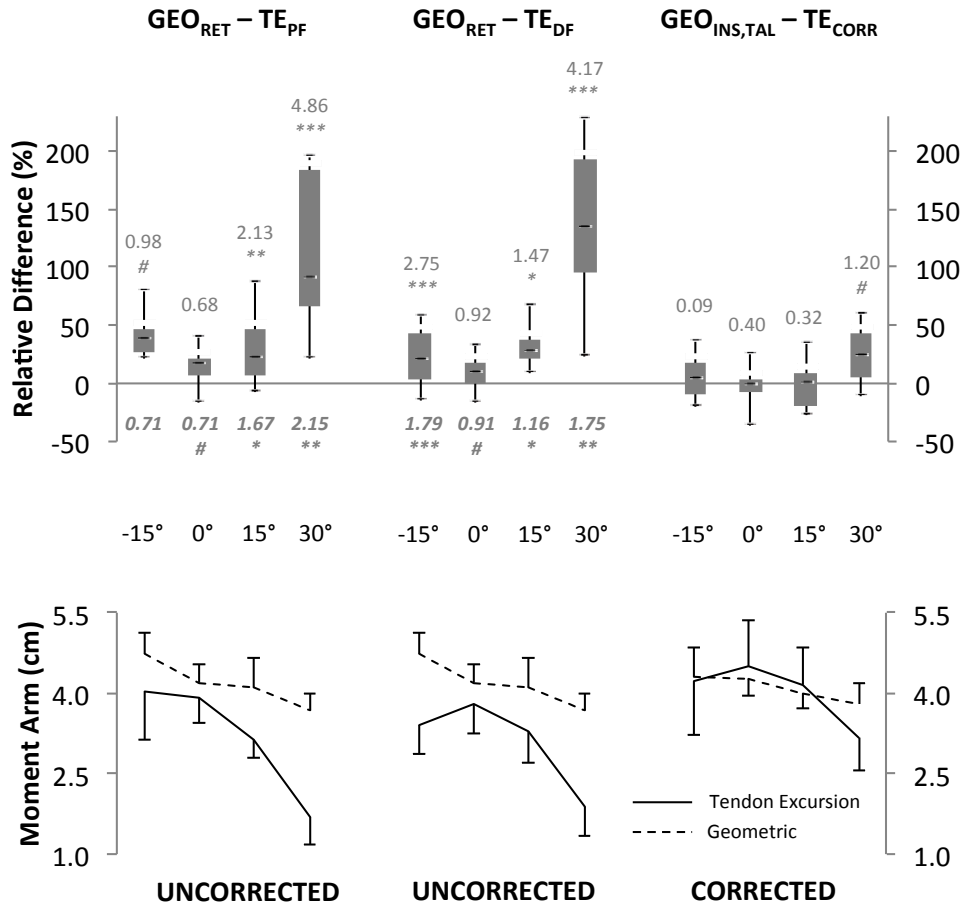
Figure 3.8: Agreement between the GEO and TE methods before (GEO_{RET}-TE_{PF} and GEO_{RET}-TE_{DF}) and after ($GEO_{INS,TAL}$-TE_{CORR}) accounting for sources of error. Agreement between the two methodologies was significantly improved after accounting for the three sources of error (tendon length change, talus rotation inconsistencies, and an alternative line of action). Effect sizes above the bars compare the difference between GEO and TE, and effect sizes below the bars compare the uncorrected and corrected differences between methodologies. # p <0.1; * p < 0.05; ** p < 0.01; *** p < 0.001.

Table 3.1: Two-way random ICC (95% confidence intervals) with absolute agreement between moment arms derived using the GEO and TE methods before (GEO_{RET}-TE_{PF} and GEO_{RET}-TE_{DF}) and after ($GEO_{INS,TAL}$-TE_{CORR}) accounting for methodological concerns. There was poor agreement across all comparisons.

Foot Angle	GEO_{RET}-TE_{PF}	GEO_{RET}-TE_{DF}	$GEO_{INS,TAL}$-TE_{CORR}
−15°	0.13	0.12	0.59
	(−0.31 − 0.67)	(−0.05 − 0.53)	(−0.19 − 0.90)
0°	0.08	−0.02	−0.03
	(−0.50 − 0.68)	(−0.46 − 0.59)	(−0.75 − 0.66)
15°	0.08	−0.09	−0.43
	(−0.10 − 0.49)	(−0.35 − 0.45)	(−1.01 − 0.42)
30°	−0.02	−0.02	−0.04
	(−0.05 − 0.14)	(−0.07 − 0.17)	(−0.37 − 0.53)

DISCUSSION

The first purpose of the present study was to determine the potential impact of different methodological approaches to the tendon excursion (TE) and geometric (GEO) methods on TA moment arm estimations.

With regards to the TE method we assessed the effect of movement direction as well as the effect of accounting for tendon length changes during the passive ankle rotation. TA moment arm estimations were larger at the most dorsiflexed position when the plantarflexion rotation was used, compared to the dorsiflexion rotation. In this condition, muscle length changes were assumed to be indicative of MTU length changes. However, MTU length changes (which are determined by changes in joint angle) were the same across both movement directions. Together, these results imply that differences in muscle length change between the rotation directions occurred simultaneously with differences in tendon lengthening. Whilst the muscle consists predominantly of the aponeurosis and fascicles, the TA aponeurosis does not change length during a passive rotation (Tilp et al., 2011). As such, the smaller muscle length change during the dorsiflexion rotation is likely due to a greater reduction in fascicle stiffness compared to tendon stiffness following the stretch caused by the plantarflexion rotation. Support for this suggestion comes from Morse et al. (2008) who showed that

47

stiffness of the fascicles is reduced following a prolonged stretch, whilst tendon stiffness is not significantly affected. Therefore, the larger TA moment arm estimated using the plantarflexion rotation compared to the dorsiflexion rotation is likely due to a greater hysteresis within the muscle fascicles compared to the tendon.

The second methodological issue within the TE methodology that we examined was how moment arm estimations would change when changes in tendon length are accounted for. In the current study, as in previous studies (e.g. Ito et al., 2000; Maganaris, 2000), the MTJ displacement was tracked in order to estimate MTU length change when using TE. However, this allows only the change in length of tissues proximal to this point (i.e. the muscle belly) to be measured and neglects any potential tendon lengthening (Herbert et al., 2002). Indeed, we found a significant tendon elongation during the passive joint rotations, which is consistent with results from Herbert et al. (2002). Accordingly, TA moment arms were ~40% larger when tendon length was accounted for compared to the uncorrected method.

When the TE method has been used in cadaveric studies, the tendon is commonly loaded with a constant mass during the joint rotation (Boyd & Ronsky, 1998; Hughes et al., 1998; Spoor & van Leeuwen, 1992). Because the load is constant the tendon would not likely have elongated during the joint rotation. However, using the present *in vivo* methodology*,* the rotating segment pulls on the tendon, causing a stretch of increasing magnitude (Fig. 3.5). Ito et al. (2000) used the TE method both without muscle activation and whilst the subjects contracted at 30 and 60% MVC. Interestingly, the moment arms reported by Ito et al. (2000) in the passive condition were smaller than the uncorrected moment arms (i.e. TE_{PF} and TE_{DF}) in the present study, whilst the moment arms reported during the active rotations within Ito's study are very similar (particularly at 30, 15 and 0°) to our moment arms that took tendon elongation into consideration (i.e. TE_{CORR}). This indicates that moment arms in Ito's experiment were only similar to our TE_{CORR} estimates when the tendon was elongated by loading, and therefore less likely to elongate during joint rotation. Whilst some of this change could be attributed to a straightening of the tendon during loading (Ito et al., 2000), which would have increased the tendon's distance from the joint centre of rotation, it is possible that tendon loading might be a useful strategy to minimise the effects of tendon lengthening during joint rotation. It would therefore be interesting to examine the validity and

48

reliability of moment arm estimations obtained during constant muscular contractions in the future.

Of all the methodological variations investigated within the current study, the incorporation of tendon length change into the TE method had the greatest effect on moment arm estimations. Therefore, tendon length change should be taken into account when using the TE method to estimate TA moment arms. Acknowledging that this can be experimentally difficult, we developed a regression equation to predict differences in corrected vs uncorrected moment arm as a function of ankle angle. The mean difference in estimated moment arms between the corrected and uncorrected TE approaches were modelled using a second-order polynomial (see Fig. 3.7 legend for equations). Whilst our R^2 values indicate a very good fit, caution should be taken when using the equation as inter-individual differences in muscle-tendon dimensions and mechanical properties exist.

With regards to the GEO method we assessed whether change in foot angle was indicative of change in talus angle and whether the method of modelling the tendon line of action would affect moment arm estimates. We found that talus rotation was not indicative of foot rotation. Previously, a non-linear relation between talus and foot rotation has been reported in cadaveric (Chen et al., 1988; Siegler et al., 1988) and *in vivo* (Lundberg et al., 1989) studies. We have found that for a given foot angular displacement talus angular displacement was noticeably smaller. Importantly, talus rotation per degree of foot rotation was not consistent across the ROM (Fig. 3.6). When this discrepancy was accounted for, we found moderate changes in TA estimates at the most dorsiflexed ankle angle. Because the magnitude of rotation of the talus relative to the foot is due to the material properties of ligaments and other tissues (Chen et al., 1988), the reduced rotation at the end of the ROM is likely due to a greater stiffness within these tissues upon stretch. As such, when employing the GEO method to derive TA moment arms, it is advisable to use a constant talus angular displacement around the foot position of interest (as opposed to a constant foot angular displacement).

We also found that for the GEO method, the location of the line of action (i.e. retinaculum vs insertion) affected the moment arm estimates at the most dorsiflexed angle. When the GEO method has been used previously, the TA tendon line of action has been taken as the line bisecting the tendon as it passes under the extensor

retinaculum (Maganaris et al., 1999; Rugg et al., 1990). However, due to the non-linear path of the TA tendon between its insertion and its intersection with the extensor retinaculum, this line of action may not be representative of that measured at the insertion; i.e. the point where the force is applied to the foot segment. Indeed, the way the tendon line of action was modelled resulted in differences in TA moment arm estimates. This was mostly evident at the more dorsiflexed angle (⁻15°; effect size = 0.58) where a greater TA tendon curvature is evident due to the more acute angle between the foot and tibia. Although the line of action located at the tendon insertion into the foot appears more appropriate, future studies need to address the validity of this.

The second aim of this study was to examine the impact of the different methodological approaches on agreement between moment arms obtained from TE and GEO methods. When the uncorrected methodologies were used, the TE-derived moment arms were ~27% smaller than GEO-derived moment arms, which is consistent with results form previous studies which indicated significant differences between moment arms derived from TE and GEO methodologies (Fath et al., 2010; Maganaris, 2000; Maganaris et al., 2000; Wilson et al., 1999; Zhu et al., 1997).

These method-related discrepancies raise the question about validity. Currently, there is no agreement on which methodology (TE or GEO) is the most valid. One approach to determine validity is to examine the agreement between different methodologies (i.e. convergent validity), with a better agreement suggesting a higher degree of validity. Therefore, we examined how the above mentioned variations in the TE and GEO methodologies would affect the agreement between the two approaches. We found that differences in moment arms between the uncorrected methods largely disappeared when tendon length changes were accounted for within TE, and retinaculum rotation was used with the line of action being modelled at the TA insertion for GEO (Fig. 3.8). Using the approach of convergent validity, one could argue that the moment arms derived from the corrected methods (TE_{CORR} and $GEO_{INS,TAL}$) yielded more accurate moment arm estimates.

Although accounting for tendon elongation within the TE method had the largest effect on moment arm estimations, it is important to acknowledge that a lack of accounting for tendon elongation during joint rotation does not fully explain the difference in moment

arm magnitudes between the TE and GEO methods reported in the current and previous studies. For example, cadaver studies utilising both methods have shown variations (Boyd & Ronsky, 1998), no difference (Spoor & van Leeuwen, 1992), and larger (Hughes et al., 1998) TE-derived moment arms when compared to GEO-derived moment arms, whilst *in vivo* TE-derived moment arms have been found to be smaller (Fath et al., 2010), larger (Wilson et al., 1999; Zhu et al., 1997) or similar (Maganaris, 2000; Maganaris et al., 2000) to those derived using GEO. If tendon elongation in the TE method was the only cause for the reported differences, then TE-derived moment arms would always be smaller than those estimated using the GEO method. The different moment arm estimations that have been observed between the uncorrected TE and GEO methods (i.e. Fath et al., 2010; Maganaris, 2000; Maganaris et al., 2000; Wilson et al., 1999; Zhu et al., 1997) are therefore likely due to a combination of the methodological variations addressed within the current study.

These findings demonstrate that accounting for various assumptions significantly affect TA moment arm estimates and the agreement between TE and GEO methods, which has direct implications for future research. In particular, when employing the TE method, we recommend accounting for tendon elongation. For the GEO methodology, the line of action should be modelled at the tendon insertion, with an equidistant talus angular displacement being used around the ankle angle of interest.

Relationship Between Moment Arm and Ankle Angle; TE v GEO

Although moment arm estimates were similar between the TE_{CORR} and $GEO_{INS,TAL}$ methods, the shape of the relationship between moment arm and ankle angle was different (curvilinear [TE_{CORR}] v linear [$GEO_{INS,TAL}$]). Rotation of the ankle joint complex occurs simultaneously around the subtalar and talocrural axes (Dettwyler, Stacoff, Kramers-de Quervain, & Stüssi, 2004; Leitch, Stebbins, & Zavatsky, 2010), neither of which results in rotation strictly in the sagittal plane. As such, the use of a single point to represent COR (used within GEO method) may not be appropriate (Zatsiorsky & Prilutsky, 2012). The TE method does not require estimation of COR and therefore is not susceptible to such errors. A further explanation for the difference in moment arm–joint angle relationship between the two methods is that the TE_{CORR} method estimates the moment arm in three dimensions, whereas the $GEO_{INS,TAL}$ estimates the moment arm only in two dimensions (sagittal plane). Previously, Hashizume et al. (2011) found the GEO-derived Achilles moment arm to change

linearly with angle when measured two dimensionally, but to have a curvilinear relationship with angle when measured in three dimensions (Fig. 4 in Hashizume et al., 2011). Unfortunately, Hashizume et al. did not compare the GEO and TE methods as they deemed the TE method to be invalid due to the estimated moment arms being smaller (based on their interpretation of Fath et al., 2010). Interestingly, the estimated 3D geometric moment arms were also smaller than the 2D geometric moment arms in their study (Hashizume et al., 2011). Therefore, the TE method (corrected for tendon lengthening; i.e. TE_{CORR}) could be more valid than the GEO method for determining the 3D moment arm *in vivo*, especially when the tendon traverses multiple joints.

Conclusions

In summary, we found that TA moment arm estimates were smaller when calculated using the TE method (ultrasound) compared to the GEO method (MRI), although several sources of error affected each method's estimate of the TA moment arm. Differences between TE- and GEO-derived moment arm estimates were removed after accounting for the tendon lengthening in the TE method as well as the talus rotation and line of action errors in the GEO method; these violations should thus be accounted for in future studies. According to the present results, however, the ideal methodology is to measure whole MTU length change in the TE method. If the complex methodologies required for this are not available, the ultrasound-based TE method may be used with a correction factor being applied to account for tendon lengthening.

Application to Musculoskeletal Modelling

The TA muscle plays an important role in a range of human movements (Cappellini et al., 2006). However, previous investigations have focused predominantly on the measurement of muscle activation. To fully understand the TA's role during movement the estimation of its force *in vivo* is vital. As *in vivo* forces during movement are typically derived from joint moments, an accurate knowledge of TA moment arms is essential. Thus, results from our study will allow researchers to estimate TA forces more accurately, which in turn may increase our ability to optimise performance (Cappellini et al., 2006; Chumanov et al., 2012) or to reduce injury (Blackman, 2000; Byrne et al., 2007).

Chapter Four

Correcting for Triceps Surae Co-Contraction During Isometric Dorsiflexion Contractions

ABSTRACT

When estimating dorsiflexor moment from ankle joint moment, it is common for co-contraction of the plantar flexors to be accounted for using plantar flexor EMG as an indirect measure of plantar flexor force, and thus moment. The aim of the present study was to determine the optimal method for correcting for plantar flexor antagonist co-contraction across the ankle joint ROM using joint moment-EMG relationships. A series of slow ramped maximal isometric plantar flexor contractions were performed across the range of motion. The moment-EMG relationships were modelled using linear and curvilinear fits, with an optimisation approach used to investigate the optimal EMG-processing procedures. Accuracy of the models were equivalent when the plantar flexors were modelled using soleus or the triceps surae. There were no differences found between a linear or curvilinear fit. Further, the change in the slope of the linear model can be modelled across joint angle with good accuracy using a 2nd-order polynomial, allowing plantar flexor moment to be estimated throughout all angles and intensities. Finally, individually optimised EMG-processing did not provide a better model than when group optimised EMG-processing was used.

INTRODUCTION

The dorsiflexor muscle group (consisting of tibialis anterior, extensor hallucis longus, extensor digitorum longus, and peroneus tertius) plays an important role in general human movement (Cappellini et al., 2006). The loading of these muscles has been suggested to be a determining factor in the walk-to-run transition speed (Bartlett & Kram, 2008; Hreljac et al., 2008) and the work performed by them has been proposed to play a causal role in disabling conditions such as chronic anterior compartment syndrome (Blackman, 2000; Tweed & Barnes, 2008; Zhang, Rennerfelt, & Styf, 2012). To further develop our understanding of the importance of the dorsiflexor muscle group in locomotion and injury contexts, it is necessary to obtain a detailed picture of its force production profile. It is, however, not currently possible to do this with a high precision with non-invasive methodologies.

Current non-invasive methods (e.g. isokinetic dynamometry; Albracht & Arampatzis, 2013; Mademli et al., 2004, and inverse dynamics; Bezodis, Kerwin, & Salo, 2008) quantify only the resultant joint torque (defined here as the resultant rotational force applied about the joint centre's axis) and do not allow for the direct measurement of the opposing agonist and antagonist joint moments (defined here as the contribution of forces acting at a distance from the joint centre and tending to rotate the joint; i.e. plantar- and dorsiflexor moments). Dorsiflexor muscle activation tends to elicit simultaneous plantarflexor co-contraction, counteracting the agonist (dorsiflexor) action (Arampatzis et al., 2005; Billot et al., 2010; Maganaris et al., 1998; Simoneau et al., 2009). Importantly, correcting for plantar flexor activity during dorsiflexion significantly alters the estimated moment and thus any conclusions drawn regarding its action (Billot et al., 2010). Clearly, the development of methods that allow for accurate correction for the antagonist (plantarflexor) moment are of significant practical importance.

Estimation of the antagonist moment generated during a dorsiflexion (agonist) contraction is commonly achieved by: (1) obtaining the relationship between joint torque and the plantar flexor surface electromyogram amplitude (EMG) during an isometric plantarflexion contraction, and (2) inferring the likely antagonist moment from the EMG signal obtained during the dorsiflexion contraction. In the simplest version of this method, the ratio between MVC torque and the maximum EMG amplitude is quantified and the relationship assumed constant for all contraction levels

(MVC-EMG$_{max}$ method; Aagaard et al., 2000; Reeves et al., 2004a, 2004b). However this method assumes a linear relationship between EMG and joint torque, which is not always appropriate (Buchanan et al., 2004; Perry & Bekey, 1981), so it may not provide accurate estimates under all conditions. To account for the potential non-linearity of the moment-EMG relationship, data can be collected through a range of submaximal intensities using either a slow ramped contraction or a series of isometric contractions at varying intensities. The data are then appropriately modelled (linear, curvilinear or exponential; Perry & Bekey, 1981) and the antagonist moment is estimated again from the antagonist EMG amplitude during the agonist contraction (moment-EMG relationship method; Billot et al., 2010; Kellis et al., 2005; Mademli et al., 2004). A third approach (Billot et al., 2010) involves performing an isometric contraction of the antagonist muscle that elicits the same EMG amplitude as measured during the agonist contraction and recording the joint torque. This method is referred to as the EMG biofeedback method. In a recent study on the ankle plantar- and dorsiflexors (Billot et al., 2010), the EMG biofeedback and moment-EMG relationship methods were shown to provide similar results, whilst the MVC-EMG$_{max}$ ratio tended to (relatively) underestimate plantar flexor antagonist moment.

Current methodologies used to correct for plantar flexor antagonist moment during dorsiflexion are subject to limitations and potential errors. Although the EMG biofeedback (Billot et al., 2010) method is comparatively simple to use, a significant number of additional contractions may be needed within an experiment, given that at least one 'antagonist correction contraction' is needed for each agonist test contraction. Thus, there would be a considerable time (both testing and post-processing) and, possibly, fatigue impact when many agonist-antagonist efforts are required within an experimental protocol. Another possible issue is that the EMG biofeedback method has yet to be employed for anisometric contractions, where a subject would be required to track the EMG activity pattern accurately throughout an intensity-varying contraction; this may not be feasible due to the substantial familiarisation that would be required. Given these potential limitations, the moment-EMG relationship method could be considered a more efficient approach in some cases (Billot et al., 2010).

Another issue affecting the accuracy of dorsiflexor joint moment estimates is that the moment-EMG relationship obtained at a single angle is not likely to be valid for use at other angles (Altenburg, de Haan, Verdijk, van Mechelen, & de Ruiter, 2009; Babault,

Pousson, Michaut, & Van Hoecke, 2003; Billot, Simoneau, Ballay, Van Hoecke, & Martin, 2011; Doheny, Lowery, Fitzpatrick, & O'Malley, 2008). Two approaches for modelling the moment-EMG relationship through the full range of motion (ROM) are: (1) to obtain the moment-EMG relationship at each angle tested, or (2) to derive a moment-EMG relationship at select angles throughout the ROM and then model the change in relationship across angles. Due to the minimal change in peak EMG amplitude across joint angles in many body segments (Doheny et al., 2008; Leedham & Dowling, 1995) and the fact that agonist moment changes consistently (curvilinearly) with joint angle, the latter option of modelling the change in moment-EMG relationship across angles may be better for estimating plantar flexor moment at any angle and intensity. Thus, one might speculate that correcting for changes in the moment-EMG relationship across the full ROM should substantially improve plantar flexor (antagonist) co-contraction accuracy, and thus dorsiflexor (agonist) moment estimation accuracy.

EMG signal processing methods have also been found to influence the accuracy of the moment-EMG model. Specifically, high-pass filtering the surface EMG signal, which removed up to 99% of the signal, allowed for better force estimates in trunk (Staudenmann, Potvin, Kingma, Stegeman, & van Dieen, 2007) and elbow flexor (Potvin & Brown, 2004a) muscles but not in three rotator cuff muscles (Brown, Brookham, & Dickerson, 2010). Thus, the optimal filter cut-off frequency likely depends on the muscle analysed (McDonald, Sanei, & Keir, 2013). The influence of the EMG filtering characteristics on the accuracy of surface EMG-based plantar flexor moment estimates has not yet been established, so its specific examination is needed.

Given the above arguments, the aim of the present study was to determine the optimal method for correcting for plantar flexor antagonist co-contraction across the ankle joint ROM using joint moment-EMG relationships. To achieve this aim, the effect of tibialis anterior (TA) co-contraction during the plantar flexor calibration contractions, the decision to use soleus or triceps surae activity to represent the plantar flexors, and the change in the moment-EMG relationship across joint angles were investigated. Whilst common EMG filtering methods were used in the first set of experiments to establish the plantar flexor moment EMG relationship, an optimisation approach was subsequently used to refine the EMG filtering procedures.

METHODS

Subjects

To determine the effects of the different modelling and processing approaches, five adults (4 men and 1 woman) who were free from musculoskeletal injury gave their informed consent and volunteered for the study (age = 26 ± 1 yr, height = 1.80 ± 0.05 m, mass = 74.5 ± y 10.7; μ ± SD). Ethics approval was granted by the Brunel University Ethics Committee, and all procedures were conducted in accordance with the Declaration of Helsinki.

Testing Overview

The study consisted of two stages. The first stage focused on developing a model to allow plantar flexor (antagonist) co-contraction to be corrected for through a full ankle joint ROM during dorsiflexion. Of importance is that this correction requires a plantar flexion contraction to be done, during which the TA muscle can act as its antagonist. Therefore the first step in this process is to determine the effect of correcting for TA antagonist co-contraction on the plantar flexor moment-EMG relationship, which was done for each of six joint angles. Additionally, the difference between linear and curvilinear model fits were investigated, and the requirement for correction for changes in the plantar flexor moment-EMG relationship across the ankle joint ROM was assessed, with a new approach for this being presented.

Generic EMG processing procedures were used for the first stage of the study, whilst optimal EMG processing procedures were determined using an optimisation approach in the second stage of the study. This used the fit of the final angle-moment-EMG relationship as the variable to optimise.

Familiarisation

Prior to the testing days, each subject completed an extensive familiarisation protocol in which the methods involved in the testing protocol were practiced. Specifically, the subjects completed the warm-up that would be used prior to the testing session (a series of sub-maximal and maximal contractions of both the plantar- and dorsiflexors), slow ramped maximal plantar flexor contractions, and low-intensity contractions of the dorsiflexors. To focus on activation of the triceps surae musculature during plantar flexions, the subjects were directed to rotate their ankle (rather than pressing with the whole leg) and to push through the ball of their foot without flexing their toes. During

dorsiflexion contractions, the subjects were instructed to rotate their foot toward their shin without deliberate extension of their toes. Following familiarisation, the seat position of the dynamometer was recorded in order to maintain consistency between the familiarisation and testing sessions.

Data Collection

The subjects were positioned in an isokinetic dynamometer (Biodex System 3, Biodex Medical Systems, Inc., NY) so that the lateral malleolus was aligned with the centre of rotation of the dynamometer, and the relative knee and hip angles in the sagittal plane were both approximately 80° (0º = full extension), with the torso being reclined to 70º relative to the horizontal. A limb-support pad was placed under the thigh proximal to the origin of the gastrocnemii muscles. Hook-and-loop straps were securely fastened over the metatarsals to prevent movement of the foot relative to the footplate, and straps were placed tightly across the thigh, torso and waist to limit movement of the upper body, leg and ankle joint. A foot angle of 0° was taken as neutral (taken when the sole of the foot was perpendicular to the tibia), with plantar flexion being a positive angle and dorsiflexion being negative. The joint angle, velocity, and torque data underwent analogue-digital conversion at 1000 Hz and were captured using Spike 2 software (version 5, CED, Cambridge, UK).

Soleus (SOL), gastrocnemius medialis (GM), gastrocnemius lateralis (GL) and tibialis anterior (TA) muscle activities were recorded synchronously with the angle, velocity and joint torque data using bipolar surface EMG procedures (Telemyo 2400R, NorAxon USA Inc., Arizona). Electrodes were positioned in accordance with the Surface Electromyography for the Non-Invasive Assessment of Muscles (SENIAM) project, and in line with the estimated fascicle line of action. Specifically, the electrodes were placed at 2/3 of the line between the medial condyle of the femur to the medial malleolus on SOL, on the most prominent bulge of GM, and at 1/3 distance on the line between the head of the fibula and the heel on GL. For TA, the electrodes were placed at 1/3 distance on the line between the tip of the fibula and the tip of the medial malleolus. A reference electrode was placed on the medial aspect of the tibia.

Prior to application of the electrodes, the skin was shaved and lightly abraded using fine sandpaper before being cleansed with an alcohol-based spray (Pink Chlorhexidine Gluconate Solution, Hyrdex). Inter-electrode spacing was 20 mm and the baseline

interference for each muscle was required to be less than 1 kΩ (Winter, 2009), assessed using an ohmmeter. When the required baseline was not achieved, a combination of using new electrodes and re-preparing the site was performed.

Experimental Procedure

Each subject performed three sub-maximal isometric contractions (at 50, 75 and 90% of perceived maximum voluntary effort) and five maximal isometric contractions of both the plantar- and dorsiflexors with the foot in the neutral position. This was done to provide a thorough warm-up and re-familiarisation, and to condition the respective tendons in order to minimise changes in tendon stiffness through the test protocol (Maganaris, 2003; Magnusson et al., 2008). Changes in tendon stiffness would affect the portion of the force-length relationship at which the muscle was working and thus potentially impact the moment-EMG relationship (Lemos, Epstein, & Herzog, 2008).

The subject's maximal ROM was determined by passively rotating the footplate to their perceived maximal plantar- and dorsiflexion angles. Eight equi-spaced angles throughout the full ROM were then determined, and the six middle angles were used for this study.

Three types of contractions were performed at each of the six angles. First, the subjects performed a series of sub-maximal isometric dorsiflexion contractions with increasing intensity at each angle (Figure 4.1), which were used to correct for TA antagonist co-contraction during the plantar flexor contractions. To determine the intensity level of these sub-maximal contractions, each subject was instructed to perform approximately four to five contractions at each angle, increasing in intensity. Each contraction was held for 3-5 s with approximately 20-30 s rest being provided between each contraction. Second, the subjects performed an isometric maximal voluntary dorsiflexion contraction (MVC) followed by a slow ramped isometric plantar flexion MVC (Figure 4.2). Plantarflexor torque rise time during MVCs was approximately 5 s, and was guided by the experimenter. Encouragement was given to the subject during all MVCs.
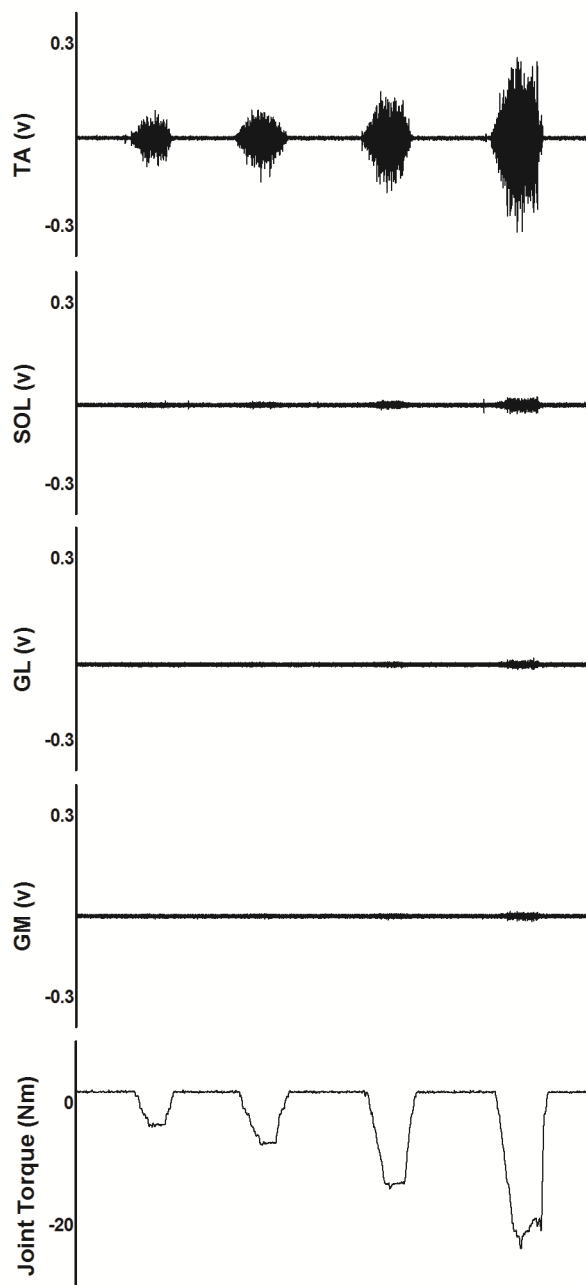
Figure 4.1. Joint torque and muscle activities during the sub-maximal isometric dorsiflexion contractions. Each contraction lasted approximately 3-5 s. Tibialis anterior (TA), soleus (SOL), gastrocnemius lateralis (GL) and gastrocnemius medialis (GM) activities were recorded using bipolar surface EMG. Raw EMG and filtered torque data are presented. Notice that EMG is negligible in SOL, GM and GL at low dorsiflexion torque magnitudes.
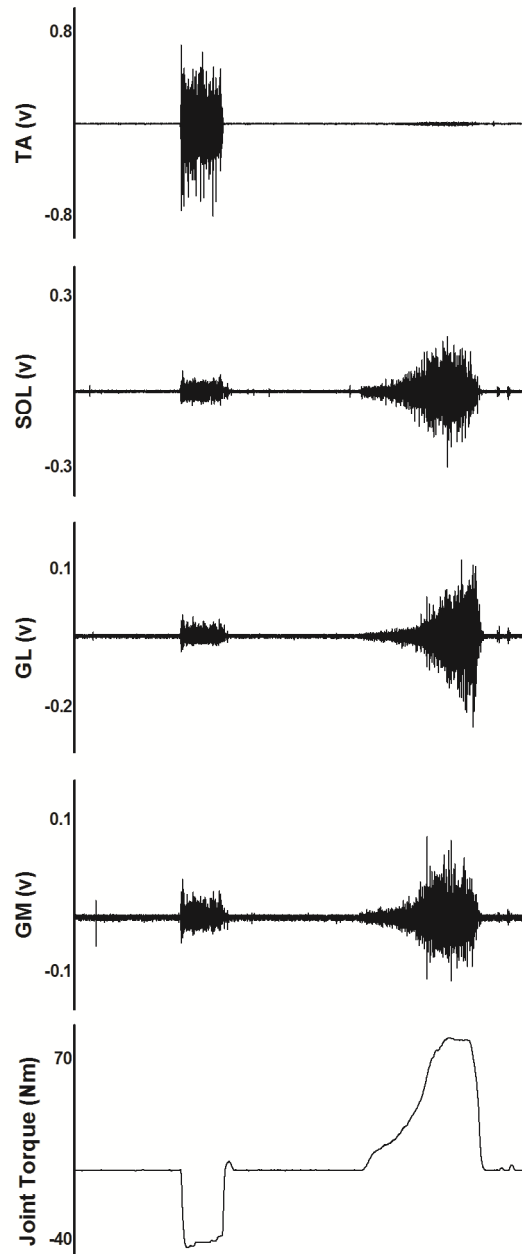
Figure 4.2. Joint torque and muscle activation during the isometric dorsiflexor MVC and slow ramped plantar flexion MVC. The dorsiflexion MVC lasted approximately 3-5 s (first observable torque production in the Joint Torque trace; bottom) and the rise of the slow ramped plantar flexion MVC approximately 5 s (second observable torque production in the Joint Torque trace). Tibialis anterior (TA), soleus (SOL), gastrocnemius lateralis (GL) and gastrocnemius medialis (GM) activities were recorded using bipolar surface EMG. Raw EMG and filtered torque data are presented.

Data Processing

All data analyses were performed off-line using MATLAB (vR2013a; Mathworks, Cambridge). Generic EMG processing procedures were used for the first stage of analyses. For these, the DC-offset was first removed before a 20-450-Hz band pass, fourth-order, zero-lag Butterworth filter was applied. The band-passed signal was then full-wave rectified and a linear-envelope was produced using a 5-Hz low pass, fourth order, zero-lag Butterworth filter. Joint angle, velocity, and moment data were filtered using a 14-Hz low pass, fourth-order, zero-lag Butterworth filter (selected following a residual analysis; Winter, 2009).

The plantar flexor muscle group was modelled using either SOL-only or whole triceps surae (TS; using the sum of the filtered SOL, GL, and GM signals) EMG signals. The flexed knee position was used because a straight–leg position induced discomfort in the subjects, in addition to increasing the passive stiffness of the plantar flexors. With the knee flexed, the contributions of GM and GL to the plantar flexor moment are substantially reduced, although the ratio of contribution of the three heads is not specifically known (Cresswell, Loscher, & Thorstensson, 1995). Therefore, with a bent knee, as in the current study, accuracy may be improved when modelling the plantar flexors using only SOL. All analyses were performed using the two approaches to modelling the plantar flexors to determine the differences between their magnitudes of correction for antagonist moment.

TA, SOL, and TS electromechanical delays were determined using a cross-correlation approach (Blanpied & Oksendahl, 2006; Staudenmann et al., 2010; Vos, Harlaar, & van Ingen Schenau, 1991; Vos, Mullender, & van Ingen Schenau, 1990). For the TA, the filtered torque and TA EMG signals from the sub-maximal isometric dorsiflexion contractions were cross-correlated. For SOL and TS, the filtered torque and EMG signals from the slow ramped plantar flexion MVC were cross-correlated. The time shift resulting in the peak correlation was then taken as the electromechanical delay. The electromechanical delay was calculated at each angle, with the median being used for subsequent analyses.

The baseline torque signal reflects the combination of passive stiffness and segment weight, whilst the baseline of the EMG signal corresponds to baseline noise, hence baseline values were removed from all signals prior to processing and analysis. At each

angle, the mean amplitude of the signal (for EMG and torque) was calculated over a 5-s rest period and then subtracted from the whole signal at each angle. Although more complex methodologies are available for accounting for baseline noise in the EMG signal (e.g. Law, Krishnan, & Avin, 2011), the subtraction of the baseline from the signal was deemed sufficient for the isometric conditions used within the present study.

The effect of correcting for TA (antagonist) co-contraction during the plantar flexor MVC was then investigated. Although TA activity is minimal during a plantar flexion MVC (Billot et al., 2010), it may be active to ~15% MVC (resultant moment ~5 Nm; Billot et al., 2010). During the sub-maximal isometric dorsiflexion contractions activity in the triceps surae was not detectable when the contraction intensity was small (Figure 1). This allowed for a moment-EMG relationship for the TA to be produced that was not affected by plantar flexor antagonist co-contraction. The ratio of the maximum TA EMG to dorsiflexor moment was calculated from the strongest contraction that produced no detectable activity within SOL, GL or GM. TA activity during this contraction was similar, if not greater, than the level of TA activity (i.e. antagonist co-contraction) during a plantar flexor MVC, and thus extrapolation of the model beyond the range used to produce it was not necessary. This provided a simple TA moment-EMG relationship that was then used to account for TA activity during subsequent plantar flexor MVCs. Specifically, the plantar flexor moment was calculated by adding the dorsiflexor moment (calculated using the ratio from the sub-maximal dorsiflexion contraction at that angle) to the resultant joint moment. To test the effect of including the correction for TA activity, the plantar flexor moment during the dorsiflexion MVC was estimated using the EMG biofeedback method (Billot et al., 2010). This was performed both with and without correcting for TA activity during the slow ramped plantar flexion MVC (Figure 4.3). All subsequent analyses correct for TA activity (i.e. antagonist co-contraction) during the slow ramped plantar flexor MVC when fitting the different models.
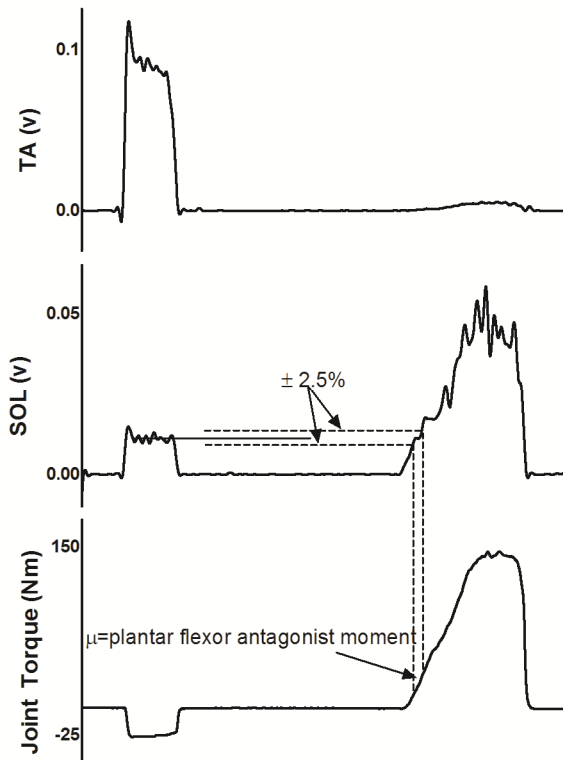
Figure 4.3. Using the biofeedback method to estimate plantar flexor (antagonist) moment during a dorsiflexion MVC. The $\mu \pm 2.5\%$ of SOL EMG activity during the dorsiflexion MVC was located during the plantar flexion MVC, and the corresponding torque was taken as being equal to the plantar flexor (i.e. antagonist) moment.

Moment-EMG Modelling

A series of approaches to modelling the plantar flexor moment-EMG relationship were investigated. For all approaches, the portion of the ramped MVC below 70% maximal torque was used. Because the aim of this study was to develop an optimal approach for plantar flexor activity correction (i.e. antagonist co-contraction), it was not necessary to use the whole range of torque up to MVC. Importantly, we hypothesised that this may improve the potential for simplifying the model through the use of a linear, as opposed to a curvilinear, fit as the main curvature of the moment-EMG relationship has been suggested to occur during contractions of greater intensity (Disselhorst-Klug, Schmitz-Rode, & Rau, 2009).

The first step was to examine differences between linear and curvilinear models at each angle. This involved fitting a linear or 2nd-order polynomial to the moment-EMG data using a linear least-squares approach. Both models were forced through the origin so

65

that muscle silence occurred at zero joint moment. The coefficients of determination (R^2) of the two models were then compared across all angles (see below).

The second step was to determine the necessity to account for potential differences in the moment-EMG relationship across the different angles. To do this, the moment-EMG model obtained from the more plantar flexed of the two mid-angles (i.e. 14 ± 4º of plantar flexion; μ ± SD; chosen as it was the middle angle, and thus more likely to be representative of the other angles) was compared to the moment-EMG model obtained at each other angle. The root mean square error (RMSE) between the modelled and real data was calculated for each model. A relative RMSE (%RMSE) was then calculated ($100 \times \text{RMSE} / \text{RMS torque}$, where *RMS torque* is the root mean square torque over the rise of the slow-ramped MVC), which was compared between the two modelling approaches using both linear and curvilinear fits.

The third step was to incorporate changes in the moment-EMG relationship across the ROM into a new model. The relationship between the joint angle and the linear slope of the moment-EMG relationship at each angle was modelled using a 2nd-order polynomial. Because the linear moment-EMG relationship was forced through the origin, only the gradient of the relationship varied with angle, allowing the relatively simple approach of using the 2nd-order polynomial to account for variations across angles. The 2nd-order polynomial was chosen as it reflected the relationship between the joint angle and the slope well (R^2 = 0.94 ± 0.07 and 0.97 ± 0.02; μ ± SD for SOL and TS approaches, respectively). To test for any reduction in accuracy of the new angle-moment-EMG model, the %RMSE of the estimated plantar flexor moment during the ramped plantar flexion MVC was compared between the new angle-incorporated model and the linear moment-EMG relationship for each angle.

Optimisation of EMG processing

For the procedures described above, generic EMG processing methods were used. However, it has been suggested that the components of both the band- and low-pass filters affect the fit of the moment-EMG relationship (McDonald et al., 2013; Potvin & Brown, 2004a; Staudenmann et al., 2007). To investigate this in the plantar flexor muscle group, an optimisation approach was used. Based on previous research the frequency and order of the high-pass component of the band-pass filter, as well as the frequency and order of the low-pass filter used to produce the linear envelope, were

altered during the optimisation; the low-pass component of the band-pass filter was kept constant (450-Hz, fourth-order, zero-lag Butterworth filter). The mean %RMSE of the estimated plantar flexor moment during the slow ramped plantar flexor MVCs was set as the variable to be minimised.

GlobalSearch and fmincon functions from the Global Optimisation Toolbox (MATLAB v2013a) were used for global and local optimisation, respectively. Specific constraints limited the filter orders to first through sixth orders, the high-pass frequency component to between 1 and 400 Hz, and the low-pass frequency component to between 1 and 10 Hz. These constraints were determined based on the ranges suggested by previous researchers who examined optimal EMG filtering procedures (McDonald et al., 2013; Olney & Winter, 1985; Potvin & Brown, 2004a; Staudenmann et al., 2007). Custom start points were used to ensure consistency across the different optimisations. In total, 3600 start points were used, which encompassed all combinations of frequencies (10-400 Hz in 10-Hz increments) and orders (2nd, 4th, and 6th) of the high-pass filter, and frequencies (1-10 Hz in 1-Hz increments) and orders (2nd, 4th, and 6th) of the low-pass filter used to produce the linear envelope.

For each run of the optimisation algorithm, the procedures described above were followed to produce the angle-moment-EMG model. This involved filtering the EMG signal, calculating the electromechanical delay, producing a linear moment-EMG model for each angle, and then fitting a 2nd-order polynomial to model the relationship between joint angle and the slope of the linear moment-EMG model. Finally, the mean %RMSE of the estimated plantar flexor moment during the ramped plantar flexion MVC was calculated using the new model. Two sets of optimisation were performed using either SOL or TS activity to represent the plantar flexor muscle group. First, an optimisation was undertaken for each subject, where the mean %RMSE of the estimated plantar flexor moment for all angles was used as the variable to be optimised. Second, an optimisation was performed across all subjects, where the mean %RMSE across all angles and subjects was used as the variable optimised. This dual approach allowed for a sensitivity analysis to be performed. The %RMSE of the estimated plantar flexor moment from the processing parameters determined from the group optimisation was compared with the %RMSE using the parameters determined using the individual optimisations.

Statistical Analysis

Coefficients of determination (R^2) were computed to compare the goodness of fit between linear and curvilinear models at each joint angle. The relative root mean square error (%RMSE) was used to compare the accuracy with which each model estimated plantar flexor moment during the ramped isometric plantar flexion MVC. Effect sizes (ES) were calculated using Cohen's *d*. The pooled SD was used as the standardiser, being calculated as the square root of the mean variances (Cohen, 1988; Fritz et al., 2012). For descriptive purposes, effect sizes of 0.2, 0.5 and 0.8 were determined as small, medium and large, respectively (Cohen, 1988). All values are presented as µ ± SD, whilst the boxplots present the minimum, 25th percentile, median, 75th percentile and maximum values.

RESULTS

Effect of TA Activity on the Plantar Flexor Moment-EMG Relationship

The effect of correcting for TA activity (i.e. antagonist co-contraction) in the estimation of plantar flexor moment was trivial-small (Figure 4.4). Regardless of whether the TA activity was accounted for, the estimated dorsiflexor moment was always larger (ES > 1.1) than the resultant joint moment measured. A trend was apparent for a greater difference between the dorsiflexor moment and the resultant joint moment at more dorsiflexed angles, i.e. when the plantar flexor muscles were longer and dorsiflexor muscles shorter. Therefore, although correcting for TA activity does not appear practically important when estimating plantar flexor moment, accounting for TS activity is clearly important when estimating dorsiflexor moment.

Effect of Modelling the Moment-EMG Relationship Using Linear vs. Curvilinear Relations

The shape of the relationship between the plantar flexor moment and EMG (modelled using either SOL or TS) was investigated comparing linear and curvilinear (2nd-order polynomial) fits. The fit of both approaches was very good for all angles ($R^2 > 0.87$), although small-large differences (range of ES = 0.2 − 1.0) were found between the linear and curvilinear approaches (see Tables 4.1 and 4.2). The large effect of model was found at the end ROM, with the four central angles (-2 ± 4° to 22 ± 4°) having only small-medium effects for model fit (i.e. range of ES = 0.2 − 0.5). With the knee flexed (80°), the plantar flexor moment-EMG relationship (modelled either using SOL or TS) can be modelled using a linear fit through the mid-range angles (-2 ± 4° to 22 ± 4°). However, a better fit was obtained at the end ROM when a curvilinear approach was used; nonetheless the absolute differences in the resultant R^2 values are small (≈ 0.05) despite the medium-large effect sizes (Table 4.1 and 4.2).
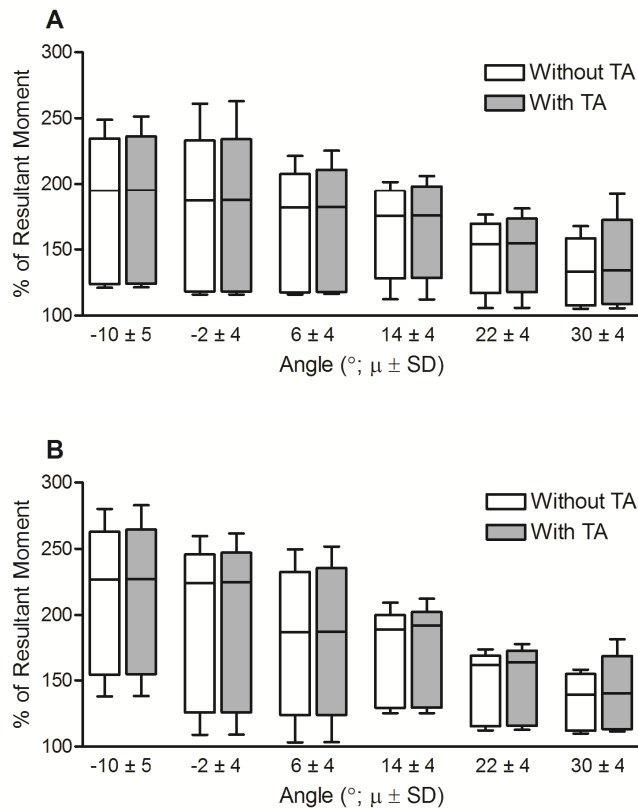
Figure 4.4. The effect of including the plantar flexor (antagonist) moment in the calculation of the dorsiflexor moment. The plantar flexors were modelled using either soleus (A) or triceps surae (B) EMG activities. The plantar flexor moment was estimated using the EMG biofeedback method both with and without TA activity (i.e. antagonist co-contraction) correction during the slow ramped plantar flexion MVC. 100%: no correction for plantarflexor activity was included, i.e. resultant ankle joint torque. For 30 ± 4°, Cohen's $d = 0.2$ (soleus and triceps surae) for the effect of inclusion of the TA, and Cohen's $d < 0.1$ for all other angles.

Error Associated with Using a Single Angle to Determine the Moment-EMG Relationship

Large errors (%RMSE of up to 200) were found when using the moment-EMG relationship calculated using only a single (mid-range; 14 ± 4°) angle, when compared to using the angle-specific relationship. Specifically, as the angle of analysis moved further from the angle in which the model was produced, larger errors were seen (Figure 4.5). These errors were independent of the model fit (linear vs. curvilinear) and whether the plantar flexor muscles were modelled as SOL or TS. Therefore, developing a moment-EMG relationship using data collected at a single angle is problematic and is therefore not recommended.

Table 4.1. Linear and curvilinear (2$^\text{nd}$-order polynomial) fits for the moment-EMG relationship during the slow ramped plantar flexion MVC. The soleus EMG was used to represent the plantar flexors. Results were similar when using the triceps surae to represent the plantar flexors (Table 4.2). Values are $\mu \pm$ SD.

Angle (°)	Linear (R^2)	Curvilinear (R^2)	Effect Size (Cohen's d)
-10 ± 5	0.87 ± 0.07	0.92 ± 0.04	1.0
-2 ± 4	0.91 ± 0.04	0.93 ± 0.03	0.5
6 ± 4	0.92 ± 0.05	0.94 ± 0.05	0.4
14 ± 4	0.94 ± 0.03	0.95 ± 0.02	0.5
22 ± 4	0.94 ± 0.04	0.95 ± 0.04	0.3
30 ± 4	0.89 ± 0.05	0.92 ± 0.06	0.5

Table 4.2. Linear and curvilinear (2$^\text{nd}$-order polynomial) fits for the moment-EMG relationship during the slow ramped plantar flexion MVC. The triceps surae EMG was used to represent the plantar flexors. Results were similar when using the soleus to represent the plantar flexors (Table 4.1). Values are $\mu \pm$ SD.

Angle (°)	Linear Fit (R^2)	Curved Fit (R^2)	Effect Size (Cohen's d)
-10 ± 5	0.90 ± 0.06	0.94 ± 0.05	0.8
-2 ± 4	0.92 ± 0.06	0.94 ± 0.06	0.2
6 ± 4	0.93 ± 0.06	0.95 ± 0.04	0.3
14 ± 4	0.94 ± 0.03	0.95 ± 0.03	0.3
22 ± 4	0.93 ± 0.06	0.94 ± 0.05	0.3
30 ± 4	0.92 ± 0.03	0.95 ± 0.03	0.9
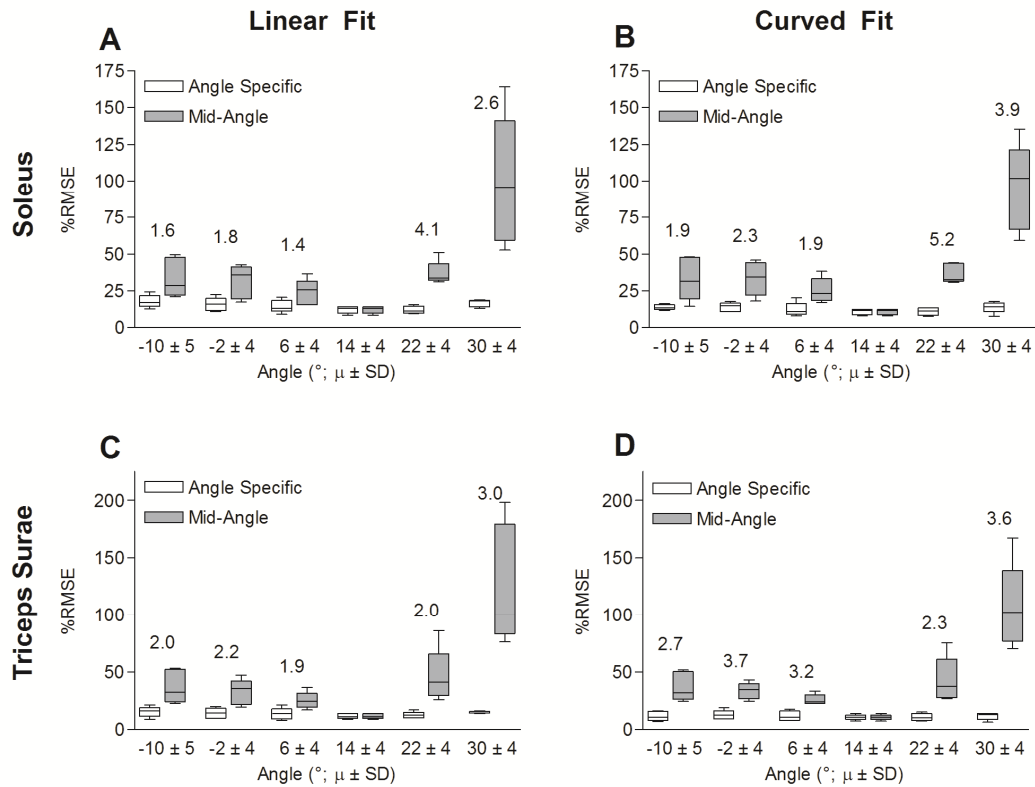
Figure 4.5. The plantarflexor moment-EMG relationships across the ROM were modelled using data collected at each angle or data collected at a single joint angle (i.e. $14 \pm 4°$). Linear (A and C) and 2nd order polynomial (B and D) models were examined. The plantar flexor muscle group was modelled using either the soleus (A and B) or triceps surae (C and D) EMG activities. %RMSE = percentage root mean square error. Cohen's d effect sizes are displayed above each comparison. No effect size is shown for angle $14 \pm 4°$ as both the angle specific and mid-angle approach used the same model.

Accounting for Joint Angle in the Moment-EMG Relationship

A modified model was developed to incorporate the changes in the moment-EMG relationship across the ROM. The accuracy of this new 'angle-incorporated' model for estimating plantar flexor moment was compared against a linear moment-EMG model at each of the six angles (Figure 4.6). When the plantar flexor muscle group was modelled using SOL, the differences between the angle-incorporated model and the angle-specific approach were small-medium (ES = 0.1 – 0.7). When the plantar flexor muscle group was modelled using TS, similar effect sizes were found for five of the six angles, whilst a very large effect size (ES = 2.5) was found for the more plantar flexed angle ($30 \pm 4°$); nonetheless, this large effect size is potentially due to the relatively small pooled SD as opposed to a large difference in %RMSE of the two approaches (%RMSE = $17.0 \pm 0.9\%$ and 14.7 ± 0.8 for the angle-incorporated and angle-specific

approaches, respectively). Therefore, although the angle-incorporated model compared well with the angle-specific linear models, it appeared to produce a better fit when the plantar flexor muscle group was modelled using SOL compared to using TS.
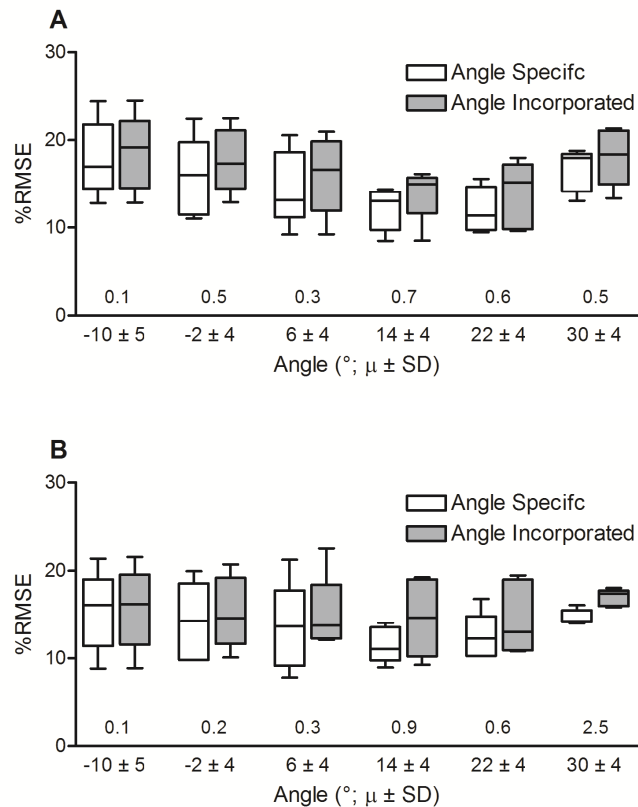
Figure 4.6. Comparison of the accuracy of the moment-EMG relationship for each angle. A linear model was fitted to the moment-EMG data at each angle for the angle-specific approach, whilst a 2nd-order polynomial was fitted to model the relationship between joint angle and the slope of the moment-EMG relationship for the angle-incorporated approach. The plantar flexor muscle group was modelled using either the soleus (A) or triceps surae (B). The new angle-incorporated model provides a good alternative for estimating plantar flexor moment across the full ROM. %RMSE = percentage root mean square of the error. Cohen's *d* effect sizes are displayed above the x-axes for each comparison.

Using Optimisation to Determine the Optimal Processing Method

The subject-specific optimisations presented a range of EMG processing parameters that were unique to the individual. For each subject, the high-pass frequency was always lower when the plantar flexors were modelled as the SOL compared to TS (Tables 4.3 and 4.4). However, when the optimisation was performed on all subjects together, the optimum high-pass frequency filter cut-off was higher when the plantar flexors were modelled as SOL (167 Hz vs. 104 Hz for SOL and TS, respectively). Reasonably consistent low-pass filter frequency ranges were produced (i.e. between 1.0 and 1.7 Hz) across all subject-specific and grouped optimisations.

73

Table 4.3. Output from the optimisation performed for each subject, and for all subjects combined. The high-pass frequency and order of the band-pass filters as well as the low-pass frequency and order of the linear envelope were modified to minimise %RMSE. The plantar flexors were modelled using SOL. Differences in the high-pass frequency were found between when plantar flexors were modelled using SOL or TS (Table 4.4).

Subject	High-pass Frequency	High-pass Order	Low-pass Frequency	Low-pass Order
1	27	4	1.2	2
2	3	4	1.6	6
3	50	2	1.5	6
4	141	4	1.0	2
5	392	6	1.0	4
Grouped	167	2	1.0	2

Table 4.4. Output from the optimisation performed for each subject, and for all subjects combined. The high-pass frequency and order of the band-pass filters as well as the low-pass frequency and order of the linear envelope were modified to minimise %RMSE. The plantar flexors were modelled using TS. Differences in the high-pass frequency were found between when plantar flexors were modelled using SOL (Table 4.3) or TS.

Subject	High Pass Frequency	High Pass Order	Low Pass Frequency	Low Pass Order
1	192	4	1.7	6
2	309	4	1.6	6
3	154	4	1.3	5
4	170	4	1.0	5
5	400	4	1.0	1
Grouped	104	4	1.5	6

A sensitivity analysis was performed to compare the subject-specific optimised filter parameters to the grouped optimised filter parameters. The use of subject-specific filter parameters produced a small to moderate improvement in the accuracy of the model (i.e. a lower %RMSE) at most joint angles (Figure 4.7). Although large effect sizes

were produced at 14 ± 4° and -10 ± 5° for SOL and TS, respectively, the absolute difference in accuracy of the models was minor (%RMSE = 2.3 ± 3.3% for SOL at 14 ± 4° and 0.9 ± 2.1% for TS at -10 ± 5°) when comparing the subject-specific filters with the group-optimised filters. Therefore, although the subject-specific optimised filter parameters were clearly different to one another, it appears that the sensitivity of the filter parameters is negligible due to the similarities in model accuracy when using the subject-specific and group-optimised filters. As such, use of globally-optimised filter parameters is acceptable when using the angle-moment-EMG model to estimate plantar flexor moment.
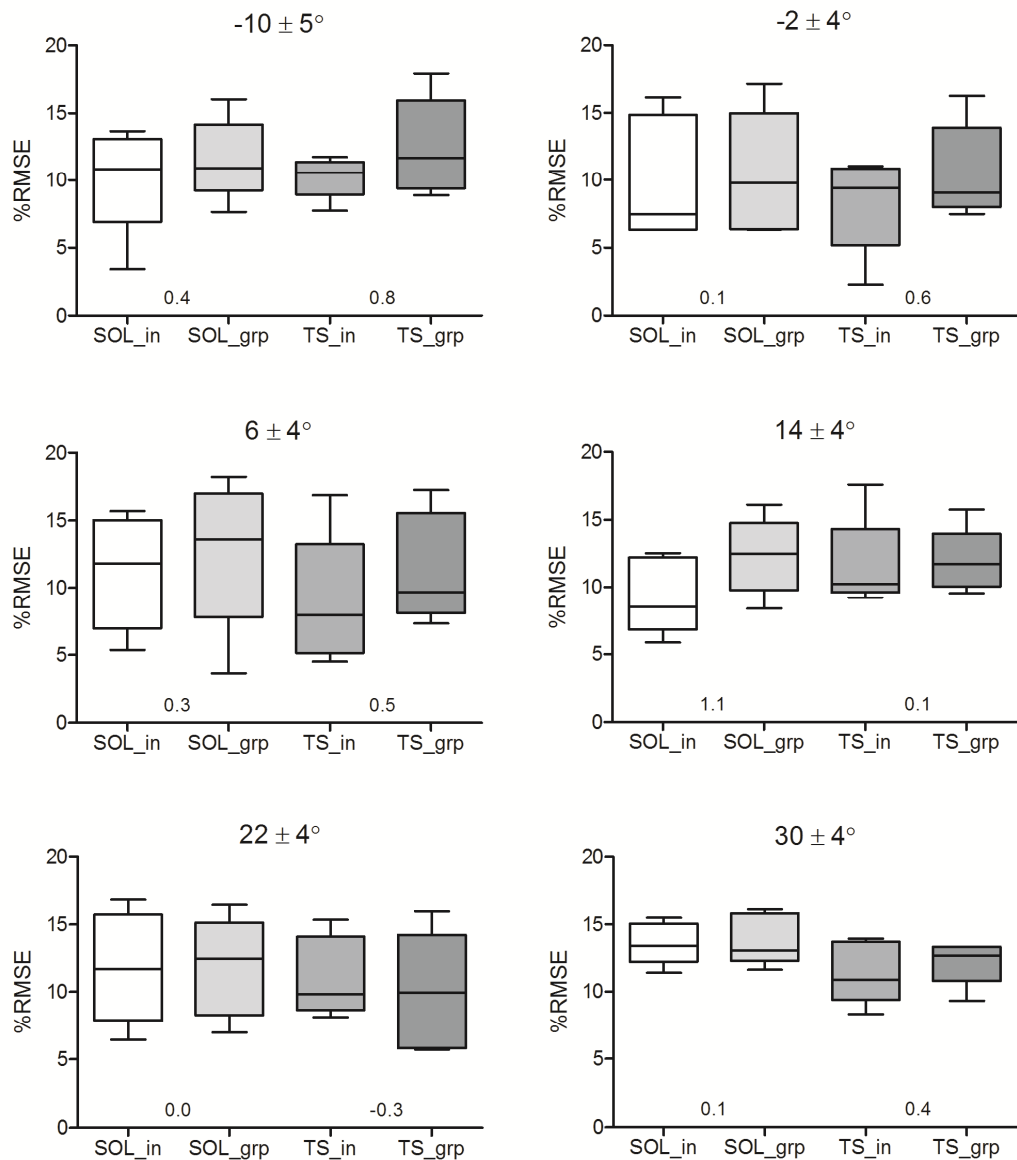
Figure 4.7. Comparison of the effect of EMG processing on the fit of the moment-EMG data. Using the angle-moment-EMG model, optimal EMG processing was determined for the soleus (SOL) and triceps surae (TS) approaches separately. Optimisation was performed to minimise the relative root mean square error (%RMSE) for each individual separately (i.e. SOL_in and TS_in) and for all subjects collectively (i.e. SOL_grp and TS_grp). Although large differences in processing parameters were produced when optimisation was performed on individual subjects compared to the group (Table 4.3 and 4.4), the effect of these differences on the model accuracy were minimal. Cohen's *d* effect sizes comparing the group and individual optimisation processing parameters are shown above the x-axes for each comparison.

DISCUSSION

The purpose of the present study was to define an optimal method for correcting for plantar flexor (antagonist) co-contraction across the ROM during dorsiflexion

contractions. In the first part of the study, methods for modelling the plantar flexor moment-EMG relationship were examined. The results showed (i) minimal differences between linear and curvilinear model fits to the moment-EMG relationship at each joint angle, and (ii) that the change in the linear slope of the moment-EMG relationship across the ROM could be modelled with good accuracy using a 2nd-order polynomial. This method provided estimates of plantar flexor moment that were similar to those obtained when the relationship was modelled at each joint angle separately. Importantly, the approach allowed for the estimation of plantar flexor moment at all joint angles and contraction intensities studied. In the second part of the study, an optimisation approach was used to define ideal EMG filtering parameters. Although large differences in the high-pass filter frequency were found when the optimisation was run for each individual subject and for all subjects grouped, model errors were similar for plantar flexor moment estimates made using the different processing methods. The frequency of the low-pass filter used to produce the linear envelope was similar across all subjects and optimisation approaches. Therefore, the high-pass filter frequency does not seem to affect model accuracy even though its optimum varied widely between individuals, but the linear envelope low-pass filter frequency appears to be of importance for the model accuracy. The EMG-processing parameters derived using the grouped-optimisation can be used for subsequent analyses as these showed similar model accuracy to the individual-optimised processing parameters.

Antagonist TA activation was detectable during the slow ramped isometric plantar flexion MVC used to derive the moment-EMG model for the plantar flexors, however it was found to have only a trivial effect on the estimated plantar flexor moment. Conversely, antagonist plantar flexor activity during the isometric dorsiflexion MVC had a large effect on estimated dorsiflexor moment. Our findings are in agreement with those of Billot et al. (2010), who found that the antagonist mechanical output (i.e. moment) of TS (~ 31 Nm) was higher than TA (~ 6 Nm) despite the TA EMG amplitudes being greater when acting as an antagonist. Additionally, Simoneau et al. (2009) found that TS antagonist activity correction significantly altered the plantar flexion:dorsiflexion ratio whereas correcting for TA antagonist activity did not. It is perhaps surprising, then, that Mademli et al. (2004) found that correcting for TA antagonist activity significantly increased plantar flexor moment estimates, although a higher antagonist activity was elicited (~ 7.7 Nm) in their study when compared to others (0.82-6 Nm; Billot et al., 2010; Gerus, Rao, Buchanan, & Berton, 2010;

Simoneau et al., 2009) and this would have increased the influence of the antagonist moment. Furthermore, TA co-contraction has been found to be higher in the weaker plantar flexor leg (Maganaris et al., 1998), which may partly explain the different effect of accounting for TA antagonist activity between studies (Billot et al., 2010; Mademli et al., 2004; Simoneau et al., 2009). Therefore, although TA activity is low during plantar flexion, it may still be important to correct it in case its influence within an individual is significant (Mademli et al., 2004; Maganaris et al., 1998).

The plantar flexor moment-EMG relationship was accurately modelled using both linear and curvilinear fits, regardless of whether soleus (SOL) only or the sum of the triceps surae (TS) EMGs was used. A large effect of model was found at the end ROM, although the R^2 difference was only ≈ 0.05; the large effect size can be attributed to the small pooled standard deviation. Thus, the moment-EMG relationship for the plantar flexors can be modelled using the simpler linear fit. Various factors have been suggested to reduce the linearity of the relationship between moment and EMG, including muscle fatigue (Moritani & deVries, 1978), muscle length change (Hof & Berg, 1977b; Moritani & deVries, 1978), electrode configuration (Moritani & deVries, 1978), contraction intensity range (Kutch & Buchanan, 2001), antagonist co-contraction correction (Brown & McGill, 2008), inclusion of all muscles involved in the action (Hof & Berg, 1977b; Kutch & Buchanan, 2001), and the EMG filtering method (Potvin & Brown, 2004a; Staudenmann et al., 2010). In fact, most of these factors were controlled for in the present study. First, a minimal number of contractions were performed and substantial rest was provided between contractions. Second, only the portion of the signal below 70% MVC was used to model the moment-EMG relationship, which reduced the contraction intensity range over which data were analysed. Finally, the triceps surae muscle group provides the majority of the plantar flexor force (Fukunaga et al., 1996b; Morse, Thom, Reeves, Birch, & Narici, 2005; Murray, Guten, Baldwin, & Gardner, 1976); this, in addition to subjects being conscious of promoting TS use (see Methods), means the input of toe flexor muscle force would have been minimal. In fact, a high linearity was found using either SOL (R^2 = 0.87-0.94) only or TS, so the influence of other muscles acting at the ankle appears to be negligible in these conditions used in the present study (Brown & McGill, 2008; Hof & Berg, 1977b; Kutch & Buchanan, 2001). Using a similar limb position (i.e. knee flexed to ~80°), Hof and van den Berg (1977b) reported that both SOL and TS (i.e. the weighted sum of the individual triceps surae muscles) EMG activities were

independently and linearly related to plantar flexor moment. With subjects in a standing position with a straight knee, however, plantar flexor moment was not linearly related to increases in SOL activation; i.e. a greater increase in GM and GL activity at higher contraction intensities provided the linear relationship between TS activity and plantar flexor moment (Hof & van den Berg, 1977b). Therefore, with the knee flexed (e.g. 80°) the plantar flexor moment-EMG relationship appears to be well represented using a linear model, regardless of whether SOL or TS is used in the model.

Although the plantar flexor moment-EMG relationship was well represented by a linear model, large differences in the slope of the relationship were found across joint angles. Furthermore, the use of a moment-EMG relationship derived at one angle was not valid for use at other angles. Therefore, the change in slope of the moment-EMG relationship across the ROM was modelled. Plantar flexor muscle length changes as the ankle joint is rotated. Since Gordon et al. (1966b) first investigated the effect of sarcomere length on force output, the "inverted-U" relationship between force and length, and subsequently joint moment and angle, has been extensively investigated (e.g. Blazevich, Cannavan, Coleman, & Horne, 2007; Kawakami, Kubo, Kanehisa, & Fukunaga, 2002; Leedham & Dowling, 1995). However, the effect of joint angle and/or muscle length on muscle activation appears less clear. Previously, no change in maximal biceps brachii, brachrioradilis or triceps brachii EMG activity was identified (Doheny et al., 2008; Leedham & Dowling, 1995), yet muscle activity for a given sub-maximal force level varied with muscle length in the quadriceps femoris (Altenburg et al., 2009; Babault et al., 2003) and triceps brachii (Doheny et al., 2008). Although sub-maximal EMG amplitudes can vary through the ROM, it appears that the change in joint moment has a greater impact on the moment-EMG relationship (Doheny et al., 2008; Leedham & Dowling, 1995). Therefore, the change in the moment-EMG relationship across angles is likely to reflect changes in the plantar flexor moment-joint angle relationship. Given this realisation, the change in gradient of the EMG-moment relationship across the ROM was modelled using a 2nd-order polynomial fit. This curvilinear model represented the data well ($R^2 = 0.94 \pm 0.07$ and 0.97 ± 0.02; $\mu \pm$ SD for SOL and TS approaches, respectively), which provides support for the initial hypothesis. Indeed, the accuracy of the angle-moment-EMG model at a particular joint angle was found to be similar to the estimates obtained using moment-EMG models developed at each angle individually. Therefore, the proposed new model is efficient for correcting for plantar flexor co-activation across the ROM and throughout the intensity range.

The second part of this study aimed to determine the optimal plantar flexor EMG filtering method. This was done using an optimisation approach, with the accuracy of the subsequent model being used as the variable to optimise. Large variations in the high-pass frequency optimum (range = 3 – 400 Hz) were found across subjects, with a lower frequency being more optimal when the plantar flexors were modelled using SOL compared to TS. Only recently has the effect of a higher cut-off frequency been investigated for high-pass filters (Brown et al., 2010; Potvin & Brown, 2004b; Staudenmann et al., 2007). Two contradicting hypotheses have been proposed to explain the mechanisms by which the high-pass filter affects the moment-EMG relationship model accuracy. These are based around whether the tissue does (Potvin & Brown, 2004b) or does not (Dimitrova, Dimitrov, & Nikitin, 2002; Staudenmann et al., 2007) act as a low-pass filter. Potvin et al. (2004b) proposed that motor unit action potentials (MUAP) originating further from the electrode location would have undergone spatial filtering as the muscle and adipose tissues act as low-pass filters. These MUAPs are more likely to emanate from muscles that are not involved in the task (i.e. cross-talk) and would thus be likely to reduce the accuracy of a moment-EMG model derived using this signal. High-pass filtering of the surface EMG would remove the portion of the signal that originates from those muscles and potentially improve the model's accuracy (Potvin et al., 2004b).

In contradiction to this, the relative weight of high frequencies from deeper motor units has been shown theoretically to increase with depth (Dimitrova et al., 2002). This is because the power of the high frequency non-propagating part of the action potential does not decrease with depth as much as the power of the slower frequency traveling wave (Dimitrova et al., 2002; Farina, Merletti, & Enoka, 2004). Therefore, the higher frequencies of the surface EMG signal would contain a greater contribution from the deeper motor units than the lower frequencies and, consequently, high-pass filtering of surface EMG should increase the contribution from deeper muscles; interestingly, this would also increase the linearity of the moment-EMG relationship (Staudenmann et al., 2007). Because the fast-type fibres, which lie more superficial in many muscles (Dahmane, Djordjevic, Simunic, & Valencic, 2005), are recruited more as contraction intensity increases (Cope & Pinter, 1995; Henneman, Somjen, & Carpenter, 1965), their contribution to the surface EMG interference signal may be disproportionately greater than their mechanical contribution as muscle force increases (Staudenmann et al.,

2007). High-pass filtering of the EMG signal would thus reduce this disproportionate representation of the superficial motor units, if it indeed increased the contribution from deeper muscles. This latter possibility may at least partly explain the higher filter frequencies found in the present study to be optimal when the plantar flexors were modelled using SOL compared to TS. Hof and van den Berg (1977b) found that SOL may contribute more than twice as much to plantar flexor moment than both GM and GL with the knee flexed. This should be reflected in a greater weighting of SOL when summing the three muscles to model the triceps surae. The three muscles were weighted equally in the present study, which may have led to an under-representation of the moment contribution of SOL. Because a small part of the GM and GL surface EMG signal likely comes from the deeper SOL (i.e. cross-talk; Hof & van den Berg, 1977b), the use of a higher filter frequency may increase SOL contribution to the GM and GL signals, and thus increase its overall weighting in the TS signal. Therefore, when using the TS EMG signal to model the plantar flexor moment-EMG relationship with the knee flexed, a higher frequency cut-off, or a greater weighting of the contribution from SOL, may be optimum in order to provide a more linear moment-EMG relationship.

When EMG filter parameters were optimised for each subject individually, large differences were found between subjects in the optimum high-pass filter frequency. Despite these variations, changes in these frequencies had little effect on the accuracy of the angle-moment-EMG model. Although large differences (26 – 296 Hz) in optimum high-pass filter frequency determined for each individual versus the whole subject group were found, the resulting moment-EMG relationships determined using the different filter parameters were very similar. Therefore, although large differences between subjects were found, the model used in this study was not sensitive to changes in the high-pass frequency. Because of this, the high-pass frequency optimised for the whole group (Table 4.3 and 4.4 for SOL and TS, respectively) is appropriate to use.

By contrast, the optimum low-pass filter frequencies for the linear envelope were consistent across subjects. Regardless of whether the plantar flexors were modelled using SOL or TS, the optimum low-pass filter frequency ranged between 1.0 – 1.7 Hz, which is similar to values that have previously been reported for the triceps surae (1.0 – 1.6 Hz; Olney & Winter, 1985) and other (1.0 – 2.8 Hz; Olney & Winter, 1985; Potvin & Brown, 2004b) muscles. The relatively low optimum frequency found in the present study accords with the slow increase in force during the ramped isometric contraction,

although similar low-pass frequencies were reported in studies investigating sinusoidal changes in moment at faster rates (Olney & Winter, 1985; Potvin & Brown, 2004b). Therefore, the optimal low-pass filter frequency appears to be more consistent across subjects and muscles than the high-pass filter frequency, and a lower frequency appears to be ideal.

Within the current results, considerations should be made in regard to the methodology. The moment-EMG model was derived using data collected during isometric contractions, however the plantar flexors can act either isometrically or eccentrically as an antagonist. As such, differences in how the muscle performs isometrically as an agonist and isometrically or eccentrically as an antagonist, may affect the accuracy of the model when used to estimate plantar flexor antagonist moment. For example, differences are found in the muscle fascicle length and pennation angle, but not activation, during an isometric contraction when the muscle is acting as an agonist compared to an antagonist (Garner, Blackburn, Weimar, & Campbell, 2008). Interestingly, plantar flexor moment was not different between isometric and eccentric contractions for maximal or submaximal activations of the soleus (Pinniger, Steele, Thorstensson, & Cresswell, 2000); however, activation parameters were different between the different contraction types (Linnamo, Moritani, Nicol, & Komi, 2003; Pinniger et al., 2000). Together, this would cause a change in the moment-EMG relationship, thus potentially reducing the validity of the model developed in the current study. Developing a more valid model would result in an increase in its complexity, which may be problematic when antagonist moment estimation is not the study's main focus. Therefore, the current angle-moment-EMG model can be recommended over other current methods when estimates of plantar flexor antagonist moments are required.

Further methodological considerations relate to the accuracy of the moment-EMG model. First, unpreventable heel-lift occurs during maximal plantar flexor MVCs, which would alter the position of the ankle and subsequently the length of the plantar flexors (Arampatzis et al., 2005). Hof and van den Berg (1977b) found that the moment-EMG relationship became more curved when heel lift occurred. The flexed knee position used in the present study would have reduced the length, and thus the force contribution, of GM and GL and subsequently reduced the overall heel-lift (Arampatzis, De Monte, & Morey-Klapsing, 2007; Simoneau, Longo, Seynnes, & Narici, 2012). Second, although

TA activity was used to represent activity of the dorsiflexors, whilst the triceps surae (SOL, GM and GL) activity was used to represent activity of the plantar flexors, other muscles do contribute force to the dorsiflexor (i.e. extensor hallucis longus, extensor digitorum longus, and peroneus tertius) and plantar flexor (i.e. flexor hallucis longus, flexor digitorum longus and tibialis posterior) moments. Nonetheless, TA is the largest dorsiflexor and contributes approximately 57% of the total volume (Fukunaga et al., 1996a), whilst SOL, GM and GL contribute approximately 75% of total plantar flexor volume (Fukunaga et al., 1996a) and approximately 70-80% of the plantar flexor moment (Murray et al., 1976; Sale, Quinlan, Marsh, McComas, & Belanger, 1982). Importantly, because linear moment-EMG relationships were found in the present study, the assumptions that heel lift was minimal and the use of TA, SOL, GM and GL are representative of the dorsi- and plantar-flexors appear to be valid (Brown & McGill, 2008; Hof & Berg, 1977b; Kutch & Buchanan, 2001). In addition, it has previously been shown that reliability of the moment-EMG model used in the current study is high both within- and between-days (Kellis et al., 2005). Therefore, effects of these methodological concerns within the present study are minimal.

Conclusion

In summary, when measurements are completed with the knee flexed, either soleus or an equal weighting of soleus, gastrocnemius medialis and gastrocnemius lateralis (i.e. triceps surae) can be used to model plantar flexor moment using a linear moment-EMG model. The change in the slope of this linear model can then be modelled across joint angle with good accuracy using a 2nd-order polynomial, allowing plantar flexor moment to be estimated throughout all angles and intensities. There were no differences in the accuracy of the model when soleus and the triceps surae muscles were used to represent the plantar flexors, whilst the knee was flexed. Of the filtering variations investigated, only the low-pass filter frequency appeared rigid in requirement, with a lower frequency (1 – 1.7 Hz) being optimal. Therefore, when it is necessary to correct for plantar flexor antagonist contribution to total joint torque the angle-moment-EMG model presented (linear moment-EMG relationship adjusted for joint angle using a 2nd-order polynomial), whilst using the grouped filtering parameters in Table 3 and 4, is recommended.

Application to Musculoskeletal Modelling

Modelling muscle force *in vivo* requires calibrating the model to the individual. This necessitates the calculation of force during the calibration procedure, of which the only non-invasive approach is to measure joint moment. Removal of the antagonist moment is important for valid calculation of TA force from the joint moment (Arampatzis et al., 2005; Billot et al., 2010; Maganaris et al., 1998; Simoneau et al., 2009). Previous methodologies to remove the antagonist plantar flexor moment have not taken into account the full range of motion and full activation profile of the muscle group. The model presented in the current study provides a more complete approach to accounting for plantar flexor co-contraction across the full range of motion and full activation profile. This is important because, as shown in the current study, plantar flexor moment-EMG relationships are not the same across the range of motion. This new plantar flexor moment-EMG model can be used to allow for a more accurate calculation of TA muscle force from ankle joint moment measures *in vivo*.

Chapter Five

Integrating Ultrasonography Into A Subject-Specific EMG-Driven Model

ABSTRACT

EMG-driven models used to calculate muscle force commonly use the joint rotation to represent the change in length of the contractile components of the muscle. Ultrasonography provides direct *in vivo* observation of the muscle itself. Using this methodology, the aim of this study was to compare two models on their accuracy of calculating tibialis anterior muscle force. The two models differed only on how the contractile component of the muscle was modelled; muscle-length or joint-angle. A "traditional" EMG-driven model was incorporated, which fits a normalised (to isometric) force-velocity relationship to the subject, with electromyography of the muscle being used to scale the isometric force. Validation of the two models was performed using two isometric, two concentric and two eccentric contractions (modelled force was compared to actual force calculated from the joint moment and tibialis anterior moment arm). The two models (muscle-length and joint-angle) performed equally for five of the validation contractions. For the fast concentric contraction, the muscle-length model performed poorly (%RMSE = 20.0 ± 4.0 vs. 67.5 ± 31.6 % for joint-angle and muscle-length models, respectively; effect size = 2.7). In conclusion, under controlled conditions where the discrepancy between muscle and whole muscle-tendon unit (estimated from joint angle change) length change is minimal, the use of ankle angle data as input into an EMG-driven model is appropriate.

INTRODUCTION

The quantification of tibialis anterior (TA) forces *in vivo* is important in order to (i) better understand its role in human movement (Chleboun et al., 2007b; Hortobágyi et al., 2009; Neptune et al., 2009; Nilsson, Thorstensson, & Halbertsma, 1985; Prilutsky & Gregor, 2001; Segers et al., 2007), (ii) allow a more complete analysis of pathological movement patterns (e.g. in drop-foot; Burridge, Wood, Taylor, & McLellan, 2001; Byrne et al., 2007; Geboers, Drost, Spaans, Kuipers, & Seelen, 2002; Lyons, Wilcox, Lyons, & Hilton, 2000; Weber et al., 2005), and (iii) provide insight into the underlying causes of overuse injuries such as chronic anterior compartment syndrome (Allen & Barnes, 1986; Birtles et al., 2002, 2003; Diebal, Gregory, Alitz, & Gerber, 2012; Edmundsson, Toolanen, & Sojka, 2007; Padhiar & King, 1996; Puranen & Alavaikko, 1981; Randall, Styf, Pedowitz, Hargens, & Gershuni, 1997). Since direct measurement of muscle and tendon forces *in vivo* cannot be performed without the use of invasive methodologies, such as the buckle transducer (Fukashiro et al., 1995; Gregor et al., 1991) or fibre-optic technologies (Arndt et al., 1998; Finni et al., 2000), most investigations requiring muscle force estimations have incorporated a modelling based approach (Hamner et al., 2010; Hardt, 1978; Neptune et al., 2009; Wright et al., 1998; Xiao & Higginson, 2010).

Estimate *in vivo* muscle forces is commonly performed using inverse dynamics, forward dynamics and electromyogram-driven (EMG-driven) modelling approaches. Forward dynamics and EMG-driven approaches are typically used when individual muscle forces are required, as inverse dynamics models are only accurate for the estimation of total joint moments. Both forward dynamics and EMG-driven approaches require the use of a series of models (or modelling steps), largely linked to the influences of muscle activation (i.e. EMG; Bigland & Lippold, 1954a, 1954b; Lippold, 1952), length (Abbott & Wilkie, 1953; Gordon et al., 1966a, 1966b) and shortening-lengthening velocity (Hill, 1938, 1964) on muscular force output. Generic versions of these models can be applied widely, although they may in some ways include scaled anthropometric parameters that are specific to an individual (e.g. Hoy et al., 1990; White & Winter, 1992). Nonetheless, the use of either generic or scaled models does not allow for accurate estimates of muscle forces, because of the significant anthropometric variability between individuals (Correa et al., 2011; Scheys et al., 2008; Scheys et al., 2008). Therefore, when accurate muscle force estimates are required, models that are uniquely designed to specifically fit an individual are required.

Musculoskeletal models commonly incorporate the muscle (or muscle-tendon) force-length and force-velocity relationships, with a scaling factor included for muscle activation intensity (i.e. amplitude). Importantly, the parameters of "length" and "velocity" must refer to that of the contractile unit itself (Ito et al., 1998) rather than the whole muscle-tendon unit, as changes in tendon length are rarely synonymous with changes in muscle length (Baratta & Solomonow, 1991; Fukashiro et al., 1995; Fukashiro et al., 1995; Ichinose et al., 2000; Ito et al., 1998; Kawakami, Ichinose, & Fukunaga, 1998; Kubo, Kawakami, & Fukunaga, 1999; Zajac, 1989). This is of particular importance when a long tendon is situated in the body segment of interest, such is the case for the TA. Previous EMG-driven models have implicitly assumed that the change in muscle length is synonymous with change in joint ankle (which is used to predict whole muscle-tendon length). However, this assumption is flawed in nearly all movement conditions because of the elastic nature of the tendon (Baratta & Solomonow, 1991; Fukashiro et al., 1995; Fukashiro et al., 1995; Ichinose et al., 2000; Ito et al., 1998; Kawakami et al., 1998; Kubo et al., 1999). Therefore, using direct measures of the change in muscle length, as opposed to change in ankle angle, as an input variable to represent the contractile components is likely to provide more accurate (e.g. compared to: Olney & Winter, 1985; White & Winter, 1992) subject-specific modelling results, and thus allow for the calculation of more realistic TA muscle force magnitudes *in vivo*.

Given the above, the aim of the present study was to develop a subject-specific EMG-driven model for TA. This model uses muscle length changes measured using ultrasonography during prescribed movements to represent the contractile components of the muscle. The model was compared to a second model, which is similar to previous models in that the change in ankle angle was used to model the contraction component (i.e. tendon length changes during contraction were not accounted for).

METHODS

Model Overview and Rationale

The model used in this study shares similarities with previous models used to estimate muscle force output (e.g. Olney & Winter, 1985; White & Winter, 1992). It is based on a force-velocity sub-model that is scaled to isometric force. As such, the model uses 'velocity' as its main input. This scaled force-velocity sub-model was then used to

calculate force across muscle lengths and activation levels. Changes in the force-velocity relationship (i.e. curvature and maximal force) across muscle lengths and activation levels are removed when normalising to isometric force (Abbott & Wilkie, 1953; Bigland & Lippold, 1954b; Matsumoto, 1967). Additionally, maximal shortening velocity has been suggested to be constant across a range of intensities and muscle lengths (Edman, 1979), and it was thus assumed that a single force-velocity sub-model, scaled to isometric force, was appropriate.

To determine the isometric force for calculation of absolute forces from the normalised force-velocity sub-model, a second sub-model was used, which calculated isometric force for all contraction intensities and muscle lengths. This second sub-model used muscle activation and length as inputs; an approach similar to that used in Study 2 for the plantar flexors was used here for TA. Briefly, a force-EMG relationship was produced for each muscle length, with the slope of this relationship being obtained over the full muscle length range. Thus, isometric force for all muscle lengths and contraction intensities was determined.

Two models were developed using the above approach, incorporating either muscle length (named "muscle-length model") or joint angle (named "joint-angle model") to represent the contractile components. Therefore, the procedures outlined below in 'developing the model' apply to both approaches.

Subjects

To assess the accuracy of the proposed model, four adults (3 men and 1 woman) who were free from musculoskeletal injury gave their informed consent and volunteered for the study (age = 26 ± 1 yr, height = 1.79 ± 0.05 m, mass = 75.6 ± 12.0 kg; μ ± SD). Ethics approval was granted by the Brunel University Ethics Committee, and all procedures were conducted in accordance with the Declaration of Helsinki.

Familiarisation

Several days before testing, each subject completed an extensive familiarisation protocol in which the methods involved in the testing were practiced. Specifically, the subjects completed the specified warm-up (a series of sub-maximal and maximal contractions of both the plantar- and dorsiflexors), slow ramped maximal plantar flexor contractions, and both low-intensity and maximal isometric, concentric and eccentric

dorsiflexor contractions. During dorsiflexions, the subjects were instructed to rotate their foot toward their shin without deliberate extension of their toes. To focus on activation of the triceps surae musculature during plantar flexion contractions, the subjects were directed to rotate their ankle (rather than pressing with the whole leg) and to push through the ball of their foot without flexing their toes. Following familiarisation, the seat position of the dynamometer was recorded in order to maintain consistency between the familiarisation and testing sessions.

Data Collection

The subjects were seated in an isokinetic dynamometer (Biodex System 3, Biodex Medical Systems, Inc., NY) so that the lateral malleolus was aligned with the centre of rotation of the dynamometer, and the relative knee and hip angles in the sagittal plane were both approximately 80° (0º = full extension), and the torso reclined to 70º relative to the horizontal. A limb-support pad was placed under the thigh proximal to the origin of the gastrocnemii muscles. Hook-and-loop straps were securely fastened over the metatarsals to prevent movement of the foot relative to the footplate, and straps were placed tightly across the thigh, torso and waist to limit movement of the upper body, leg and ankle joint. An ankle angle of 0° was taken as neutral (taken when the sole of the foot was perpendicular to the tibia), with plantar flexion being a positive angle and dorsiflexion being negative. The joint angle, velocity, and torque data underwent analogue-digital conversion at 1000 Hz and were captured using Spike 2 software (version 5, CED, Cambridge, UK).

Soleus (SOL), gastrocnemius medialis (GM), gastrocnemius lateralis (GL) and tibialis anterior (TA) muscle activities were recorded synchronously with the angle, velocity and joint moment data using bipolar surface EMG procedures (Telemyo 2400R, NorAxon USA Inc., Arizona). Electrodes were positioned in accordance with the Surface Electromyography for the Non-Invasive Assessment of Muscles (SENIAM) project, and in line with the estimated fascicle line of action. Specifically, the electrodes were placed at 2/3 of the line between the medial epicondyle of the femur to the medial malleolus on SOL, on the most prominent bulge of the GM, and at 1/3 distance on the line between the head of the fibula and the heel on GL. For the TA, the electrodes were placed at 1/3 distance on the line between the tip of the fibula and the tip of the medial malleolus. A reference electrode was placed on the medial aspect of the tibia. All EMG signals were band-pass filtered before being full-wave-rectified and then low-pass

filtered to produce a linear envelope. The triceps surae muscles (SOL, GM and GL) were processed using the methods developed in Study 2, i.e. a 4th-order, zero-lag, Butterworth filter with a band pass of 104-450 Hz, followed by a 6th-order, zero-lag, Butterworth filter with a 1.5-Hz cut-off. TA EMG signals were filtered using a similar procedure, but a 20-450 Hz band pass, and 4 Hz low pass, cut-off was used (Winter, 2009).

Prior to application of the electrodes, the skin was shaved and lightly abraded using fine sandpaper before being cleansed with an alcohol-based spray (Chlorhexidine Gluconate Solution, Hyrdex). Inter-electrode spacing was 20 mm and the baseline interference for each muscle was required to be less than 1 kΩ (Winter, 2009), assessed using an ohmmeter. When the required baseline was not achieved, a combination of using new electrodes and re-preparing the site was performed.

A 10-MHz, 50-mm linear-array, B-mode ultrasound probe (Esaote Megas GPX, Genova, Italy) was housed in a custom-made foam case and strapped to the anterior lower leg in line with the TA tendon-aponeurosis complex in order to track the muscle-tendon junction (MTJ) during the passive ankle rotations. An electroconductive gel was placed on the surface of the probe prior to fixation to aid acoustic contact, with a thin echo-absorbent strip being placed on the skin under the probe to allow probe movement to be quantified, and then mathematically corrected in post-processing if required. The ultrasound images were continuously recorded to VHS tape at 25 Hz and synchronised with the dynamometer-derived joint angle data using a 5-V electrical trigger (model DS7A stimulator, Digitimer, Hertfordshire, UK).

Experimental Procedures

Each subject's full range of motion (ROM) was determined and subsequently used during testing. Eight equidistant ankle angles were determined for each subject. These positions were used when isometric contractions of the plantar- and dorsiflexors were performed. The foot was rotated passively about the ankle at $20°·s^{-1}$ through its ROM for three consecutive rotations (start and finish in dorsiflexion) whilst ultrasound recordings of the MTJ were obtained. Data from this procedure were used to determine TA moment arm values (described below).

To account for plantar flexor co-contraction in subsequent dorsiflexion contractions, a series of maximal plantar flexor contractions were performed across the ROM. At each of the eight equidistant angles, the subjects performed a slow ramped isometric plantar flexor maximal voluntary contraction (MVC). Joint moment rise time during MVCs was approximately 5 s, and was guided by the experimenter.

At each of the eight angles the subjects performed a dorsiflexion MVC and a series of submaximal dorsiflexion contractions. The dorsiflexion MVC was used to determine peak EMG, thus it was not deemed important to strictly control the rate of force rise. Subjects were encouraged to maintain a maximal contraction for approximately three seconds. For the sub-maximal isometric dorsiflexion contraction, the subjects were guided to increase the contraction intensity until the MTJ (seen on the ultrasound monitor) reached a marker placed on the screen, with approximately four contractions being performed at each muscle length. The same marker was used for measurements obtained at each of the 8 ankle angles, thus resulting in the acquisition of data during isometric contractions at a range of contraction intensities but at the same muscle length. The marker was then moved and the contractions repeated so that data were obtained at 6-8 muscle lengths (fewer muscle lengths were tested if a subject was unable to accurately target the marker, in order to minimise fatigue). Each sub-maximal isometric contraction was held for approximately 2-3 s. These contractions were then used to produce the force-EMG relationship for each muscle length.

To produce the force-velocity relationship, a series of maximal contractions were performed at six concentric and five eccentric joint angular velocities. For the concentric contractions, the foot was placed in full plantar flexion before the subject maximally dorsiflexed through their full ROM. Concentric contractions were performed at 10, 20, 45, 60, 90 and $120°·s^{-1}$. These velocities were chosen because subjects found it difficult to accelerate the footplate to the required velocity when the system was set to higher angular velocities during pilot testing, meaning that no iso-velocity phase was achieved (this is an essential element of measurement validity; Bartlett & Payton, 2007). For the eccentric contractions, the subject rotated their foot to full dorsiflexion before resisting the lever arm rotation caused by the isokinetic dynamometer through the ROM. Eccentric contractions were performed at 10, 20, 45, 60 and $90°·s^{-1}$. The $120°·s^{-1}$ velocity was not used for eccentric testing because it was found that eccentric

forces plateaued prior to this velocity during pilot testing. Thus, because this velocity was deemed unnecessary, it was excluded.

To assess the accuracy of the model, a separate series of six contractions were performed. Two isometric contractions were performed each at 0 and 20° plantar flexion. No guidance was provided on the rate of rise, but the subjects were instructed to maintain maximum intensity for approximately 2-3 s. Two concentric and eccentric contractions were performed at 10 and $90°·s^{-1}$, using the same procedures as the main data collection.

Data Processing

TA Muscle Length Measurement

MTJ displacement was manually digitised in all ultrasound video fields (50 Hz; Peak Motus, Peak Performance Technologies Inc., Colorado) and the data low-pass filtered with a fourth-order, zero-lag, Butterworth filter with a 6-Hz cut-off frequency. This filter protocol was selected following residual analysis (as described in Winter, 2009) and was used for all repetitions except for calculation of TA moment arm, where a sixth-order, zero-lag, Butterworth filter with a 1-Hz cut-off frequency was used (see Study 1). The distance between the MTJ and the shadow caused by the echo-absorbent strip on the skin was measured continuously during digitisation. A stationary ultrasound scan was taken of the TA origin on the proximal head of the tibia, with a second thin echo-absorbent strip being placed on the skin under the probe. The distance between the TA origin and the shadow of this strip was calculated during digitisation. Finally, the distance between the two echo-absorbent strips on the skin was measured using an anthropometric tape measure placed against the skin. The TA muscle length was then calculated as the sum of these three distances (i.e. MTJ-strip one, strip one-strip two and strip two-origin).

TA Force Calculation

TA force (F_{TA}) was calculated from dorsiflexor moment (M_{DF}) and TA moment arm (r) using the equation:

$$F_{TA} = M_{DF}/r$$

Dorsiflexor moment was calculated from total joint moment (M_J), passive joint moment (M_{pass}) and plantar flexor moment (M_{PF}) using the equation:

$$M_{DF} = M_J - M_{pass} - M_{PF}$$

93

Because M_{PF} is acting in the opposite direction, subtraction of this is equivalent to adding the absolute plantar flexor moment.

Moment Arm Calculation

The TA moment arm was calculated using the tendon excursion method derived in Study 1. Specifically, a passive dorsiflexion rotation was used, with the correction for tendon length change included. This correction for tendon length change, was modelled on the group mean from Study 1. Although individual differences will be present, the validation contractions will utilise the same moment arm measurements, and so any errors will be consistent between model development and validation. As such, any errors due to moment arm measurements may affect the validity of the force measurements, but not the accuracy of the modelling process used.

Importantly, this procedure only provides muscle-tendon moment arm distance under passive conditions, yet TA moment arm increases with contractile intensity (Maganaris, 2000). To account for this, it was assumed that moment arm increases were linearly related to contractile intensity, allowing a correction using TA EMG as a measure of contractile intensity to be utilised. The resultant model was:

$$(1 + [0.3 \times EMG / EMG_{max}]) \times passive\ moment\ arm$$

where *EMG* is the TA EMG collected during the measurement and EMG_{max} is the maximum TA EMG (see below). This allowed for a linear increase in moment arm with contractile intensity, up to a 30% increase in moment arm for maximal contractions (based on findings from Maganaris, 2000).

Maximal TA EMG

Maximal TA EMG was required to allow for the correction of moment arm with intensity. Only a single value was used for EMG_{max} as maximal TA EMG was found to be similar across the ROM (coefficient of variation [CV] for individual subjects was $10.6 - 18.5\%$). The maximum mean EMG over a 250-ms range from each of the 8 isometric dorsiflexion MVCs was calculated, with the mean of these taken to represent maximal TA EMG (i.e. EMG_{max}).

Accounting for Plantar Flexor Co-Contraction

The model derived in Study 2 was used. Briefly, a linear relationship was fitted to the moment-EMG data of the plantar flexors collected during the slow-ramped plantar

flexion MVCs at each angle. The linear relationship was forced through the origin so that zero activation related in zero plantar flexor moment being calculated. The slope of this relationship was then plotted against joint angle, with a second-order polynomial being fitted to this relationship. The equation of the 2nd-order polynomial was then used to find the slope of the moment-EMG relationship at any muscle length or ankle angle, allowing plantar flexor moment (M_{PF}) to be estimated from plantar flexor EMG. The plantar flexors were modelled as the equal weighting of SOL, GM, and GL (i.e. the triceps surae muscle group).

Passive Ankle Joint Moment

At each of the eight equidistant angles, mean passive ankle joint moment was measured during a 3-s period in which the subject relaxed. The mean passive joint moment-angle data was fitted with a 3rd-order polynomial (which optimised the R^2 value). This was then used to calculate M_{pass}, which was required to calculate dorsiflexor moment (M_{DF}).

Developing the Model

The main aim of this study was to compare an EMG-driven model utilising muscle length (muscle-length model) or ankle angle (joint-angle model) to represent the contractile components. As such, two models were developed. The processes described below refer to the muscle-length model. However, these procedures were also used in the joint-angle model.

Force-EMG Sub-Model

For each sub-maximal contractions, ankle angle, TA muscle length and TA force were recorded. The mean for each variable over the portion of constant muscle length during the sub-maximal contraction was calculated. Data were then grouped by muscle lengths, providing force-EMG data for 6-8 muscle lengths. A similar procedure to that used for modelling plantar flexor moment-EMG relationships was incorporated here to model TA force-EMG relationships. The force-EMG data were modelled with a linear fit (forced through the origin) at each muscle length. The slope of this relationship was then modelled with a 2nd-order polynomial across muscle lengths. This then allowed the force-EMG relationship to be calculated at any muscle length.

Force-Velocity Sub-Model

Only the iso-velocity regions of the concentric and eccentric contractions were used (Bartlett & Payton, 2007) to develop the force-velocity relationships. As previously described, a single force-velocity relationship normalised to isometric force was produced. Force was normalised using the estimated isometric force for the specific muscle length and activation (using the force-EMG sub-model developed). The mean normalised force for the full contraction at each velocity was calculated, and used to fit the force-velocity model. As such, there were a total of 11 points (mean normalised force for each velocity) to which the model could be fitted. It was observed that muscle velocity was constant throughout each contraction. Therefore, the slope of a linear fit applied to the muscle length-time data was taken as the muscle velocity for each contraction. Ankle velocity data were obtained from the isokinetic dynamometer.

Concentric data were modelled using the Hill-equation (Fenn & Marsh, 1935; Hill, 1938, 1964), fitted using a non-linear least squares approach:

$$F = (F_{iso} \times b - a \times v) / (b + v)$$

where F is TA force, F_{iso} is the calculated isometric force for the specific muscle length and activation level, v is the velocity of the muscle length change, and a and b are constants. Because force was normalised to the isometric force, the term '$F_{iso} \times b$' was reduced to 'b' (i.e. $F_{iso} = 1$).

Eccentric force, and its relation with movement velocity, has not been investigated in as much detail as concentric force (Nigg & Herzog, 2006). A consequence of this is that no generically accepted model has been developed to represent the eccentric portion of the force-velocity relationship. Of note, a much greater rise in force for given change in velocity of lengthening compared to shortening has been reported around the isometric point (Edman, 1988), resulting in an almost plateau-like relationship between force and lengthening velocity. This was found in the present study (supported by the %RMSE values for this portion of the force-velocity relationship; see "Results"). Thus, for the purposes of this study, the eccentric portion was modelled as a constant, taken as the mean of the data from the five eccentric contraction velocities.

Model Use and Validation

To estimate force using the model, TA EMG and muscle length (or ankle angle in the joint-angle model) and velocity data were required. Muscle velocity was input into the

force-velocity sub-model to determine the relative (to isometric) force. TA EMG and muscle lengths (or ankle angle) were entered into the force-EMG model to determine the isometric force. This allowed for absolute force to be calculated from the relative (to isometric) force.

For each of the six validation contractions, force was calculated in three ways: (1) directly from the data collected (accounting for plantar flexor co-contraction and using the moment arm to calculate muscle force), (2) using the EMG-driven model based on muscle kinematics and (3) using the EMG-driven model based on ankle kinematics.

The joint moment data from the point at which 50% MVC (measured using M_J) was achieved during the initial rise until the ankle joint moment dropped below 50% MVC was used. For the concentric and eccentric contractions, only the data obtained during the iso-velocity (constant angular velocity) phase were used (Bartlett & Payton, 2007).

Statistical Analysis

The relative root mean square error (%RMSE) was used to compare the accuracy with which each model estimated TA force during the validation contractions. Effect sizes were used to compare between the different approaches (muscle-length vs. joint-angle) for each validation contraction. Effect sizes (ES) were calculated using Cohen's *d*. The pooled SD was used as the standardiser, being calculated as the square root of the mean variances (Cohen, 1988; Fritz et al., 2012). For descriptive purposes, effect sizes of 0.2, 0.5 and 0.8 were determined as small, medium and large, respectively (Cohen, 1988).

RESULTS

Force-EMG Sub-Model

Force-EMG relationship at each position was fitted with a linear relationship, with the slope of these linear relationships modelled across the muscle lengths or ankle angles using a 2nd-order polynomial. This model fit was equivalent when either muscle length or ankle angle was used to represent the contractile components (%RMSE = 18.3 ± 10.1 and 18.1 ± 6.5 % for angle and length models, respectively; %RMSE calculated across all positions and subjects). Mean %RMSE for individual subjects across positions ranged from 15 ± 9 to 23 ± 12% for the angle model and from 15 ± 8 to 21 ± 5% for the length model. Therefore, although error was associated with this approach to modelling

the force-EMG relationship, using either ankle angle or muscle length to represent the contractile components produced similar results.

Force-Velocity Sub-Model

The accuracy of the sub-model derived using the force-velocity relationship was assessed for concentric and eccentric parts individually. Small differences in the accuracy of the concentric force-velocity model (%RMSE = 9.1 ± 1.9 and 10.1 ± 4.4% for angle and length, respectively; ES = 0.3) and the eccentric force-velocity model (%RMSE = 9.5 ± 2.7 and 10.4 ± 3.9% for angle and length, respectively; ES = 0.3) were found between angle and length approaches. There was no difference in the fit between the concentric and eccentric force-velocity models when the contractile components were modelled using the ankle angle (ES = 0.16) or muscle length (ES = 0.07).

Ankle Angle vs. Muscle Length as Model Inputs

The TA contractile component was modelled using either 'ankle angle' or 'muscle length' as inputs, with six different contractions being used to assess the accuracy of these approaches (see Table 5.1). For four of the six validation conditions, small differences were found between the two approaches to modelling the contractile components of TA. For the fast concentric condition, the angle model predicted TA force better (ES = 2.7) whilst the length model predicted TA force better for the slow eccentric condition (ES = 0.7), although this was only a difference in %RMSE of 2.8 %.

Table 5.1. Validation results of the muscle-length and joint-angle models. Overall, minimal differences were seen between the two approaches, although the model performed poorly for the fast concentric contraction when 'muscle length' was used as the model input. *large effect size.

Condition	Joint-angle model	Muscle-length model	ES
Isometric (0°)	15.1 ± 4.4	16.3 ± 6.1	0.2
Isometric (20°)	20.4 ± 8.6	19.9 ± 7.1	0.1
Concentric ($10°·s^{-1}$)	16.6 ± 5.6	19.2 ± 6.4	0.4
Concentric ($90°·s^{-1}$)	20.0 ± 4.0	67.5 ± 31.6	2.7*
Eccentric ($10°·s^{-1}$)	17.1 ± 3.6	14.3 ± 4.7	0.7
Eccentric ($90°·s^{-1}$)	13.5 ± 7.3	15.5 ± 7.4	0.3

DISCUSSION

The main aim of present study was to investigate the effect of using 'muscle length' (muscle-length model) instead of 'joint angle' (joint-angle model) as the input in a subject-specific EMG-driven TA muscle force model. The model was designed to eliminate potential errors in assuming that the length of the whole muscle-tendon unit (calculated from changes in joint angle) is synonymous with actual muscle length, and thus both muscle length and shortening-lengthening velocity inputs were altered. The results showed that the use of 'muscle length' and 'joint angle' inputs in the model resulted in similar muscle force estimates through most joint ranges of motion, however the muscle-length model produced poorer estimates of TA force during fast ($90°·s^{-1}$) concentric dorsiflexion contractions. Under the conditions used to determine the validity of the models in the current study, the joint-angle model provided a better approach to estimating TA force. However, as discussed below, important considerations must be made when discussing further application of these models to more complex movements (e.g. walking) where greater discrepancies between 'muscle' and 'muscle-tendon' length might occur.

For most of the muscular contractions used for model validation, both approaches to estimating muscle force (i.e. direct measurement of muscle length using ultrasound

versus the estimation of 'muscle' length from changes in ankle joint angle) performed with similar levels of accuracy. Both models were developed using the same procedures and, importantly, the validation conditions used were similar to those incorporated into the modelling process. As such, it is not surprising that both approaches performed similarly, due to the validation being comparable to that used for developing the models. Unfortunately, use of isokinetic dynamometry limits the possible variability of contractions due to the requirement for an iso-velocity movement phase to be achieved (Bartlett & Payton, 2007). Further research should focus on testing these two approaches for estimating muscle forces in more complex (unconstrained) movements, e.g. gait. However, measuring force directly, which is required to check the accuracy of the models under such conditions, is not possible in these movements without the use of invasive technologies (Arndt et al., 1998; Finni et al., 2000; Fukashiro et al., 1995; Gregor et al., 1991).

Muscle forces estimated using the muscle-length EMG-driven model were very different (i.e. the model performed poorly) to those measured from joint moment recordings during fast concentric dorsiflexions but not during slow concentric or fast eccentric dorsiflexions. In other muscle groups, during fast isokinetic concentric knee extensions, shortening of the vastus lateralis was not constant (Ichinose et al., 2000), with the action of the vastus lateralis muscle and tendon mirroring that of a slingshot (i.e. muscle velocity increased during the first half, before reducing during the second half of the contraction). One possibility is that the potentially difference between muscle and muscle-tendon unit shortening velocity was not detectable during the validation contractions because the resolution or sampling frequency (25 Hz) was insufficient. However, Ichinose et al. (2000) used an ultrasound sampling rate of 30 Hz with success, so any mismatch between muscle and muscle-tendon unit action should have been visible using the techniques in the present study as well.

An alternative explanation is that the force-velocity sub-model was not appropriate for estimating muscle force at the faster concentric velocities. Data from only one contraction at each velocity was used to fit the force-velocity model. Although more contractions would have been preferred, a large number of contractions had to be performed by the subjects throughout the testing session. Increasing the number of contractions and thus the total contraction time would have also increased the likelihood of fatigue. However, the goodness-of-fit of the force-velocity sub-model on the original

data was adequate (10.1 ± 4.4%) and was similar to when ankle angle was used as the input to the model (9.1 ± 1.9%). Although a complete familiarisation procedure was used on a previous day, and the fit of the force-velocity model was good, differences in technique used by the subject in the validation contraction at the faster concentric velocity and that used to fit the model may explain the poor accuracy of the length-based model in this condition. Interestingly, this poor accuracy was observed for all four subjects (%RMSE = 25.5, 80.7, 63.8 and 99.9% for the individual subjects), but was not mirrored when the joint-angle model was used instead of the muscle-length model despite the same contractions being used. As it is unlikely that all four subjects performed differently in this one condition, and that it thus only affected the muscle-length model, differences in the contractions used to fit the model versus those used to test the model are not likely to be the source for the findings at the fast concentric speeds. Future research should test whether this finding is repeatable, and to investigate the mechanisms underpinning it.

Although similar levels of accuracy were found between the two approaches for modelling the contractile component, caution must be employed before deciding on the use of ankle angle as a model input (which may be useful because it simplifies the approach) instead of muscle length. Of note, validation conditions were very controlled within the current study and, although differences between joint angle-derived and directly-measured (ultrasound-based) muscle length changes do occur under these controlled conditions (i.e.Fukashiro et al., 1995; Ichinose et al., 2000; Ito et al., 1998), these differences are small compared to those that occur in complex movements involving stretch-shorten cycle actions, such as walking (Chleboun et al., 2007a; Ishikawa et al., 2007; Lichtwark et al., 2007), running (Ishikawa & Komi, 2008; Ishikawa et al., 2007; Lichtwark et al., 2007), hopping (Lichtwark & Wilson, 2005; Sano et al., 2012) and jumping (Fukashiro et al., 2006; Kurokawa et al., 2001). As such, future studies are required to further investigate the possible differences between the two modelling approaches in more complex movements.

Conclusion

In conclusion, under controlled conditions where the discrepancy between muscle and whole muscle-tendon unit (estimated from joint angle change) length change is minimal, the use of ankle angle data as input into an EMG-driven model is appropriate. However, further research is required to ascertain the validity of this simplification in

more complex movements where stretch-shorten cycle actions might produce a greater discrepancy between muscle and muscle-tendon length.

Application to Musculoskeletal Modelling

Within the current study, it has been shown to be viable to use ultrasonography to separate the actions of the tendon and muscle when modelling muscle forces *in vivo*. This has important implications for future approaches to modelling muscle forces. Previously, *in vivo* muscle forces have been estimated through tracking of the length changes of the whole muscle-tendon unit. Importantly, this does not account for tendon length changes being different to muscle length changes (Baratta & Solomonow, 1991; Fukashiro et al., 1995; Fukashiro et al., 1995; Ichinose et al., 2000; Ito et al., 1998; Kawakami, Ichinose, & Fukunaga, 1998; Kubo, Kawakami, & Fukunaga, 1999; Zajac, 1989). As such, tracking muscle-tendon unit length changes may lead to invalid estimates of muscle force. The alternative approach to modelling the contractile component in the current study is a potential solution that accounts for the problems accounted when using the muscle-tendon unit to represent the contractile component. Future applications of this modelling approach in more dynamic conditions provides an opportunity to estimate muscle forces *in vivo* with more validity when tendon and muscle actions are not synonymous i.e. walking (Chleboun et al., 2007a; Ishikawa et al., 2007; Lichtwark et al., 2007), running (Ishikawa & Komi, 2008; Ishikawa et al., 2007; Lichtwark et al., 2007), hopping (Lichtwark & Wilson, 2005; Sano et al., 2012) and jumping (Fukashiro et al., 2006; Kurokawa et al., 2001).

Chapter Six

General Discussion

SUMMARY OF FINDINGS

Introduction

The tibialis anterior (TA) muscle plays an important role in human locomotion (Byrne et al., 2007; Franz & Kram, 2013; Gazendam & Hof, 2007; Kyrolainen et al., 2005; Scott et al., 2012), including assisting in improving efficiency by guiding the commencement of running over walking (Bartlett & Kram, 2008; Hreljac et al., 2008; Segers et al., 2007). Overuse of the TA muscle, particularly during gait, has been found to lead to the onset of chronic exertional compartment syndrome (Allen & Barnes, 1986; Edwards et al., 2005; Mouhsine et al., 2006; Touliopolous & Hershman, 1999). TA is therefore an important muscle and plays a key role in human movement and injury; measuring TA force production during the above scenarios would allow for a greater understanding of the role it has.

The overall purpose of this thesis was to develop a subject-specific EMG-driven force model whilst accounting for methodological concerns outlined above, which would allow for the accurate estimation of TA muscle force during complex movement. Within the first two studies (Chapters 3 and 4) the optimal procedures to allow calculation of TA force were investigated. These were utilised in Study 3 (Chapter 5) to assist in developing a subject-specific EMG-driven force model.

Measuring Tibialis Anterior Moment Arm

Two methods are commonly used to measure TA moment arm: the tendon excursion and the geometric method. In Study 1 it was shown that both of these methods, as they are currently employed, have methodological issues that reduce their validity. The greatest variable affecting accuracy was the changes in tendon length that affected the tendon excursion approach. However, it was also determined that two sources of error were present within the geometric method. The talus rotation, which is used to represent foot rotation when determining the centre of rotation, was not synonymous with foot rotation. Additionally, an alternative location of the TA line of action was presented, leading to a better agreement between the tendon excursion and geometric methods. Although the sources of error with the geometric approach were not as large as the error caused by tendon length changes, they still altered the subsequent moment arm estimations. Interestingly, once tendon length changes had been accounted for, the tendon excursion-derived moment arms presented a more physiologically valid relationship across joint angle.

Correcting for Plantar Flexor Antagonist Co-Contraction

When calculating agonist moment from joint moment, it is common practice to use a simple EMG-moment relationship to account for antagonist co-contraction. For this, an EMG-moment relationship is fitted to a series of contractions performed by the antagonist muscle group whilst, somewhat ironically, assuming the opposing muscle group is silent (something that is not assumed during collection of agonist moment). Additionally, an EMG-moment relationship is not collected for the full range of motion, and therefore may not be valid. These are important considerations, as any inaccuracies with accounting for co-contraction will affect the validity of the main data.

Accounting for plantar flexor antagonist co-contraction across the full range of motion was found to be possible through the use of modelling changes in the linear EMG-moment relationship across ankle angle. Importantly, this was regardless of whether the plantar flexors were modelled using all three triceps surae muscles, or only soleus, whilst the knee is bent. Along with the optimal EMG-processing procedures that were derived, this approach provides a good method for accounting for plantar flexor antagonist co-contraction, allowing a good estimation of dorsiflexor moment.

Modelling TA Force Using EMG and Muscle Length

The final part of this thesis (Study 3) was to investigate whether improvements in TA force estimations could be made when using muscle length, instead of joint angle, to model the TA muscle. Previous (e.g. Olney & Winter, 1985; White & Winter, 1992) attempts to model TA force output utilised joint angle. However, this assumed that the tendon is a stiff structure that does not change length. This is completely invalid, and thus may affect the accuracy of TA force estimations.

Interestingly, during the validation conditions utilised, the joint-angle approach provided a better estimate of TA force. Although potentially due to methodological concerns, these were counter-argued within Chapter 5 as not being likely. As such, the reason why the muscle-length approach was very poor at the fast concentric velocity is not known. This was found for all subjects, and thus should be further investigated.

APPLICATION TO MUSCULOSKELETAL MODELLING

The main aim of this thesis was to develop a subject specific EMG-driven model of the TA. However, the output from studies one and two can be implemented independently of this final modelling approach. When joint moment is measured (i.e. isokinetic dynamometry or inverse dynamics), the outputs from the first two studies can be used to calculate TA force in vivo from the data collected.

Calculation of TA (and other muscles) force production is performed using many different approaches with varying degrees of complexity. One main non-invasive *in vivo* approach is to use the ratio of joint moment to moment arm as an estimate of the muscle force. Within this approach, sometimes co-contraction of the plantar flexor muscle group is used to separate the joint moment into dorsi- and plantar flexor moments. Although this is a fairly simple procedure, errors are associated with the approach as presented in studies one and two within this thesis.

The output from this thesis allows for a more valid approach to using the ratio of joint moment to moment arm as an estimate of the muscle force. Specifically, the new method of measuring TA moment arm, whilst incorporating tendon length changes into the tendon excursion method, accounts for the moderate to large sources of error present in previous methodologies. Whereas previous methods were reliable and thus appropriate for within-subject comparison (i.e. repeated-measures study designs), due to errors, these methods are limited when valid measures were required for between-subject comparisons. Importantly, these errors would have led to invalid estimates of muscle force. As such, comparisons between individuals of both moment arm and force measures will be possible with good accuracy. For example, this provides the potential for investigations into the understanding of overuse injuries, such as chronic anterior compartment syndrome, through comparisons between symptomatic and asymptomatic individuals (see "future work").

A second improvement to future musculoskeletal modelling that is derived from this thesis is in relation to calculation of the dorsiflexor moment from the resultant joint moment. Accounting for plantar flexor co-contraction is necessary as presented in study two and other studies (Arampatzis et al., 2005; Billot et al., 2010; Maganaris et al., 1998; Simoneau et al., 2009). Therefore, appropriate methodology should be incorporated in future testing. The model developed in study 2 provides a good

approach to allow the experimenter to account for co-contraction of the planter flexor muscle group. Important improvements on previous approaches include the estimation of plantar flexor moment throughout all activation intensities and joint ROM, which are paramount for more valid estimations. Finally, this new approach requires few contractions to be performed during the testing procedure (six slow-ramped contractions used in this thesis), causing less fatigue than other approaches i.e. EMG biofeedback method (Billot et al., 2010). This provides experimenters the possibility of utilising a greater range of positions and intensities when investigating the role of the TA in human actions.

The inclusion of ultrasonography into subject specific EMG-driven musculoskeletal modelling provides an interesting approach going forward. It has been shown that the actions of the tendon and muscle are not synonymous with one another during dynamic human movements (Baratta & Solomonow, 1991; Fukashiro et al., 1995; Fukashiro et al., 1995; Ichinose et al., 2000; Ito et al., 1998; Kawakami et al., 1998; Kubo et al., 1999). Therefore, the separation of these two tissues is important to enhance the accuracy of musculoskeletal modelling. Interestingly, within the controlled conditions used in study 3, the accuracy at the fast concentric velocities of this new approach was less than the traditional approach of modelling the contractile components using joint rotation. However, this may be due to complications arising within the calibration and testing procedure that need to be investigated in future work (see "future work"). Nevertheless, the extension of these findings to more dynamic movements needs to be investigated as the accuracy of the new approach is likely to improve relative to the traditional approach within these dynamic movements.

FUTURE WORK

Future research based on the output of this thesis is primarily centred on two research aims. The first aim is to develop the final model, with the second aim being to implement the final model into gaining a greater understanding of the role of the TA.

Development of the EMG-driven model

The model developed in study 3 did not perform as well across all conditions as the traditional approach. This may be due to the complexities associated with calculating muscle force (i.e. force produced by the muscle and applied to the tendon) as opposed to calculating tendon force (i.e. force applied to the foot from the tendon). Within study 3,

it was assumed that muscle force and tendon force were synonymous. However, due to tendon lengthening and recoiling occurring, energy will be stored within and released from the tendon. This is likely to develop an inconsistency between the muscle force and tendon force. Consequently, new methodologies need to be developed to allow measurement of muscle and tendon force. Invasively, buckle transducers (Fukashiro, Komi, Järvinen, & Miyashita, 1995; Gregor, Komi, Browning, & Järvinen, 1991) or fibre optic technologies (Arndt, Komi, Brüggemann, & Lukkariniemi, 1998; Finni, Komi, & Lepola, 2000) can be used. Non-invasively, modelling of the complex interaction between tendon length, velocity and history (i.e. duration of stretch) will need to be included. Preliminary testing can then be used to associate these variables (i.e. tendon length, velocity and history) with force output of the tendon (i.e. stiffness, viscoelastic properties and creep). This tendon model can then be incorporated into the model proposed in study 3 to differentiate muscle force and tendon force.

Importantly, this will require constant monitoring of tendon length. For the TA, this would require an approach similar to that used in study 1 (i.e. combination of MRI and ultrasound). However, for other muscle groups, regression equations have been commonly used (i.e. triceps surae muscle group; Grieve, Pheasant, & Cavanagh, 1978) making these possible MTUs to assess the validity of the model without the need for more expensive MRI testing. Conversely, the simplicity of the mechanical set-up of the TA (i.e. single tendon) provides a potentially more controlled setting if tendon length changes are to be accounted for.

Finally, in addition to developing the fitting procedure of the model, future derivations of the model should also investigate the potential for tracking fascicle length and pennation angle changes in order to develop a more precise measure of the contractile component. Together, these two additions to the model developed in study 3 should provide a more valid approach to modelling muscle force in vivo. Thus, allowing the model to be used to investigate the role of TA in more dynamic movements and injuries.

Application of the EMG-drive model
The second aim of the research following this PhD is to apply the EMG-driven model to investigate the role of the TA in human movement and injuries. Of specific relevance to the theme of this thesis (see "general introduction") is the role of the TA during gait,

and the potential effect of overloading the TA on susceptibility to chronic anterior compartment syndrome.

The work performed by the TA has been suggested to be a trigger for the walk-run transition speed; the speed at which an individual starts to run. The activation of the TA and the dorsiflexor moment have both been shown to increase with increasing walking speeds, only to reduce upon commencement of running (Bartlett & Kram, 2008; Hreljac et al., 2008). Additionally, the walk-run transition speed reduced after fatiguing the dorsiflexor muscle group (Segers et al., 2007). Importantly, studies have only studied the activation of the TA, or the joint moment at the ankle in relation to the walk-run transition speed. The action (concentric, eccentric or isometric), length, profile of the activation, and importantly the force output of the TA have not been measured in relation to the walk-run transition speed. As such, the parameters of the TA performance in determining the walk-run transition speed are not known.

With a more forefoot landing style reducing the onset of symptoms associated with chronic anterior compartment syndrome (Diebal et al., 2012), postulated to be due to a reduced TA workload, work performed by the TA is hypothesised to be a mechanism for chronic anterior compartment syndrome (Allen & Barnes, 1986; Bong, Polatsch, Jazrawi, & Rokito, 2005; de Fijter, Scheltinga, & Luiting, 2006). Application of the model in symptomatic and asymptomatic individuals will provide an opportunity to assess the action, force, and subsequently work, performed by TA in this injured population and investigate the hypothesis that TA work is a mechanism underpinning chronic anterior compartment syndrome. Development of this research could be focused on monitoring changes in TA work during a gait re-education programme such as that implemented by Diebal et al. (2012) who trained patients to adopt a more forefoot strike during running. The combined cross-sectional and longitudinal approaches to this research will provide a deeper understanding on potential preventative measures in those susceptible to chronic anterior compartment syndrome.

CONCLUSION

Overall, the studies undertaken within this thesis provide some very important advances in our understanding of the mechanical factors affecting TA force production. Accurate measurements of the moment arm are vital for valid TA force calculation. In Study 1, the sources of error were explained, and the most optimal methodology currently

available was developed. In Study 2, current approaches to accounting for plantar flexor antagonist co-contraction were investigated and a more complete method was developed. The effect of tendon length changes on the accuracy of an EMG-driven model for the TA was investigated in Study 3. Under the controlled validation conditions, accounting for tendon length changes during the fitting of, and subsequent use of, the model were found to not be necessary. However, this is not likely to be true for movements involving stretch-shortening contractions where the TA muscle and ankle perform in opposite directions (i.e. Chleboun et al., 2007b).

The outputs of studies one and two, and the model developed in study three, provide an exciting development in our ability to investigate the role of the muscle non-invasively in vivo. Future work applying these findings to more dynamic human movement provides an opportunity to investigate fundamental movement patterns and potential mechanisms linked to overuse injuries.

References

Aagaard, P., Simonsen, E. B., Andersen, J. L., Magnusson, S. P., Bojsen-Moller, F., & Dyhre-Poulsen, P. (2000). Antagonist muscle coactivation during isokinetic knee extension. *Scand J Med Sci Sports*, *10*(2), 58-67.

Abbott, B. C., & Wilkie, D. R. (1953). The relation between velocity of shortening and the tension-length curve of skeletal muscle. *J Physiol*, *120*(1-2), 214-23.

Ackland, D. C., Lin, Y. C., & Pandy, M. G. (2012). Sensitivity of model predictions of muscle function to changes in moment arms and muscle-tendon properties: A monte-carlo analysis. *Journal of Biomechanics*, *45*(8), 1463-71.

Albracht, K., & Arampatzis, A. (2013). Exercise-induced changes in triceps surae tendon stiffness and muscle strength affect running economy in humans. *European Journal of Applied Physiology.* doi:10.1007/s00421-012-2585-4

Allen, M. J., & Barnes, M. R. (1986). Exercise pain in the lower leg. Chronic compartment syndrome and medial tibial syndrome. *J Bone Joint Surg Br*, *68*(5), 818-23.

Altenburg, T. M., de Haan, A., Verdijk, P. W., van Mechelen, W., & de Ruiter, C. J. (2009). Vastus lateralis single motor unit EMG at the same absolute torque production at different knee angles. *Journal of Applied Physiology*, *107*(1), 80-9.

Antman, S., & Osborn, J. (1979). The principle of virtual work and integral laws of motion. *Archive for Rational Mechanics and Analysis*, *69*(3).

Arampatzis, A., De Monte, G., & Morey-Klapsing, G. (2007). Effect of contraction form and contraction velocity on the differences between resultant and measured ankle joint moments. *Journal of Biomechanics*, *40*(7), 1622-1628.

Arampatzis, A., Karamanidis, K., Morey-Klapsing, G., De Monte, G., & Stafilidis, S. (2007). Mechanical properties of the triceps surae tendon and aponeurosis in relation to intensity of sport activity. *J Biomech*, *40*(9), 1946-52.

Arampatzis, A., Morey-Klapsing, G., Karamanidis, K., DeMonte, G., Stafilidis, S., & Brüggemann, G. P. (2005). Differences between measured and resultant joint moments during isometric contractions at the ankle joint. *Journal of Biomechanics*, *38*(4), 885-92.

Arampatzis, A., Peper, A., Bierbaum, S., & Albracht, K. (2010). Plasticity of human achilles tendon mechanical and morphological properties in response to cyclic strain. *J Biomech*, *43*(16), 3073-9.

Arndt, A. N., Komi, P. V., Brüggemann, G. P., & Lukkariniemi, J. (1998). Individual muscle contributions to the in vivo achilles tendon force. *Clinical Biomechanics (Bristol, Avon)*, *13*(7), 532-541.

Arnold, A. S., Salinas, S., Asakawa, D. J., & Delp, S. L. (2000). Accuracy of muscle moment arms estimated from mri-based musculoskeletal models of the lower extremity. *Comput Aided Surg*, *5*(2), 108-19.

Arnold, E. M., & Delp, S. L. (2011). Fibre operating lengths of human lower limb muscles during walking. *Philosophical Transactions of the Royal Society of London. Series B, Biological Sciences*, *366*(1570), 1530-9.

Axelson, H. (2005). *Muscle thixotropy: Implications for human motor control.* Acta Universitatis Upsaliensis,.

Babault, N., Pousson, M., Michaut, A., & Van Hoecke, J. (2003). Effect of quadriceps femoris muscle length on neural activation during isometric and concentric contractions. *Journal of Applied Physiology*, *94*(3), 983-90.

Baddar, A., Granata, K., Damiano, D. L., Carmines, D. V., Blanco, J. S., & Abel, M. F. (2002). Ankle and knee coupling in patients with spastic diplegia: Effects of gastrocnemius-soleus lengthening. *J Bone Joint Surg Am*, *84-A*(5), 736-44.

Baratta, R., & Solomonow, M. (1991). The effect of tendon viscoelastic stiffness on the dynamic performance of isometric muscle. *Journal of Biomechanics*, *24*(2), 109-116.

Baratta, R. V., Solomonow, M., Best, R., Zembo, M., & D'Ambrosia, R. (1995). Architecture-based force-velocity models of load-moving skeletal muscles. *Clin Biomech (Bristol, Avon)*, *10*(3), 149-155.

Bartlett, J., & Kram, R. (2008). Changing the demand on specific muscle groups affects the walk–run transition speed. *The Journal of Experimental Biology*, *211*(8), 1281-1288.

Bartlett, R., & Payton, C. (2007) B*iomechanical Evaluation of Movement in Sport and Exercise: The British Association of Sport and Exercise Sciences Guidelines*. London; New York: Routledge.

Bezodis, I. N., Kerwin, D. G., & Salo, A. I. (2008). Lower-limb mechanics during the support phase of maximum-velocity sprint running. *Med Sci Sports Exerc*, *40*(4), 707-15.

Biewener, A. A., Farley, C. T., Roberts, T. J., & Temaner, M. (2004). Muscle mechanical advantage of human walking and running: Implications for energy cost. *Journal of Applied Physiology*, *97*(6), 2266-2274.

Bigland, B., & Lippold, O. C. (1954a). Motor unit activity in the voluntary contraction of human muscle. *J Physiol*, *125*(2), 322-35.

Bigland, B., & Lippold, O. C. (1954b). The relation between force, velocity and integrated electrical activity in human muscles. *J Physiol*, *123*(1), 214-24.

Billot, M., Simoneau, E., Van Hoecke, J., & Martin, A. (2010). Coactivation at the ankle joint is not sufficient to estimate agonist and antagonist mechanical contribution. *Muscle & Nerve*, *41*(4), 511-8.

Billot, M., Simoneau, E. M., Ballay, Y., Van Hoecke, J., & Martin, A. (2011). How the ankle joint angle alters the antagonist and agonist torques during maximal efforts in dorsi- and plantar flexion. *Scandinavian Journal of Medicine & Science in Sports*, *21*(6), e273-81.

Birtles, D. B., Minden, D., Wickes, S. J., KP, M. P., MG, A. L., Casey, A., . . . Newham, D. J. (2002). Chronic exertional compartment syndrome: Muscle changes with isometric exercise. *Med Sci Sports Exerc*, *34*(12), 1900-6.

Birtles, D. B., Rayson, M. P., Jones, D. A., Padhiar, N., Casey, A., & Newham, D. J. (2003). Effect of eccentric exercise on patients with chronic exertional compartment syndrome. *Eur J Appl Physiol*, *88*(6), 565-71.

Blackman, P. G. (2000). A review of chronic exertional compartment syndrome in the lower leg. *Med Sci Sports Exerc*, *32*(3 Suppl), S4-10.

Blanpied, P., & Oksendahl, H. (2006). Reaction times and electromechanical delay in reactions of increasing and decreasing force. *Perceptual and Motor Skills*, *103*(3), 743-54.

Blazevich, A. J., Cannavan, D., Coleman, D. R., & Horne, S. (2007). Influence of concentric and eccentric resistance training on architectural adaptation in human quadriceps muscles. *J Appl Physiol*, *103*(5), 1565-75.

Bobbert, & Frank, M. (2012). Why is the force-velocity relationship in leg press tasks quasi-linear rather than hyperbolic? *Journal of Applied Physiology (Bethesda, Md. : 1985).*

Bong, M. R., Polatsch, D. B., Jazrawi, L. M., & Rokito, A. S. (2005). Chronic exertional compartment syndrome: Diagnosis and management. *Bull Hosp Jt Dis*, *62*(3-4), 77-84.

Bottinelli, R., Canepari, M., Pellegrino, M. A., & Reggiani, C. (1996). Force-velocity properties of human skeletal muscle fibres: Myosin heavy chain isoform and temperature dependence. *Journal of Physiology-London*, *495 (Pt 2)*, 573-86.

Boyd, S. K., & Ronsky, J. L. (1998). Instantaneous moment arm determination of the cat knee. *J Biomech*, *31*(3), 279-83.

Brenner, E. (2002). Insertion of the tendon of the tibialis anterior muscle in feet with and without hallux valgus. *Clinical Anatomy*, *15*(3), 217-223.

Brown, S. H., & McGill, S. M. (2008). Co-activation alters the linear versus non-linear impression of the emg--torque relationship of trunk muscles. *Journal of Biomechanics*, *41*(3), 491-497.

Brown, S. H., Brookham, R. L., & Dickerson, C. R. (2010). High-pass filtering surface EMG in an attempt to better represent the signals detected at the intramuscular level. *Muscle & Nerve*, *41*(2), 234-239.

Buchanan, T. S., Lloyd, D. G., Manal, K., & Besier, T. F. (2004). Neuromusculoskeletal modeling: Estimation of muscle forces and joint moments and movements from measurements of neural command. *J Appl Biomech*, *20*(4), 367-95.

Buchanan, T. S., Lloyd, D. G., Manal, K., & Besier, T. F. (2005). Estimation of muscle forces and joint moments using a forward-inverse dynamics model. *Medicine and Science in Sports and Exercise*, *37*(11), 1911-1916.

Burkholder, T. J., & Lieber, R. L. (2001). Sarcomere length operating range of vertebrate muscles during movement. *Journal of Experimental Biology*, *204*(Pt 9), 1529-36.

Burridge, J. H., Wood, D. E., Taylor, P. N., & McLellan, D. L. (2001). Indices to describe different muscle activation patterns, identified during treadmill walking, in people with spastic drop-foot. *Medical Engineering & Physics*, *23*(6), 427-34.

Byrne, C. A., O'Keeffe, D. T., Donnelly, A. E., & Lyons, G. M. (2007). Effect of walking speed changes on tibialis anterior EMG during healthy gait for FES envelope design in drop foot correction. *Journal of Electromyography and Kinesiology*, *17*(5), 605-16.

Cappellini, G., Ivanenko, Y. P., Poppele, R. E., & Lacquaniti, F. (2006). Motor patterns in human walking and running. *Journal of Neurophysiology*, *95*(6), 3426-37.

Chen, J., Siegler, S., & Schneck, C. D. (1988). The three-dimensional kinematics and flexibility characteristics of the human ankle and subtalar joint--part II: Flexibility characteristics. *J Biomech Eng*, *110*(4), 374-85.

Cheung, R. T., & Ng, G. Y. (2010). Motion control shoe delays fatigue of shank muscles in runners with overpronating feet. *The American Journal of Sports Medicine*, *38*(3), 486-91.

Chleboun, G. S., Busic, A. B., Graham, K. K., & Stuckey, H. A. (2007a). Fascicle length change of the human tibialis anterior and vastus lateralis during walking. *J Orthop Sports Phys Ther*, *37*(7), 372-9.

Chleboun, G. S., Busic, A. B., Graham, K. K., & Stuckey, H. A. (2007b). Fascicle length change of the human tibialis anterior and vastus lateralis during walking. *Journal of Orthopaedic & Sports Physical Therapy*, *37*(7), 372-379.

Chumanov, E. S., Wille, C. M., Michalski, M. P., & Heiderscheit, B. C. (2012). Changes in muscle activation patterns when running step rate is increased. *Gait & Posture*, *36*(2), 231-5.

Cohen, J. (1988). *Statistical power analysis for the behavioral sciences* (reprint, revised ed., p. 567). Hillsdale, N.J.: L. Erlbaum Associates
.
Cope, T. C., & Pinter, M. J. (1995). The size principle: Still working after all these years. *Physiology*, *10*(6), 280-286.

Correa, T. A., Baker, R., Graham, H. K., & Pandy, M. G. (2011). Accuracy of generic musculoskeletal models in predicting the functional roles of muscles in human gait. *Journal of Biomechanics*, *44*(11), 2096-105.

Cresswell, A. G., Loscher, W. N., & Thorstensson, A. (1995). Influence of gastrocnemius muscle length on triceps surae torque development and electromyographic activity in man. *Exp Brain Res*, *105*(2), 283-90.

Csapo, R., Maganaris, C. N., Seynnes, O. R., & Narici, M. V. (2010). On muscle, tendon and high heels. *The Journal of Experimental Biology*, *213*(Pt 15), 2582-8.

Dahmane, R., Djordjevic, S., Simunic, B., & Valencic, V. (2005). Spatial fiber type distribution in normal human muscle histochemical and tensiomyographical evaluation. *Journal of Biomechanics*, *38*(12), 2451-9.

Delp, S. L., Loan, J. P., Hoy, M. G., Zajac, F. E., Topp, E. L., & Rosen, J. M. (1990). An interactive graphics-based model of the lower extremity to study orthopaedic surgical procedures. *IEEE Trans Biomed Eng*, *37*(8), 757-67.

Dettwyler, M., Stacoff, A., Kramers-de Quervain, I. A., & Stüssi, E. (2004). Modelling of the ankle joint complex. Reflections with regards to ankle prostheses. *Foot and Ankle Surgery*, *10*(3), 109-119.

Devrome, A. N., & MacIntosh, B. R. (2007). The biphasic force-velocity relationship in whole rat skeletal muscle in situ. *J Appl Physiol*, *102*(6), 2294-300.

Diebal, A. R., Gregory, R., Alitz, C., & Gerber, J. P. (2012). Forefoot running improves pain and disability associated with chronic exertional compartment syndrome. *The American Journal of Sports Medicine*, *40*(5), 1060-7.

Dimitrova, N. A., Dimitrov, G. V., & Nikitin, O. A. (2002). Neither high-pass filtering nor mathematical differentiation of the EMG signals can considerably reduce cross-talk. *Journal of Electromyography and Kinesiology*, *12*(4), 235-46.

Disselhorst-Klug, C., Schmitz-Rode, T., & Rau, G. (2009). Surface electromyography and muscle force: Limits in semg-force relationship and new approaches for applications. *Clin Biomech (Bristol, Avon)*, *24*(3), 225-35.

Doheny, E. P., Lowery, M. M., Fitzpatrick, D. P., & O'Malley, M. J. (2008). Effect of elbow joint angle on force-emg relationships in human elbow flexor and extensor muscles. *Journal of Electromyography and Kinesiology*, *18*(5), 760-70.

Edman, K. A. (1979). The velocity of unloaded shortening and its relation to sarcomere length and isometric force in vertebrate muscle fibres. *J Physiol, 291*, 143-59.

Edman, K. A. (1988). Double-hyperbolic force-velocity relation in frog muscle fibres. *J Physiol, 404*, 301-21.

Edmundsson, D., Toolanen, G., & Sojka, P. (2007). Chronic compartment syndrome also affects nonathletic subjects - A prospective study of 63 cases with exercise-induced lower leg pain. *Acta Orthopaedica, 78*(1), 136-142.

Edwards, P. H. J., Wright, M. L., & Hartman, J. F. (2005). A practical approach for the differential diagnosis of chronic leg pain in the athlete. *Am J Sports Med, 33*(8), 1241-9.

Farina, D., Merletti, R., & Enoka, R. M. (2004). The extraction of neural strategies from the surface EMG. *Journal of Applied Physiology, 96*(4), 1486-95.

Fath, F. (2012). Methodological and anatomical modifiers of achilles tendon moment arm estimates implications for biomechanical modelling: Implications for biomechanical modelling. *School of Sport and Education.*

Fath, F., Blazevich, A. J., Waugh, C. M., Miller, S. C., & Korff, T. (2010). Direct comparison of in vivo achilles tendon moment arms obtained from ultrasound and MR scans. *Journal of Applied Physiology: Respiratory, Environmental and Exercise Physiology, 109*, 1644-1653.

Fenn, W. O., & Marsh, B. S. (1935). Muscular force at different speeds of shortening. *J Physiol, 85*(3), 277-97.

de Fijter, W. M., Scheltinga, M. R., & Luiting, M. G. (2006). Minimally invasive fasciotomy in chronic exertional compartment syndrome and fascial hernias of the anterior lower leg: Short- and long-term results. *Mil Med, 171*(5), 399-403.

Finni, T., Komi, P. V., & Lepola, V. (2000). In vivo human triceps surae and quadriceps femoris muscle function in a squat jump and counter movement jump. *European Journal of Applied Physiology, 83*(4 -5), 416-26.

Franz, J. R., & Kram, R. (2013). How does age affect leg muscle activity/coactivity during uphill and downhill walking? *Gait & Posture*, 37(3), 378-384

Fritz, C. O., Morris, P. E., & Richler, J. J. (2012). Effect size estimates: Current use, calculations, and interpretation. *Journal of Experimental Psychology. General*, *141*(1), 2-18.

Fukashiro, S., Hay, D. C., & Nagano, A. (2006). Biomechanical behavior of muscle-tendon complex during dynamic human movements. *J Appl Biomech*, *22*(2), 131-47.

Fukashiro, S., Itoh, M., Ichinose, Y., Kawakami, Y., & Fukunaga, T. (1995). Ultrasonography gives directly but noninvasively elastic characteristic of human tendon in vivo. *Eur J Appl Physiol Occup Physiol*, *71*(6), 555-7.

Fukashiro, S., Komi, P. V., Järvinen, M., & Miyashita, M. (1995). In vivo achilles tendon loading during jumping in humans. *European Journal of Applied Physiology and Occupational Physiology*, *71*(5), 453-8.

Fukunaga, T., Kawakami, Y., Kuno, S., Funato, K., & Fukashiro, S. (1997). Muscle architecture and function in humans. *Journal of Biomechanics*, *30*(5), 457-463.

Fukunaga, T., Kubo, K., Kawakami, Y., Fukashiro, S., Kanehisa, H., & Maganaris, C. N. (2001). In vivo behaviour of human muscle tendon during walking. *Proc Biol Sci*, *268*(1464), 229-33.

Fukunaga, T., Roy, R. R., Shellock, F. G., Hodgson, J. A., & Edgerton, V. R. (1996a). Specific tension of human plantar flexors and dorsiflexors. *Journal of Applied Physiology*, *80*(1), 158-65.

Fukunaga, T., Roy, R. R., Shellock, F. G., Hodgson, J. A., & Edgerton, V. R. (1996b). Specific tension of human plantar flexors and dorsiflexors. *Journal of Applied Physiology*, *80*(1), 158-65.

Fukunaga, T., Roy, R. R., Shellock, F. G., Hodgson, J. A., Day, M. K., Lee, P. L., . . . Edgerton, V. R. (1992). Physiological cross-sectional area of human leg muscles based on magnetic resonance imaging. *Journal of Orthopaedic Research : Official Publication of the Orthopaedic Research Society*, *10*(6), 928-34.

Gareis, H., Solomonow, M., Baratta, R., Best, R., & D'Ambrosia, R. (1992). The isometric length-force models of nine different skeletal muscles. *J Biomech*, *25*(8), 903-16.

Garner, J. C., Blackburn, T., Weimar, W., & Campbell, B. (2008). Comparison of electromyographic activity during eccentrically versus concentrically loaded isometric contractions. *Journal of Biomechanics*, *18*(3), 466 - 471.

Garrett, W. E., Safran, M. R., Seaber, A. V., Glisson, R. R., & Ribbeck, B. M. (1987). Biomechanical comparison of stimulated and nonstimulated skeletal muscle pulled to failure. *The American Journal of Sports Medicine*, *15*(5), 448-454.

Gazendam, M. G. J., & Hof, A. L. (2007). Averaged EMG profiles in jogging and running at different speeds. *Gait & Posture*, *25*(4), 604-614.

Geboers, J. F., Drost, M. R., Spaans, F., Kuipers, H., & Seelen, H. A. (2002). Immediate and long-term effects of ankle-foot orthosis on muscle activity during walking: A randomized study of patients with unilateral foot drop. *Arch Phys Med Rehabil*, *83*(2), 240-5.

Gerus, P., Rao, G., Buchanan, T. S., & Berton, E. (2010). A clinically applicable model to estimate the opposing muscle groups contributions to isometric and dynamic tasks. *Annals of Biomedical Engineering*, *38*(7), 2406-17.

Gordon, A. M., Huxley, A. F., & Julian, F. J. (1966a). Tension development in highly stretched vertebrate muscle fibres. *J Physiol*, *184*(1), 143-69.

Gordon, A. M., Huxley, A. F., & Julian, F. J. (1966b). The variation in isometric tension with sarcomere length in vertebrate muscle fibres. *J Physiol*, *184*(1), 170-92.

Gregor, R. J., Komi, P. V., Browning, R. C., & Järvinen, M. (1991). A comparison of the triceps surae and residual muscle moments at the ankle during cycling. *Journal of Biomechanics*, *24*(5), 287-97.

Grieve, D. W., Pheasant, S., & Cavanagh, P. R. (1978). Prediction of gastrocnemius length from knee and ankle joint posture. In E. Asmussen & K. Jorgensen (Eds.), Biomechanics vi-a (Vol. 2, pp. 405-412). Baltimore: University Park Press.

Hamner, S. R., Seth, A., & Delp, S. L. (2010). Muscle contributions to propulsion and support during running. *Journal of Biomechanics*, *43*(14), 2709-16.

Hansen, P., Aagaard, P., Kjaer, M., Larsson, B., & Magnusson, S. P. (2003). Effect of habitual running on human achilles tendon load-deformation properties and cross-sectional area. *J Appl Physiol*, *95*(6), 2375-80.

Hardt, D. E. (1978). Determining muscle forces in the leg during normal human walking—an application and evaluation of optimization methods. *Journal of Biomechanical Engineering*, *100*(2), 72.

Hashizume, S., Iwanuma, S., Akagi, R., Kanehisa, H., Kawakami, Y., & Yanai, T. (2011). In vivo determination of the achilles tendon moment arm in three-dimensions. *Journal of Biomechanics*.

Hawkins, D., & Bey, M. (1997). Muscle and tendon force-length properties and their interactions in vivo. *J Biomech*, *30*(1), 63-70.

Henneman, E., Somjen, G., & Carpenter, D. O. (1965). Functional significance of cell size in spinal motoneurons. *Journal of Neurophysiology*, *28*, 560-80.

Herbert, R. D., Moseley, A. M., Butler, J. E., & Gandevia, S. C. (2002). Change in length of relaxed muscle fascicles and tendons with knee and ankle movement in humans. *J Physiol*, *539*(Pt 2), 637-45.

Herzog, W., Guimaraes, A. C., Anton, M. G., & Carter-Erdman, K. A. (1991). Moment-length relations of rectus femoris muscles of speed skaters/cyclists and runners. *Medicine and Science in Sports and Exercise*, *23*(11), 1289-96.

Herzog, W., Read, L. J., & Ter Keurs, H. E. (1991). Experimental determination of force-length relations of intact human gastrocnemius muscles. *Clinical Biomechanics*, *6*(4), 230-8.

Hill, A. V. (1938). The heat of shortening and the dynamic constants of muscle. *Proceedings of the Royal Society of London. Series B, Biological Sciences*, *126*(843), 136-195.

Hill, A. V. (1964). The effect of load on the heat of shortening of muscle. *Proc R Soc Lond B Biol Sci*, *159*, 297-318.

Hof, A. L., & Berg, J. V. D. (1977a). Linearity between the weighted sum of the emgs of the human triceps surae and the total torque. *Journal of Biomechanics*, *10*(9), 529 - 539.

Hof, A. L., & Berg, J. V. D. (1977b). Linearity between the weighted sum of the emgs of the human triceps surae and the total torque. *Journal of Biomechanics*, *10*(9), 529 - 539.

Hortobágyi, T., Finch, A., Solnik, S., Rider, P., & DeVita, P. (2011). Association between muscle activation and metabolic cost of walking in young and old adults. *The Journals of Gerontology. Series A, Biological Sciences and Medical Sciences*, *66*(5), 541-7.

Hortobágyi, T., Solnik, S., Gruber, A., Rider, P., Steinweg, K., Helseth, J., & DeVita, P. (2009). Interaction between age and gait velocity in the amplitude and timing of antagonist muscle coactivation. *Gait & Posture*, *29*(4), 558-64.

Hoy, M. G., Zajac, F. E., & Gordon, M. E. (1990). A musculoskeletal model of the human lower extremity: The effect of muscle, tendon, and moment arm on the moment-angle relationship of musculotendon actuators at the hip, knee, and ankle. *J Biomech*, *23*(2), 157-69.

Hreljac, A., Imamura, R. T., Escamilla, R. F., Edwards, W. B., & MacLeod, T. (2008). The relationship between joint kinetic factors and the walk-run gait transition speed during human locomotion. *Journal of Applied Biomechanics*, *24*(2), 149-57.

Hughes, R. E., Niebur, G., Liu, J., & An, K. N. (1998). Comparison of two methods for computing abduction moment arms of the rotator cuff. *J Biomech*, *31*(2), 157-60.

Huxley, A. F., & Niedergerke, R. (1954). Structural changes in muscle during contraction; interference microscopy of living muscle fibres. *Nature*, *173*(4412), 971-3.

Huxley, H., & Hanson, J. (1954). Changes in the cross-striations of muscle during contraction and stretch and their structural interpretation. *Nature*, *173*(4412), 973-6.

Ichinose, Y., Kawakami, Y., Ito, M., Kanehisa, H., & Fukunaga, T. (2000). In vivo estimation of contraction velocity of human vastus lateralis muscle during "isokinetic" action. *J Appl Physiol*, *88*(3), 851-6.

Ishikawa, M., & Komi, P. V. (2008). Muscle fascicle and tendon behavior during human locomotion revisited. *Exercise and Sport Sciences Reviews*, *36*(4), 193-9.

Ishikawa, M., Pakaslahti, J., & Komi, P. V. (2007). Medial gastrocnemius muscle behavior during human running and walking. *Gait Posture*, *25*(3), 380-4.

Ito, M., Akima, H., & Fukunaga, T. (2000). In vivo moment arm determination using b-mode ultrasonography. *J Biomech*, *33*(2), 215-8.

Ito, M., Kawakami, Y., Ichinose, Y., Fukashiro, S., & Fukunaga, T. (1998). Nonisometric behavior of fascicles during isometric contractions of a human muscle. *J Appl Physiol*, *85*(4), 1230-5.

Kawakami, Y., Ichinose, Y., & Fukunaga, T. (1998). Architectural and functional features of human triceps surae muscles during contraction. *Journal of Applied Physiology*, *85*(2), 398-404.

Kawakami, Y., Kubo, K., Kanehisa, H., & Fukunaga, T. (2002). Effect of series elasticity on isokinetic torque-angle relationship in humans. *Eur J Appl Physiol*, *87*(4-5), 381-7.

Kellis, E., Kouvelioti, V., & Ioakimidis, P. (2005). Reliability of a practicable emg-moment model for antagonist moment prediction. *Neurosci Lett*, *383*(3), 266-71.

Klein, P., Mattys, S., & Rooze, M. (1996). Moment arm length variations of selected muscles acting on talocrural and subtalar joints during movement: An in vitro study. *J Biomech*, *29*(1), 21-30.

Koh, T. J., & Herzog, W. (1998). Increasing the moment arm of the tibialis anterior induces structural and functional adaptation: Implications for tendon transfer. *J Biomech*, *31*(7), 593-9.

Kubo, K., Kanehisa, H., & Fukunaga, T. (2002). Effects of resistance and stretching training programmes on the viscoelastic properties of human tendon structures in vivo. *Journal of Physiology-London*, *538*(Pt 1), 219-26.

Kubo, K., Kawakami, Y., & Fukunaga, T. (1999). Influence of elastic properties of tendon structures on jump performance in humans. *J Appl Physiol*, *87*(6), 2090-6.

Kues, J. M., & Mayhew, T. P. (1996). Concentric and eccentric force-velocity relationships during electrically induced submaximal contractions. *Physiother Res Int*, *1*(3), 195-204.

Kurokawa, S., Fukunaga, T., & Fukashiro, S. (2001). Behavior of fascicles and tendinous structures of human gastrocnemius during vertical jumping. *Journal of Applied Physiology*, *90*(4), 1349-58.

Kutch, J. J., & Buchanan, T. S. (2001). Human elbow joint torque is linearly encoded in electromyographic signals from multiple muscles. *Neuroscience Letters*, *311*(2), 97 - 100.

Kyrolainen, H., Avela, J., & Komi, P. V. (2005). Changes in muscle activity with increasing running speed. *J Sports Sci*, *23*(10), 1101-9.

Labeit, S., & Kolmerer, B. (1995, October). Titins: Giant proteins in charge of muscle ultrastructure and elasticity. *Science (New York, N.Y.)*, *270*(5234), 293-296.

Law, L. F., Krishnan, C., & Avin, K. (2011). Modeling nonlinear errors in surface electromyography due to baseline noise: A new methodology. *Journal of Biomechanics*, *44*(1), 202-5.

Lay, A. N., Hass, C. J., & Gregor, R. J. (2006). The effects of sloped surfaces on locomotion: A kinematic and kinetic analysis. *Journal of Biomechanics*, *39*(9), 1621-8.

Lay, A. N., Hass, C. J., Richard Nichols, T., & Gregor, R. J. (2007). The effects of sloped surfaces on locomotion: An electromyographic analysis. *Journal of Biomechanics*, *40*(6), 1276-85.

Lee, S. J., & Hidler, J. (2008). Biomechanics of overground vs. Treadmill walking in healthy individuals. *J Appl Physiol*, *104*(3), 747-55.

Leedham, J. S., & Dowling, J. J. (1995). Force-length, torque-angle and emg-joint angle relationships of the human in vivo biceps brachii. *Eur J Appl Physiol Occup Physiol*, *70*(5), 421-6.

Leitch, J., Stebbins, J., & Zavatsky, A. B. (2010). Subject-specific axes of the ankle joint complex. *Journal of Biomechanics*, *43*(15), 2923 - 2928.

Lemos, R., Epstein, M., & Herzog, W. (2008). Modeling of skeletal muscle: The influence of tendon and aponeuroses compliance on the force–length relationship. *Medical & Biological Engineering & Computing*, *46*(1), 23-32.

Lichtwark, G. A., & Wilson, A. M. (2005). In vivo mechanical properties of the human achilles tendon during one-legged hopping. *Journal of Experimental Biology*, *208*(Pt 24), 4715-25.

Lichtwark, G. A., Bougoulias, K., & Wilson, A. M. (2007). Muscle fascicle and series elastic element length changes along the length of the human gastrocnemius during walking and running. *Journal of Biomechanics*, *40*(1), 157-64.

Lieber, R. L., & Brown, C. G. (1992). Sarcomere length-joint angle relationships of seven frog hindlimb muscles. *Acta Anatomica*, *145*(4), 289-95.

Lieber, R. L., & Ward, S. R. (2011). Skeletal muscle design to meet functional demands. *Philosophical Transactions of the Royal Society of London. Series B, Biological Sciences*, *366*(1570), 1466-76.

Lieber, R. L., Loren, G. J., & Fridén, J. (1994). In vivo measurement of human wrist extensor muscle sarcomere length changes. *Journal of Neurophysiology*, *71*(3), 874-81.

Lieber, R. L., Raab, R., Kashin, S., & Edgerton, V. R. (1992). Short communication. Sarcomere length changes during fish swimming. *Journal of Experimental Biology*, *169*, 251-4.

Linnamo, V., Moritani, T., Nicol, C., & Komi, P. V. (2003). Motor unit activation patterns during isometric, concentric and eccentric actions at different force levels. *Journal of Electromyography and Kinesiology*, *13*(1), 93-101.

Linnamo, V., Strojnik, V., & Komi, P. V. (2006). Maximal force during eccentric and isometric actions at different elbow angles. *European Journal of Applied Physiology*, *96*(6), 672-678.

Lippold, O. C. (1952). The relation between integrated action potentials in a human muscle and its isometric tension. *J Physiol*, *117*(4), 492-9.

Lundberg, A., Goldie, I., Kalin, B., & Selvik, G. (1989). Kinematics of the ankle/foot complex: Plantarflexion and dorsiflexion. *Foot & Ankle*, *9*(4), 194.

Lyons, G. M., Wilcox, D. J., Lyons, D. J., & Hilton, D. (2000). Evaluation of a drop foot stimulator FES intensity envelope matched to tibialis anterior muscle activity

during walking. In *Proceedings of the 5th annual international functional electrical stimulation society conference* (pp. 448-451).

Mademli, L., Arampatzis, A., Morey-Klapsing, G., & Brüggemann, G. P. (2004). Effect of ankle joint position and electrode placement on the estimation of the antagonistic moment during maximal plantarflexion. *Journal of Electromyography and Kinesiology*, *14*(5), 591-7.

Maganaris, C. N. (2000). In vivo measurement-based estimations of the moment arm in the human tibialis anterior muscle-tendon unit. *J Biomech*, *33*(3), 375-9.

Maganaris, C. N. (2001). Force-length characteristics of in vivo human skeletal muscle. *Acta Physiol Scand*, *172*(4), 279-85.

Maganaris, C. N. (2002). Tensile properties of in vivo human tendinous tissue. *J Biomech*, *35*(8), 1019-27.

Maganaris, C. N. (2003). Tendon conditioning: Artefact or property? *Proc Biol Sci*, *270 Suppl 1*, S39-42.

Maganaris, C. N. (2004). Imaging-based estimates of moment arm length in intact human muscle-tendons. *Eur J Appl Physiol*, *91*(2-3), 130-9.

Maganaris, C. N., & Paul, J. P. (1999). In vivo human tendon mechanical properties. *J Physiol*, *521 Pt 1*, 307-13.

Maganaris, C. N., & Paul, J. P. (2000a). Hysteresis measurements in intact human tendon. *J Biomech*, *33*(12), 1723-7.

Maganaris, C. N., & Paul, J. P. (2000b). In vivo human tendinous tissue stretch upon maximum muscle force generation. *J Biomech*, *33*(11), 1453-9.

Maganaris, C. N., & Paul, J. P. (2002). Tensile properties of the in vivo human gastrocnemius tendon. *J Biomech*, *35*(12), 1639-46.

Maganaris, C. N., Baltzopoulos, V., & Sargeant, A. J. (1998). Differences in human antagonistic ankle dorsiflexor coactivation between legs; can they explain the moment deficit in the weaker plantarflexor leg? *Experimental Physiology*, *83*(6), 843-55.

Maganaris, C. N., Baltzopoulos, V., & Sargeant, A. J. (1999). Changes in the tibialis anterior tendon moment arm from rest to maximum isometric dorsiflexion: In vivo observations in man. *Clin Biomech (Bristol, Avon)*, *14*(9), 661-6.

Maganaris, C. N., Baltzopoulos, V., & Sargeant, A. J. (2000). In vivo measurement-based estimations of the human achilles tendon moment arm. *Eur J Appl Physiol*, *83*(4 - 5), 363-9.

Maganaris, C. N., Baltzopoulos, V., & Sargeant, A. J. (2002). Repeated contractions alter the geometry of human skeletal muscle. *J Appl Physiol*, *93*(6), 2089-94.

Magid, A., & Law, D. J. (1985, December). Myofibrils bear most of the resting tension in frog skeletal muscle. *Science (New York, N.Y.)*, *230*(4731), 1280-1282.

Magnusson, S. P., Narici, M. V., Maganaris, C. N., & Kjaer, M. (2008). Human tendon behaviour and adaptation, in vivo. *J Physiol*, *586*(1), 71-81.

Manal, K., Cowder, J. D., & Buchanan, T. S. (2013). Subject-specific measures of achilles tendon moment arm using ultrasound and video-based motion capture. *Physiological Reports*, *1*(6), n/a.

Manal, K., Gravare-Silbernagel, K., & Buchanan, T. S. (2012). A real-time emg-driven musculoskeletal model of the ankle. *Multibody System Dynamics*, *28*(1-2), 169-180.

Marsh, E., Sale, D., McComas, A. J., & Quinlan, J. (1981). Influence of joint position on ankle dorsiflexion in humans. *J Appl Physiol*, *51*(1), 160-7.

Matsumoto, Y. (1967). Validity of the force-velocity relation for muscle contraction in the length region, l less than or equal to l-o. *J Gen Physiol*, *50*(5), 1125-37.

McDonald, A. C., Sanei, K., & Keir, P. J. (2013). The effect of high pass filtering and non-linear normalization on the emg--force relationship during sub-maximal finger exertions. *Journal of Electromyography and Kinesiology*.

Milner-Brown, H. S., Stein, R. B., & Yemm, R. (1973). Changes in firing rate of human motor units during linearly changing voluntary contractions. *J Physiol*, *230*(2), 371-90.

Moritani, T., & deVries, H. A. (1978). Reexamination of the relationship between the surface integrated electromyogram (IEMG) and force of isometric contraction. *American Journal of Physical Medicine*, *57*(6), 263-77.

Morse, C. I., Degens, H., Seynnes, O. R., Maganaris, C. N., & Jones, D. A. (2008). The acute effect of stretching on the passive stiffness of the human gastrocnemius muscle tendon unit. *The Journal of Physiology*, *586*(Pt 1), 97.

Morse, C. I., Thom, J. M., Reeves, N. D., Birch, K. M., & Narici, M. V. (2005). In vivo physiological cross-sectional area and specific force are reduced in the gastrocnemius of elderly men. *Journal of Applied Physiology*, *99*(3), 1050-5.

Mouhsine, E., Garofalo, R., Moretti, B., Gremion, G., & Akiki, A. (2006). Two minimal incision fasciotomy for chronic exertional compartment syndrome of the lower leg. *Knee Surg Sports Traumatol Arthrosc*, *14*(2), 193-7.

Muraoka, T., Muramatsu, T., Fukunaga, T., & Kanehisa, H. (2004). Influence of tendon slack on electromechanical delay in the human medial gastrocnemius in vivo. *J Appl Physiol*, *96*(2), 540-4.

Murley, G. S., Landorf, K. B., Menz, H. B., & Bird, A. R. (2009). Effect of foot posture, foot orthoses and footwear on lower limb muscle activity during walking and running: A systematic review. *Gait & Posture*, *29*(2), 172-87.

Murray, M. P., Guten, G. N., Baldwin, J. M., & Gardner, G. M. (1976). A comparison of plantar flexion torque with and without the triceps surae. *Acta Orthopaedica Scandinavica*, *47*(1), 122-4.

Neptune, R. R., Clark, D. J., & Kautz, S. A. (2009). Modular control of human walking: A simulation study. *Journal of Biomechanics*, *42*(9), 1282-7.

Nigg, B. M., & Herzog, W. (2006). *Biomechanics of the musculo-skeletal system* (3 ed.). New Jersey: Wiley.

Nilsson, J., Thorstensson, L. F., & Halbertsma, Ñ. (1985). Changes in leg movements and muscle activity with speed of locomotion and mode of progression in humans. *Acta Physiologica Scandinavica*, *123*(4), 457-475.

Nishikawa, K. C., Monroy, J. A., Uyeno, T. E., Yeo, S. H., Pai, D. K., & Lindstedt, S. L. (2012). Is titin a 'winding filament'? A new twist on muscle contraction. *Proceedings. Biological Sciences / the Royal Society*, *279*(1730), 981-90.

Olney, S. J., & Winter, D. A. (1985). Predictions of knee and ankle moments of force in walking from EMG and kinematic data. *J Biomech*, *18*(1), 9-20.

Padhiar, N., & King, J. B. (1996). Exercise induced leg pain-chronic compartment syndrome. Is the increase in intra-compartment pressure exercise specific? *Br J Sports Med*, *30*(4), 360-2.

Perry, J., & Bekey, G. A. (1981). EMG-force relationships in skeletal muscle. *Crit Rev Biomed Eng*, *7*(1), 1-22.

Pinniger, G. J., Steele, J. R., Thorstensson, A., & Cresswell, A. G. (2000). Tension regulation during lengthening and shortening actions of the human soleus muscle. *European Journal of Applied Physiology*, *81*(5), 375-83.

Podolsky, R. J., & Teichholz, L. E. (1970). Relation between calcium and contraction kinetics in skinned muscle fibres. *Journal of Physiology-London*, *211*(1), 19-35.

Potvin, J. R., & Brown, S. H. M. (2004a). Less is more: High pass filtering, to remove up to 99% of the surface EMG signal power, improves emg-based biceps brachii muscle force estimates. *Journal of Electromyography and Kinesiology*, *14*(3), 389-399.

Potvin, J. R., & Brown, S. H. M. (2004b). Less is more: High pass filtering, to remove up to 99% of the surface EMG signal power, improves emg-based biceps brachii muscle force estimates. *Journal of Electromyography and Kinesiology*, *14*(3), 389-399.

Prado, L. G., Makarenko, I., Andresen, C., Krüger, M., Opitz, C. A., & Linke, W. A. (2005). Isoform diversity of giant proteins in relation to passive and active contractile properties of rabbit skeletal muscles. *The Journal of General Physiology*, *126*(5), 461-80.

Prilutsky, B. I., & Gregor, R. J. (2001). Swing- and support-related muscle actions differentially trigger human walk-run and run-walk transitions. *J Exp Biol*, *204*(Pt 13), 2277-87.

Puranen, J., & Alavaikko, A. (1981). Intracompartmental pressure increase on exertion in patients with chronic compartment syndrome in the leg. *J Bone Joint Surg Am*, *63*(8), 1304-9.

Rack, P. M., & Westbury, D. R. (1969). The effects of length and stimulus rate on tension in the isometric cat soleus muscle. *Journal of Physiology-London*, *204*(2), 443-60.

Ramsey, R. W., & Street, S. F. (1940). The isometric length-tension diagram of isolated skeletal muscle fibers of the frog. *Journal of Cellular and Comparative Physiology*, *15*(1), 11-34.

Randall, L., Styf, J. R., Pedowitz, R. A., Hargens, A. R., & Gershuni, D. H. (1997). Intramuscular deoxygenation during exercise in patients who have chronic anterior compartment syndrome of the leg. *Journal of Bone and Joint Surgery-American Volume*, *79A*(6), 844-849.

Rassier, D. E., MacIntosh, B. R., & Herzog, W. (1999). Length dependence of active force production in skeletal muscle. *J Appl Physiol*, *86*(5), 1445-57.

Reeves, N. D., & Narici, M. V. (2003). Behavior of human muscle fascicles during shortening and lengthening contractions in vivo. *J Appl Physiol*, *95*(3), 1090-6.

Reeves, N. D., Narici, M. V., & Maganaris, C. N. (2003). Strength training alters the viscoelastic properties of tendons in elderly humans. *Muscle & Nerve*, *28*(1), 74-81.

Reeves, N. D., Narici, M. V., & Maganaris, C. N. (2004a). Effect of resistance training on skeletal muscle-specific force in elderly humans. *Journal of Applied Physiology*, *96*(3), 885-92.

Reeves, N. D., Narici, M. V., & Maganaris, C. N. (2004b). In vivo human muscle structure and function: Adaptations to resistance training in old age. *Experimental Physiology*, *89*(6), 675-89.

Reuleaux, F., & Kennedy, A. B. W. (1876). *The kinematics of machinery. Outlines of a theory of machines* (pp. xvi, 622 p.). London,: Macmillan.

Rosager, S., Aagaard, P., Dyhre-Poulsen, P., Neergaard, K., Kjaer, M., & Magnusson, S. P. (2002). Load-displacement properties of the human triceps surae aponeurosis and tendon in runners and non-runners. *Scand J Med Sci Sports*, *12*(2), 90-8.

Rugg, S. G., Gregor, R. J., Mandelbaum, B. R., & Chiu, L. (1990). In vivo moment arm calculations at the ankle using magnetic resonance imaging (MRI). *J Biomech*, *23*(5), 495-501.

Ryan, E. D., Herda, T. J., Costa, P. B., Walter, A. A., Hoge, K. M., Stout, J. R., & Cramer, J. T. (2010). Viscoelastic creep in the human skeletal muscle-tendon unit. *European Journal of Applied Physiology*, *108*(1), 207-11.

Sale, D., Quinlan, J., Marsh, E., McComas, A. J., & Belanger, A. Y. (1982). Influence of joint position on ankle plantarflexion in humans. *Journal of Applied Physiology: Respiratory, Environmental and Exercise Physiology*, *52*(6), 1636-42.

Sano, K., Ishikawa, M., Nobue, A., Danno, Y., Akiyama, M., Oda, T., Ito, A., Hoffren, M., Nicol, C., Locatelli, E., & Komi, P. V. (2012). Muscle-tendon interaction and EMG profiles of world class endurance runners during hopping. *European Journal of Applied Physiology*.

Scheys, L., Spaepen, A., Suetens, P., & Jonkers, I. (2008). Calculated moment-arm and muscle-tendon lengths during gait differ substantially using MR based versus rescaled generic lower-limb musculoskeletal models. *Gait Posture, 28*(4), 640-8.

Scheys, L., Van Campenhout, A., Spaepen, A., Suetens, P., & Jonkers, I. (2008). Personalized mr-based musculoskeletal models compared to rescaled generic models in the presence of increased femoral anteversion: Effect on hip moment arm lengths. *Gait & Posture, 28*(3), 358-65.

Scott, L. A., Murley, G. S., & Wickham, J. B. (2012). The influence of footwear on the electromyographic activity of selected lower limb muscles during walking. *Journal of Electromyography and Kinesiology : Official Journal of the International Society of Electrophysiological Kinesiology.*

Scott, S. H., Brown, I. E., & Loeb, G. E. (1996). Mechanics of feline soleus: I. Effect of fascicle length and velocity on force output. *Journal of Muscle Research and Cell Motility, 17*(2), 207-219.

Segers, V., Lenoir, M., Aerts, P., & De Clercq, D. (2007). Influence of M. Tibialis anterior fatigue on the walk-to-run and run-to-walk transition in non-steady state locomotion. *Gait & Posture, 25*(4), 639-47.

Sheehan, F. T. (2007). The 3D patellar tendon moment arm: Quantified in vivo during volitional activity. *J Biomech, 40*(9), 1968-74.

Sheehan, F. T. (2012). The 3D in vivo achilles' tendon moment arm, quantified during active muscle control and compared across sexes. *Journal of Biomechanics, 45*(2), 225-30.

Siegler, S., Chen, J., & Schneck, C. D. (1988). The three-dimensional kinematics and flexibility characteristics of the human ankle and subtalar joints—part I: Kinematics. *Journal of Biomechanical Engineering, 110*, 364.

Simoneau, E. M., Billot, M., Martin, A., & Van Hoecke, J. (2009). Antagonist mechanical contribution to resultant maximal torque at the ankle joint in young and older men. *Journal of Electromyography and Kinesiology : Official Journal of the International Society of Electrophysiological Kinesiology*, *19*(2), e123-31.

Simoneau, E. M., Longo, S., Seynnes, O. R., & Narici, M. V. (2012). Human muscle fascicle behavior in agonist and antagonist isometric contractions. *Muscle & Nerve*, *45*(1), 92-9.

Sparto, P. J., Parnianpour, M., Marras, W. S., Granata, K. P., Reinsel, T. E., & Simon, S. (1998). Effect of electromyogram-force relationships and method of gain estimation on the predictions of an electromyogram-driven model of spinal loading. *Spine*, *23*(4), 423-429.

Spoor, C. W., & van Leeuwen, J. L. (1992). Knee muscle moment arms from MRI and from tendon travel. *J Biomech*, *25*(2), 201-6.

Spoor, C. W., van Leeuwen, J. L., Meskers, C. G., Titulaer, A. F., & Huson, A. (1990). Estimation of instantaneous moment arms of lower-leg muscles. *J Biomech*, *23*(12), 1247-59.

Staudenmann, D., Potvin, J. R., Kingma, I., Stegeman, D. F., & van Dieen, J. H. (2007). Effects of EMG processing on biomechanical models of muscle joint systems: Sensitivity of trunk muscle moments, spinal forces, and stability. *Journal of Biomechanics*, *40*(4), 900-909.

Staudenmann, D., Roeleveld, K., Stegeman, D. F., & van Dieën, J. H. (2010). Methodological aspects of SEMG recordings for force estimation--a tutorial and review. *Journal of Electromyography and Kinesiology*, *20*(3), 375-87.

Theis, N., Mohagheghi, A. A., & Korff, T. (2012). Method and strain rate dependence of achilles tendon stiffness. *Journal of Electromyography and Kinesiology : Official Journal of the International Society of Electrophysiological Kinesiology*, *22*(6), 947-

Thorstensson, A., Grimby, G., & Karlsson, J. (1976). Force-velocity relations and fiber composition in human knee extensor muscles. *Journal of Applied Physiology*, *40*(1), 12-6.

Tilp, M., Steib, S., & Herzog, W. (2011). Length changes of human tibialis anterior central aponeurosis during passive movements and isometric, concentric, and eccentric contractions. *European Journal of Applied Physiology.*

Touliopolous, S., & Hershman, E. B. (1999). Lower leg pain. Diagnosis and treatment of compartment syndromes and other pain syndromes of the leg. *Sports Med*, *27*(3), 193-204.

Tsaopoulos, D. E., Baltzopoulos, V., & Maganaris, C. N. (2006). Human patellar tendon moment arm length: Measurement considerations and clinical implications for joint loading assessment. *Clin Biomech (Bristol, Avon)*, *21*(7), 657-67.

Tsaopoulos, D. E., Baltzopoulos, V., Richards, P. J., & Maganaris, C. N. (2007). In vivo changes in the human patellar tendon moment arm length with different modes and intensities of muscle contraction. *J Biomech*, *40*(15), 3325-32.

Turnipseed, W. D., Hurschler, C., & Vanderby, R. (1995). The effects of elevated compartment pressure on tibial arteriovenous flow and relationship of mechanical and biochemical characteristics of fascia to genesis of chronic anterior compartment syndrome. *Journal of Vascular Surgery*, *21*(5), 810-817.

Tweed, J. L., & Barnes, M. R. (2008). Is eccentric muscle contraction a significant factor in the development of chronic anterior compartment syndrome? A review of the literature. *Foot (Edinb)*, *18*(3), 165-70.

de Vet, H. C. W., Terwee, C. B., Knol, D. L., & Bouter, L. M. (2006). When to use agreement versus reliability measures. *Journal of Clinical Epidemiology*, *59*(10), 1033-1039.

Vos, E. J., Harlaar, J., & van Ingen Schenau, G. J. (1991). Electromechanical delay during knee extensor contractions. *Medicine and Science in Sports and Exercise*, *23*(10), 1187-93.

Vos, E. J., Mullender, M. G., & van Ingen Schenau, G. J. (1990). Electromechanical delay in the vastus lateralis muscle during dynamic isometric contractions. *European Journal of Applied Physiology and Occupational Physiology*, *60*(6), 467-71.

Weber, D. J., Stein, R. B., Chan, K. M., Loeb, G., Richmond, F., Rolf, R., & Chong, S. L. (2005). BIONic walkaide for correcting foot drop. *IEEE Trans Neural Syst Rehabil Eng*, *13*(2), 242-6.

White, S. C., & Winter, D. A. (1992). Predicting muscle forces in gait from {EMG} signals and musculotendon kinematics. *Journal of Electromyography and Kinesiology*, *2*(4), 217 - 231.

Williams, C. D., Salcedo, M. K., Irving, T. C., Regnier, M., & Daniel, T. L. (2013). The length-tension curve in muscle depends on lattice spacing. *Proceedings. Biological Sciences / the Royal Society*, *280*(1766), 697.

Wilson, D. L., Zhu, Q., Duerk, J. L., Mansour, J. M., Kilgore, K., & Crago, P. E. (1999). Estimation of tendon moment arms from three-dimensional magnetic resonance images. *Annals of Biomedical Engineering*, *27*(2), 247-256.

Wilson, N. A., & Sheehan, F. T. (2009). Dynamic in vivo 3-dimensional moment arms of the individual quadriceps components. *Journal of Biomechanics*, *42*(12), 1891-7.

Winter, D. A. (2009). *Biomechanics and motor control of human movement* (4th ed., pp. xiv, 370 p.). Hoboken, N.J.: Wiley.

Wright, I. C., Neptune, R. R., van Den Bogert, A. J., & Nigg, B. M. (1998). Passive regulation of impact forces in heel-toe running. *Clinical Biomechanics (Bristol, Avon)*, *13*(7), 521-531.

Xiao, M., & Higginson, J. (2010). Sensitivity of estimated muscle force in forward simulation of normal walking. *Journal of Applied Biomechanics*, *26*(2), 142-9.

Zajac, F. E. (1989). Muscle and tendon: Properties, models, scaling, and application to biomechanics and motor control. *Critical Reviews in Biomedical Engineering*, *17*(4), 359-411.

Zajac, F. E., Neptune, R. R., & Kautz, S. A. (2002). Biomechanics and muscle coordination of human walking. Part I: Introduction to concepts, power transfer, dynamics and simulations. *Gait Posture*, *16*(3), 215-32.

Zatsiorsky, V. M., & Prilutsky, B. I. (2012). *Biomechanics of skeletal muscles* (p. 536). Champaign, IL: Human Kinetics.

Zhang, Q., Rennerfelt, K., & Styf, J. (2012). The magnitude of intramuscular deoxygenation during exercise is an unreliable measure to diagnose the cause of leg pain. *Scandinavian Journal of Medicine & Science in Sports*, *22*(5), 690-4.

Zhu, Q., Duerk, J. L., Mansour, J. M., Crago, P. E., & Wilson, D. L. (1997). Tendon moment arm measurement using 3D MRI images. *Proceedings of the 19th Annual International Conference of the Ieee Engineering in Medicine and Biology Society, Vol 19, Pts 1-6*, *19*, 480-482.

Appendices

Ethical Approval

Head of School of Sport & Education
Professor Susan Capel

Brunel
UNIVERSITY
WEST LONDON

Stuart Miller
Research Student
School of Sport and Education
Brunel University

Heinz Wolff Building,
Brunel University, Uxbridge,
Middlesex, UB8 3PH, UK
Telephone +44 (0)1895 266494
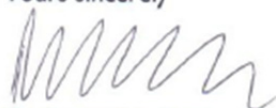Fax +44 (0)1895 269769
Web www.brunel.ac.uk

1st May 2008

Dear Stuart

RE71- 07 – Validation of Reuleaux's method using motion analysis

I am writing to confirm the Research Ethics Committee of the School of Sport and Education received your application connected to the above project. Your application has been independently reviewed and I am pleased to confirm your application complies with the research ethics guidelines issued by the University.

On behalf of the Research Ethics Committee, I wish you every success with your study.

Yours sincerely

Dr Simon Bradford
Chair of Research Ethics Committee

Head of School of Sport & Education
Professor Susan Capel

Brunel
UNIVERSITY
WEST LONDON

Mr Stuart Miller
c/o School of Sport and Education
Brunel University

12th August 2009

Dear Stuart

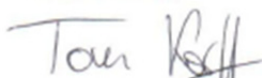### RE71-07 – Validation of Reuleaux's method using motion analysis

I am writing to confirm the Research Ethics Committee of the School of Sport and Education received your application to amend the above mentioned research study. Your application has been independently reviewed to ensure it complies with the University Research Ethics requirements and guidelines.

The Chair, acting under delegated authority, is satisfied with the decision reached by the independent reviewers and is pleased to confirm there is no objection on ethical grounds to the proposed amendment to your study.

Any further changes to the protocol contained within your application and any unforeseen ethical issues which arise during the conduct of your study must be notified to the Research Ethics Committee for further consideration.

On behalf of the Research Ethics Committee for the School of Sport and Education, I wish you every success with your amended study.

Yours sincerely

Signed on behalf of Dr Simon Bradford
Chair of Research Ethics Committee
School Of Sport and Education

Head of School of Sport & Education
Professor Susan Capel

Brunel
UNIVERSITY
L O N D O N

Stuart Miller
PhD (Sport Sciences) Student
School of Sport and Education
Brunel University

7th June 2012

Dear Stuart

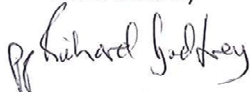**RE71-07 – Validation of Reuleaux's method using motion analysis**

I am writing to confirm the Research Ethics Committee of the School of Sport and Education received your application to amend the above mentioned research study. Your amendments have been independently reviewed to ensure they comply with the University Research Ethics requirements and guidelines.

The Chair, acting under delegated authority, is satisfied with the decision reached by the independent reviewers and is pleased to confirm there is no objection on ethical grounds to you amending your study as proposed.

Any further changes to the protocol contained within your application and any unforeseen ethical issues which arise during the conduct of your study must be notified to the Research Ethics Committee for further consideration.

On behalf of the Research Ethics Committee for the School of Sport and Education, I wish you every success with your revised study.

Yours sincerely

Dr Gary Armstrong
Chair of Research Ethics Committee
School Of Sport and Education

Brunel is proud to host

Team Korea

Canadian | Comité
Paralympic | paralympique
Committee | canadien

THE QUEEN'S
ANNIVERSARY PRIZES
FOR HIGHER AND FURTHER EDUCATION
2011